Annu. Rev. Astron. Astrophys. 2004. 42:603–83
doi: 10.1146/annurev.astro.42.053102.134024

First published online as a Review in Advance on June 2, 2004

SECULAR EVOLUTION AND THE FORMATION OF PSEUDOBULGES IN DISK GALAXIES

John Kormendy
Department of Astronomy, University of Texas, Austin, Texas 78712; email: kormendy@astro.as.utexas.edu

Robert C. Kennicutt, Jr.
Department of Astronomy, Steward Observatory, University of Arizona, Tucson, Arizona 85721; email: rkennicutt@as.arizona.edu

Key Words galaxy dynamics, galaxy structure, galaxy evolution

■ **Abstract** The Universe is in transition. At early times, galactic evolution was dominated by hierarchical clustering and merging, processes that are violent and rapid. In the far future, evolution will mostly be secular—the slow rearrangement of energy and mass that results from interactions involving collective phenomena such as bars, oval disks, spiral structure, and triaxial dark halos. Both processes are important now. This review discusses internal secular evolution, concentrating on one important consequence, the buildup of dense central components in disk galaxies that look like classical, merger-built bulges but that were made slowly out of disk gas. We call these pseudobulges.

We begin with an "existence proof"—a review of how bars rearrange disk gas into outer rings, inner rings, and stuff dumped onto the center. The results of numerical simulations correspond closely to the morphology of barred galaxies. In the simulations, gas is transported to small radii, where it reaches high densities and plausibly feeds star formation. In the observations, many barred and oval galaxies have dense central concentrations of gas and star formation. Optical colors and spectra often imply young stellar populations. So the formation of pseudobulges is well supported by theory and observations. It is embedded in a broader evolution picture that accounts for much of the richness observed in galaxy structure.

If secular processes built dense central components that masquerade as bulges, how can we distinguish them from merger-built bulges? Observations show that pseudobulges retain a memory of their disky origin. That is, they have one or more characteristics of disks: (*a*) flatter shapes than those of classical bulges, (*b*) correspondingly large ratios of ordered to random velocities, (*c*) small velocity dispersions σ with respect to the Faber-Jackson correlation between σ and bulge luminosity, (*d*) spiral structure or nuclear bars in the "bulge" part of the light profile, (*e*) nearly exponential brightness profiles, and (*f*) starbursts. All these structures occur preferentially in barred and oval galaxies, where secular evolution should be most rapid. So the cleanest examples of pseudobulges are recognizable.

Are their formation timescales plausible? We use measurements of central gas densities and star-formation rates to show that pseudobulges of the observed densities form on timescales of a few billion years.

Thus a large variety of observational and theoretical results lead to a new picture of galaxy evolution that complements hierarchical clustering and merging. Secular evolution consists of more than the aging of stellar populations. Every galaxy is dynamically evolving.

1. INTRODUCTION

This paper reviews internal processes of secular evolution in disk galaxies. We concentrate on one important consequence: the buildup of dense central components that look like classical, i.e., merger-built bulges but that were made slowly by disks out of disk material. These are called pseudobulges. Our discussion updates a review by Kormendy (1993).

The relative importance of the different physical processes of galaxy evolution (Figure 1) changes as the Universe expands. Rapid processes that happen in discrete events are giving way to slow, ongoing processes.

At early times, galactic evolution was dominated by a combination of dissipative collapse (Eggen, Lynden-Bell & Sandage 1962; Sandage 1990) and mergers (Toomre 1977a) of galaxies that virialized out of the density fluctuations of cold dark matter. These are the top processes shown in Figure 1. The evolution timescale was short, $t_{\rm dyn} \sim (1/G\rho)^{1/2}$, where ρ is the mean density and G is the gravitational constant. The processes were violent. Many present-day galaxies owe their properties to this violence. Because mergers scramble disks and induce dissipation and starbursts, they are thought to make classical bulges and elliptical galaxies. We do not review classical bulges other than to contrast them to pseudobulges. Most work on galaxy evolution in the past 25 years has concentrated on hierarchical clustering and mergers. As the Universe expands, and as galaxy clusters virialize and acquire large internal velocities, mergers get less common (Toomre 1977a, Conselice et al. 2003).

In the distant future, internal secular processes will become dominant. These are defined to be slow processes, i.e., ones that have timescales much longer than $t_{\rm dyn}$. To be interesting, they must operate over long times. Some secular processes, such as disk heating via stellar enounters with molecular clouds, are well known (Spitzer & Schwarzschild 1951, 1953). But star-star relaxation is too slow to be important almost everywhere in almost every galaxy. Therefore, relevant secular processes generally involve the interactions of individual stars or gas clouds with collective phenomena such as bars, oval distortions, spiral structure, and triaxial dark matter halos. Also important are the interactions of these collective phenomena with each other. Given that hierarchical clustering continues today, has there been time for slow processes to be important? For secular evolution to have a significant effect, a galaxy must be free of major mergers for a long time, because merger violence erases the signature of secular processes. Hierarchical clustering results in so many

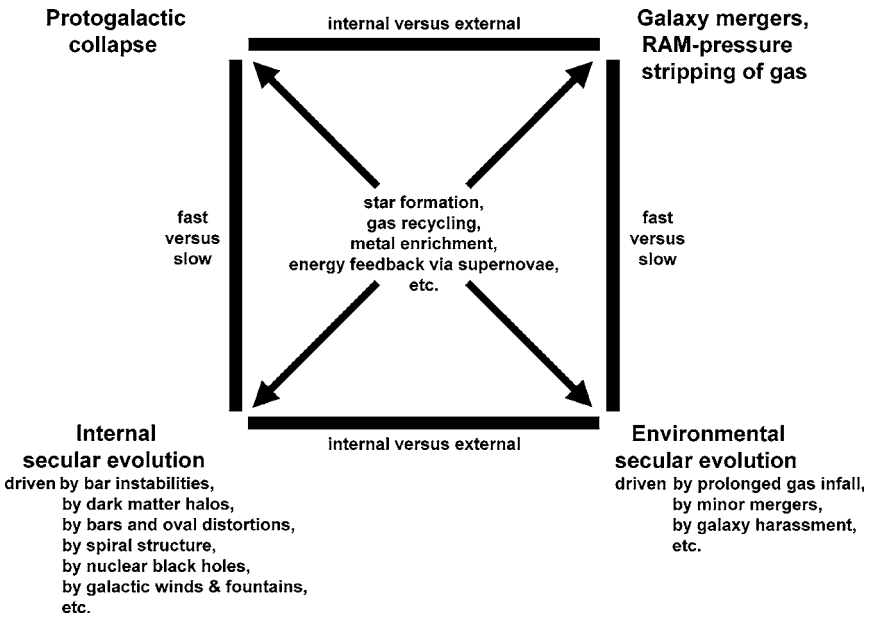

Figure 1 Morphological box (Zwicky 1957) of processes of galactic evolution updated from Kormendy (1982a). Processes are divided vertically into fast (*top*) and slow (*bottom*). Fast evolution happens on a free-fall ("dynamical") timescale, $t_{\rm dyn} \sim (G\rho)^{-1/2}$, where ρ is the density of the object produced and G is the gravitational constant. Slow means many galaxy rotation periods. Processes are divided horizontally into ones that happen purely internally in one galaxy (*left*) and ones that are driven by environmental effects such as galaxy interactions (*right*). The processes at center are aspects of all types of galaxy evolution. This paper is about the internal and slow processes at lower left.

mergers that one might guess that secular processes are relatively unimportant. A clue that this is frequently not the case is provided by galaxies with superthin—and fragile—disks but apparently no bulges (e.g., Matthews, Gallagher & van Driel 1999b; Freeman 2000; van der Kruit et al. 2001). They show that many galaxies have suffered no major merger violence since the onset of star formation in the disk (Tóth & Ostriker 1992). Therefore there has been time for secular evolution to be important in at least some galaxies. Given that mergers make bulges and ellipticals, these tend to be late-type galaxies. Actually, because the latest-type galaxies are (pseudo)bulgeless, secular evolution is likely to be most important in intermediate-late-type galaxies, i.e., Sbcs. But even some S0 and Sa galaxies contain pseudobulges. Secular processes have received less attention than galaxy mergers.

Still, this subject has made rapid progress. Many reviews discuss secular evolution in barred and oval galaxies (Kormendy 1979a,b; 1981, 1982a; Norman 1984; Combes 1991, 1998, 2000, 2001; Martinet 1995; Pfenniger 1996a,b, 2000;

Sellwood & Debattista 1996; Buta 1995, 1999, 2000; Athanassoula 2002; and especially Sellwood & Wilkinson 1993 and Buta & Combes 1996). Discussions of pseudobulge formation include, besides the above, Pfenniger & Norman (1990); Courteau (1996b); Carollo, Ferguson & Wyse (1999); Balcells et al. (2003); and especially Kormendy (1993) and Carollo (2003).

Theory and observations point to a variety of processes that redistribute energy in disks. In Section 2, we review evidence that bars and ovals rearrange disk gas into outer rings, inner rings, and central mass concentrations. The resulting star formation produces a central stellar subsystem that has the high density and steep density gradient of a bulge but that was not formed by galaxy mergers.

Secular evolution is not confined to barred and oval galaxies. Bars can self-destruct by building up the central mass concentration, so secular evolution may have happened even if no bar is seen today. Global spiral structure also makes galaxies evolve, albeit more slowly than do bars.

These processes are manifestations of very general dynamical principles. Disks spread in radius—the inner parts shrink and the outer parts expand—because this lowers the total energy for fixed total angular momentum (Lynden-Bell & Kalnajs 1972, Tremaine 1989). Two-dimensional spreading by angular momentum transport is as fundamental for rotation-dominated disks as is three-dimensional spreading by energy transport in the core collapse of ellipsoidal systems dominated by random motions. The reason is the same, too. Self-gravitating systems have negative specific heats, so increasing the central density by flinging away the periphery lowers the total energy (Lynden-Bell & Wood 1968, Binney & Tremaine 1987). What makes evolution important in some systems and not in others? The determining factor is whether any evolution process is fast enough. Core collapse requires short relaxation times. Galaxy disks have long relaxation times, so their evolution is interesting only if they have an alternative to relaxation. Nonaxisymmetries provide the engine for rapid evolution.

We argue here that pseudobulges are one result of this evolution. Of key importance is the observation that they retain some memory of their disky origin. We review this subject in detail (Section 4), because it is central to any conclusion that evolution has happened and because it is the only way that we can recognize pseudobulges.

Next we review observations of gas content and star-formation rates. From these, we estimate pseudobulge growth times. These prove to be in good agreement with stellar population ages. So the picture of pseudobulge growth from rearranged disk gas is internally consistent.

Our purpose is to connect up a large number of apparently disparate results into a well-developed and (as we hope to show) a well-supported paradigm. Still, many questions remain unanswered. In particular, we need a better understanding of the relative importance of mergers and secular evolution as a function of galaxy type and luminosity. We hope that this review will provide a concrete context that will allow efficient progress in this subject.

1.1. What is a Bulge? Classical and Physical Morphology

What do we mean by a bulge? The answer shows why, for some galaxies, we use the term pseudobulge.

Renzini (1999) clearly states the canonical interpretation of Hubble-Sandage-de Vaucouleurs classifications: "It appears legitimate to look at bulges as ellipticals that happen to have a prominent disk around them [and] ellipticals as bulges that for some reason have missed the opportunity to acquire or maintain a prominent disk." We adopt this point of view. However, as observations improve, we discover more and more features that make it difficult to interpret every example of what we used to call a bulge as an elliptical living in the middle of a disk. This leads authors to agonize: "Are bulges of early-type and late-type spirals different? Are their formation scenarios different? Can we talk about bulges in the same way for different types of galaxies?" (Fathi & Peletier 2003).

We conclude that early- and late-type galaxies generally do make their dense central components in different ways. This is not recognized in classical morphology, because it defines classification bins—deliberately and with good reason—without physical interpretation. Sandage & Bedke (1994) describe how, in the early stages of investigating a subject, a classifier should look for "natural groups" (Morgan 1951) of objects with similar features. Sandage emphasizes that it is important not to be led astray by preconceptions: "The extreme empiricist claims that no whiff of theory may be allowed into the *initial* classification procedures, decisions, and actions." Nevertheless, some choice of which features to consider as important and which to view as secondary must be made. After all, the goal is to understand the physics, and the exercise is useful only if classification bins at least partly isolate unique physics or order galaxies by physically relevant parameters. The Hubble-Sandage-de Vaucouleurs classification scheme has done these things remarkably well.

However, it is reasonable to expect that improved understanding of galaxies will show that the classification missed some of the physics. Also, some features of galaxies could not be observed well enough in the photographic era to be included. These include high-surface-brightness disky substructures in galaxy centers. Consistent with physical morphology as discussed in Kormendy (1982a), we wish to distinguish components in galaxies that have different origins.

At the level of detail that we nowadays try to understand, the time has passed when we can make effective progress by defining morphological bins with no guidance from a theory. Disks, bulges, and bars were different enough that we could do this. Afterward, robust conclusions could be reached, e.g., about the relative timescales of collapse and star formation (Eggen, Lynden-Bell & Sandage 1962). But even inner rings and spiral arms—which are not subtle—do not scream the appropriate message, which is that spiral arms are details that would disappear quickly and without a trace if the driving mechanism switched off, whereas we will see that rings are a permanent rearranging of disk material. Inner rings are, in this sense, more fundamental than spiral arms. Years ago, people commonly

reacted badly to a classification as complicated as (R)SB(r)b (de Vaucouleurs et al. 1991). The reason, we believe, was that the phenomenology alone did not sell itself. People did not see why this level of detail was important. Now, we will show that every letter in the above classification has a clear-cut meaning in terms of formation physics. This is the goal of physical morphology.

We adopt the view that bulges are ellipticals living in the middle of disks. Ellipticals form via mergers (Toomre 1977a, Schweizer 1990). Therefore, we do not use the term bulge for every central component that is in excess of the inward extrapolation of an exponential fitted to the disk brightness profile. If the evidence suggests that such a component formed by secular processes, we call it a pseudobulge. In practice, we cannot be certain about formation mechanisms. Therefore, if the component in question is very E-like, we call it a bulge, and if it is disk-like, we call it a pseudobulge. Intermediate cases are discussed in Sections 4, 7, and 9.1.

Finally, we comment on one of the biggest problems in this subject. It is exceedingly easy to get lost in the details. Many authors interpret observations or simulations in much more detail than we do here. For example, it is common for observers to distinguish nuclei, nuclear bars, nuclear disks, nuclear spiral structure, exponential bulges, boxy bulges, and star-formation rings. We discuss all these features, because they are central to the developing picture of what secular evolution can accomplish. But we consider them all to be features of pseudobulges, because the evidence is that they are all built by secular evolution out of disk material. In the same way, global spiral structure, flocculent spiral structure, and the absence of spiral structure in S0 galaxies are all features of disks.

2. SECULAR EVOLUTION OF BARRED GALAXIES

We see only snapshots of galaxy evolution, so it is difficult to study slow processes.[1] Why do we think that secular evolution is happening? We begin with an existence proof—a review of how *n*-body simulations account for the morphological features seen in barred galaxies. Our suggestion that pseudobulges are constructed out of rearranged disk gas is embedded in this larger picture of SB secular evolution.

2.1. Morphology of Barred Galaxies

Barred galaxies are reviewed in detail by Sellwood & Wilkinson (1993). Their morphology is discussed by de Vaucouleurs (1959, 1963), Sandage (1961, 1975), Kormendy (1979b), Sandage & Bedke (1994), Buta & Crocker (1991), Buta & Combes (1996), and Buta (1995, 1999). We use these diagnostic features:

1. Barred spiral galaxies are divided into subclasses SB(s), in which the spiral arms begin at the ends of the bar, and SB(r), in which a complete inner

[1]Mergers are an easier problem—transient phenomena such as tidal tails are readily recognizable (Toomre & Toomre 1972, Schweizer 1990).

ring of stars connects the ends of the bar. In the latter case, the spiral arms start somewhere on the ring, "often downstream from the ends of the bar" (Sandage & Bedke 1994). SB(r) and SB(s) galaxies are contrasted in Figure 6; additional SB(r) galaxies are shown in Figure 3 and Figure 5, and additional SB(s) galaxies are shown in Figure 7.

2. Some barred and oval galaxies have outer rings (R) that are 2.2 ± 0.1 times the diameter of the bar or inner disk. Outer rings in barred and unbarred galaxies are similar [Figure 2 and Figure 5]. Inner and outer rings are different; there is no size overlap. Some galaxies contain both (Figure 5).
3. At intermediate Hubble types, when the bar is made mostly of old stars and the disk contains many young stars, the stellar population of inner and outer rings is like that of the disk, not like that of the bar (Figures 2 and 3). Inner and outer rings generally contain gas.
4. In SB(s) galaxies, an almost-straight dust lane parallels the ridge line of the bar but is displaced slightly forward in the direction of galactic rotation. Such dust lanes are analogous to and connect up with the prominent dust lanes seen on the trailing side of the arms in global-pattern spirals. Examples are shown in Figure 6 and in Figures 7 and 8. These dust lanes are almost never present in SB(r) galaxies (Sandage 1961). NGC 1512 in Figure 3 is a rare exception.
5. Many barred and oval galaxies have very active star formation near their centers, in what is conventionally identified as the bulge. Often the star formation is concentrated in a ring. Figures 3, 7, and 8 show examples.
6. Many barred galaxies have pseudobulges that are elongated into a structure resembling a bar. Examples are shown in Figure 14.
7. Many early-type SB galaxies contain a lens in the disk—a shelf of slowly decreasing surface brightness with a sharp outer edge. Lenses have intrinsic axial ratios of $\sim$0.85; the bar usually fills the longest dimension. These properties are discussed in Kormendy (1979a,b, 1981, 1982a) and in Athanassoula et al. (1982). Lenses are sometimes seen in unbarred galaxies; NGC 1553 is the best example (Freeman 1975, Kormendy 1984). Lenses in early-type galaxies look similar to oval disks in late-type galaxies (Section 3.2); it is not clear whether or not they are physically similar. Lenses are illustrated in Figures 2 and 5.

These features can be understood at least qualitatively as results of secular evolution driven by nonaxisymmetric gravitational potentials. An exact correspondence between *n*-body simulations and observations cannot be expected, because real galaxies have a complicated interplay between gas, star formation, and energy feedback from massive young stars back into the interstellar medium. Such effects, along with the self-gravity of the gas, are often omitted from simulations and at best are included only approximately. Nevertheless, *n*-body

simulations have been conspicuously successful in reproducing the structure of barred galaxies.

2.2. Dynamics of Barred Galaxies: The Importance of Resonances

To understand bar-driven evolution, we need to dip briefly into the dynamics of bars. An in-depth review is provided by Sellwood & Wilkinson (1993). Here we need a primer on the nature and importance of orbital resonances.

Seen from an inertial frame, an orbit in a galactic disk is an unclosed rosette. That is, there are a nonintegral number of radial oscillations for every revolution around the center. However, in a frame of reference that rotates at the average angular velocity of the star, the star's mean position is fixed, and its radial oscillation makes it move in a small ellipse around that mean position.[2] Any global density pattern such as a bar that rotates at the above angular velocity will pull gravitationally on the star in essentially the same way at all times and will therefore make large perturbations in its orbit. Corotation is the strongest of a series of resonances in which the pattern repeatedly sees the star in the same way.

For example, there is another rotating frame in which the star executes two radial oscillations for each circuit around the center. If a bar rotates at this angular velocity, it sees the stellar orbit as closed, roughly elliptical, and centered on the galactic center (Figure 4). This is called inner Lindblad resonance (ILR). It occurs when the pattern speed of the bar is $\Omega_p = \Omega - \kappa/2$, where Ω is the average angular velocity of revolution of the star and κ is its frequency of radial oscillation. The limit of small radial oscillations is called the epicyclic approximation; then $\kappa^2 = (2V/r)(V/r + dV/dr)$, where $V(r)$ is the circular-orbit rotation curve (Mihalas & Routly 1968 provide a particularly transparent discussion).

[2]It is an ellipse and not just radial motion because the star revolves faster than average near pericenter and slower than average near apocenter.

Figure 4 (*Top*) Frequencies $\Omega(r) = V(r)/r$ and $\Omega \pm \kappa/2$, where $\kappa^2 = (2V/r)(V/r + dV/dr)$ is the epicyclic frequency of radial oscillations for almost circular orbits. This figure (Sparke & Gallagher 2000) is for a Plummer potential, but the behavior is generic. For a pattern speed Ω_p, the most important resonances occur where $\Omega_p = \Omega$ (corotation), $\Omega_p = \Omega + \kappa/2$ [outer Lindblad resonance (OLR)], and $\Omega_p = \Omega - \kappa/2$ [two inner Lindblad resonances (ILR), marked with vertical dashes]. (*Bottom*) From Englmaier & Gerhard (1997), examples of the principal orbit families for a bar oriented at 45° as in Figure 7. The elongated orbits parallel to the bar are the x_1 family out of which the bar is constructed. Interior to ILR (or outer ILR, if there are two LRs), the x_2 family is perpendicular to the bar. Near corotation is the 4:1 ultraharmonic resonance; the almost-square orbit makes four radial oscillations during each circuit around the center. Since the principal orbits change orientation by 90° at each resonance shown, they must cross near the resonances.

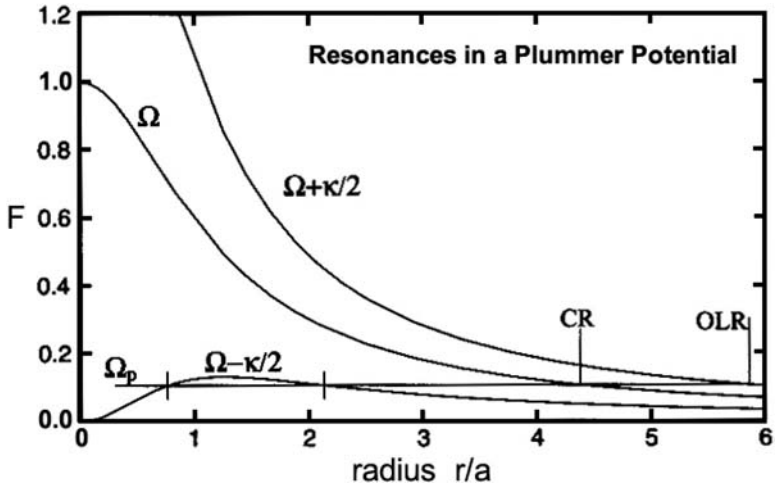

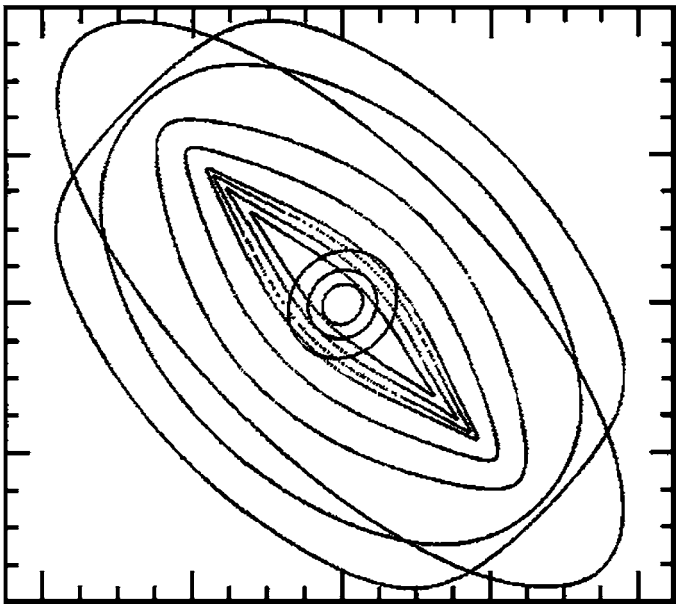

Outer Lindblad resonance (OLR) is like inner Lindblad resonance, except that the star drifts backward with respect to the rotating frame while it executes two radial oscillations for each revolution: $\Omega_p = \Omega + \kappa/2$.

Resonances are important for several reasons. Figure 4 shows generic frequency curves and the most important periodic orbit families in a barred galaxy. We can begin to understand how a self-consistent bar is constructed by exploiting the fact that $\Omega - \kappa/2$ varies only slowly with radius (except near the center, if there is an ILR). Calculations of orbits in a barred potential show that the main family of orbits (called x_1) is elongated parallel to the bar between ILR and corotation. Bars are largely made of x_1 orbits and similar, nonperiodic orbits that are trapped around them by the bar's self-gravity. Typical x_1 orbits are shown in the bottom panel of Figure 4. They are not nearly circular, but the essence of their behavior is captured if we retain the language of the epicyclic approximation and say that orbits of different radii look closed in frames that rotate at different angular velocities $\Omega - \kappa/2$. But if $\Omega - \kappa/2$ varies only a little with radius, then it is possible to pick a single pattern speed Ω_p in which the orbits precess almost together. If they precessed exactly together, then one could make a bar by aligning elongated orbits as in the bottom panel of the figure. Because $\Omega - \kappa/2$ is not quite constant, it is the job of self-gravity to make the orbits precess not approximately but exactly together. This idea was used to understand self-consistent bars by Lynden-Bell & Kalnajs (1972) and by Lynden-Bell (1979) and to demystify spiral structure by Kalnajs (1973) and by Toomre (1977b). They were following in the pioneering footsteps of Bertil Lindblad (1958; see section 20 of Lindbald 1959).

Calculations of orbits in barred potentials reveal other orbit families (e.g., Contopolous & Mertzanides 1977; Athanassoula 1992a,b; Sellwood & Wilkinson 1993), only a few of which are relevant here. Next in importance is the x_2 family, which lives interior to ILR and which is oriented perpendicular to the bar (Figure 4, bottom). Between corotation and OLR, the principal orbits are elongated perpendicular to the bar, and outside OLR, they are again oriented parallel to the bar. Near corotation is the 4:1 ultraharmonic resonance in which a star executes 4 radial oscillations for every revolution: $\Omega_p = \Omega - \kappa/4$. We need these results in the following sections.

The important consequence is emphasized by Sellwood & Wilkinson (1993): "Not only do the eccentricities of the orbits increase as exact resonance is approached, but the major axes switch orientation across all three principal resonances, making the crossing of orbits from opposite sides of a resonance inevitable" (bottom panel of Figure 4). This is important mainly when the orbits are very noncircular, as they are in strongly barred galaxies. Now, orbits that cross are no problem for stars. But gas clouds that move on such orbits must collide near resonances. Dissipation is inevitable; the consequence is an increase in the gas density and star formation. This heuristic discussion helps to explain the numerical results reviewed in the following sections, in which gas tends to build up in rings and to form stars there.

2.3. Bar-Driven Radial Transport of Gas: The Formation of Rings

Theory (Binney & Tremaine 1987; Sellwood & Wilkinson 1993; Lynden-Bell 1979, 1996) and *n*-body simulations (Sellwood 1981, Sparke & Sellwood 1987, Pfenniger & Friedli 1991, Athanassoula 2003) show that bars grow by transferring angular momentum to the outer disk, thereby driving spiral structure. As a result, stellar orbits in the bar get more elongated, and the bar grows in amplitude. Its pattern speed slows down.

The essence of the response of gas to a bar is captured in figure 3 of Simkin, Su & Schwarz (1980), reproduced here as Figure 5. Outside corotation, gas is driven outward by the angular momentum transfer from bar to disk that makes the bar

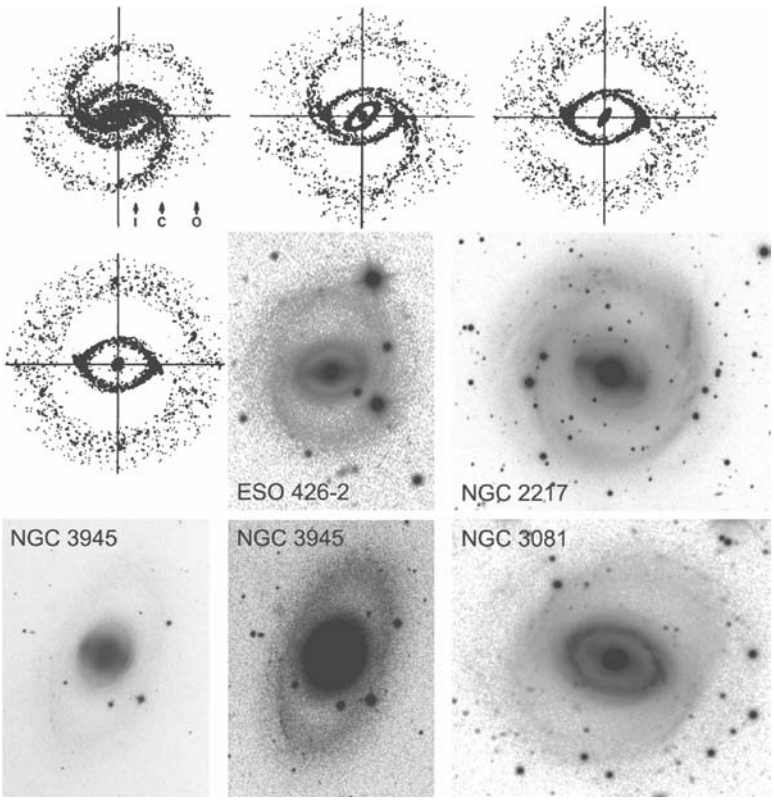

Figure 5 Evolution of gas in a rotating oval potential (Simkin, Su, & Schwarz 1980; see also Schwarz 1981, 1984). The gas particles in this sticky-particle *n*-body model are shown after 2, 3, 5, and 7 bar rotations (*top-left through center-left*). Arrows show the radii of ILR, corotation, and OLR. Four SB0 or SB0/a galaxies are shown that have outer rings and a lens (NGC 3945) or an inner ring (obvious in ESO 426-2 and in NGC 3081, but poorly developed in NGC 2217). Sources: NGC 3945 (Kormendy 1979b); NGC 2217, NGC 3081 (Buta et al. 2003); ESO 426-2 (Buta & Crocker 1991).

grow. This gas collects into an outer ring near OLR. As discussed earlier, outer rings are oriented perpendicular to the bar when they are interior to OLR; this is the usual situation (Kormendy 1979b, Buta 1995). At radii well inside corotation, gas falls toward the center. This is the gas that is believed to make pseudobulges. Within an annular region around corotation, gas is collected into an inner ring near corotation or near the 4:1 ultraharmonic resonance.

This behavior is seen in a variety of simulations starting as early as Prendergast (1964), Duus & Freeman (1975), and Sørensen et al. (1976). By the early 1980s, there was already an extensive literature on the subject (see Kormendy 1982a and Prendergast 1983 for reviews).

The reason why SB(r) and SB(s) galaxies are different was investigated by Sanders & Tubbs (1980). They simulated the response of gas to an imposed, rigid bar potential that they grew inside a disk galaxy. Examples of the steady-state gas response are shown in Figure 6. In the top two rows of panels, the strength of the bar increases from left to right, either because the ratio of bar mass to disk mass increases (top row), or because the bar gets more elongated (second row). In both cases, weak bars tend to produce an SB(s) response, while strong bars produce ring-like structures that resemble SB(r) galaxies. If the bar gets too strong (top-right panel), the result does not look like a real galaxy. The bottom row of simulations explores the effect of varying the bar's pattern speed. Rapid pattern speeds produce dramatically SB(s) structure. Slower pattern speeds in which corotation is near the end of the bar produce inner rings. Very slow pattern rotation (right panel, in which corotation is at 3 bar radii) produce responses that do not look like real galaxies. This is because Ω_p is now so small that the radius of ILR is large. Inside ILR, closed gas orbits align perpendicular to the bar. These can never have substantially the same radius as the bar, as they do in the bottom-right simulation in Figure 6. If the response to the bar were perpendicular to the bar over most of the radius of the bar, it would be impossible to make that response add up to a self-consistent bar. Pattern speeds are never so slow that corotation radii are so far out in the disk that the entire bar is inside ILR. This was possible in Sanders & Tubbs (1980) only because the bar was inserted by hand and given a chosen (not a self-consistent) pattern speed. Theoretical arguments tell us that bars end inside or near corotation (Contopoulos 1980, Sellwood & Wilkinson 1993). Observations agree (Kent 1987b; Merrifield & Kuijken 1995; Gerssen, Kuijken & Merrifield 1999, 2003; Debattista & Williams 2001; Debattista, Corsini & Aguerri 2002; Aguerri, Debattista & Corsini 2003; Corsini, Debattista & Aguerri 2003; see Elmegreen 1996 for a review) except in late-type galaxies in which $V \propto r$ rotation curves imply that the bar is safely clear of ILR anyway (Elmegreen 1996; Elmegreen, Wilcots & Pisano 1998).

Despite the above successes, Sanders & Tubbs (1980) share a number of technical problems with other early simulations of gas response to bars. Their beam scheme (Sanders & Prendergast 1974) code has coarse spatial resolution and unphysical numerical viscosity (see Athanassoula 1992b and Sellwood & Wilkinson 1993). In fact, there are conflicting views on whether viscosity is important at all;

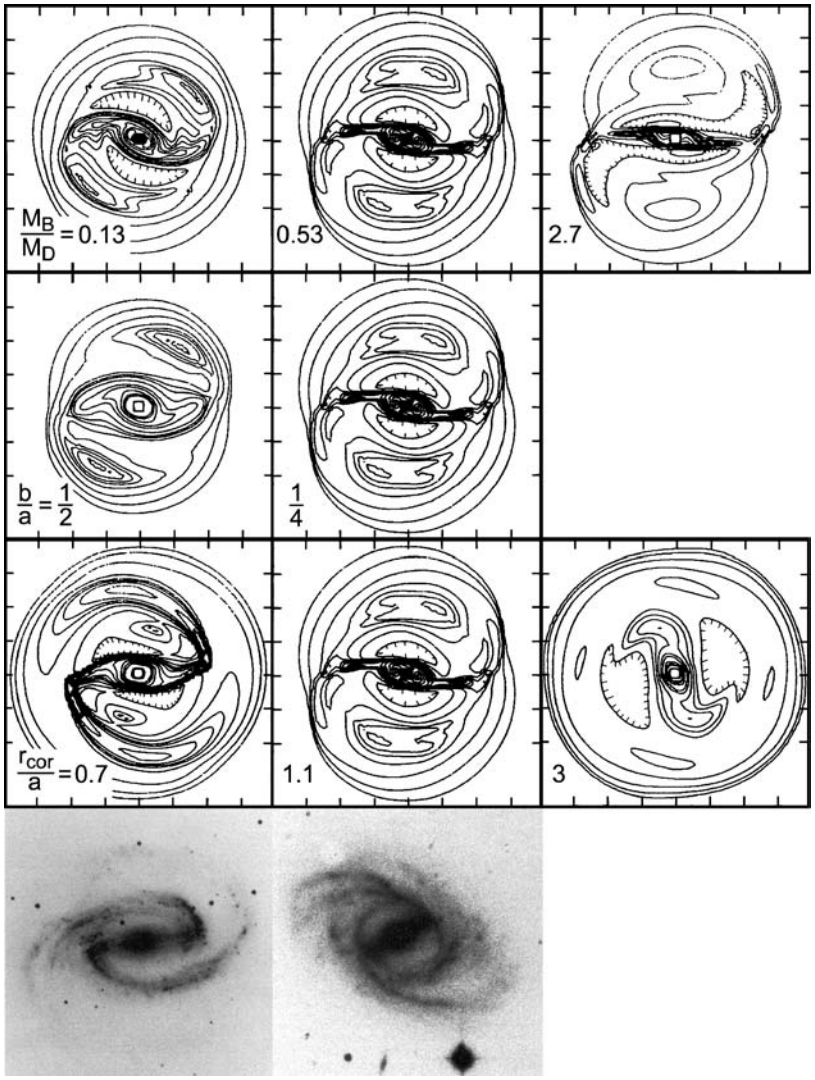

Figure 6 Contours of steady-state gas density in response to a bar (adapted from Sanders & Tubbs 1980, who also show intermediate cases). The bar is horizontal and has a length equal to four axis tick marks. The top row explores the effect of varying the ratio M_B/M_D of bar mass to disk mass. The second row varies the bar's axial ratio b/a. The third row varies the bar pattern speed, parameterized by the ratio $r_{\rm cor}/a$ of the corotation radius to the disk scale length. The middle column is the same standard model in each row; it approximates an SB(r) galaxy such as NGC 2523 (*bottom center*). The left panels resemble SB(s) galaxies such as NGC 1300 (*bottom left*). The right panels carry the parameter sequences to unrealistic extremes; they do not resemble real galaxies.

Combes (1998) suggests that it is negligible compared with gravitational torques, whereas Sellwood & Wilkinson (1993) at least consider the possibility that it is important. Gas infall timescales are very uncertain in early simulations.

Still, the main conclusion reached by Sanders & Tubbs (1980)—that weak, fast bars favor SB(s) structure and that strong, slow bars favor SB(r) structure—has largely been confirmed by higher-quality simulations (e.g., Schwarz 1984, Byrd et al. 1994, Salo et al. 1999). Well-motivated hints of these results came much earlier (Freeman 1970b). Therefore a widespread feeling has developed that we understand the essentials of ring formation.

Nearly radial dust lanes in bars (see Section 2.1 and Figures 3, 6, 7, 8) are a particularly important diagnostic of SB evolution. They are widely believed to be the observational signatures of shocks that drive gas infall. The idea was proposed by Prendergast (1964); other early studies include Sørensen, Matsuda, & Fujimoto (1976); Roberts, Huntley, & van Albada (1979), and, as discussed above, Sanders & Tubbs (1980).

In an important paper, Athanassoula (1992b) explored the response of inviscid gas to a bar using a high-resolution code. Her main focus was gas shocks and their relation to dust lanes. Typical results are shown in Figure 7. If the mass distribution is centrally concentrated enough to result in an ILR, then the dust lanes are offset in the forward (rotation) direction from the ridge line of the bar. Because of the presence of the x_2 orbits—the ones that align perpendicular to the bar inside ILR—the offset is largest near the center (Figure 7). The models reproduce the observation that the dust lanes in many bars curve around the center of the galaxy at small radii and become nearly azimuthal. Athanassoula found that the dust lanes are more curved into an open S shape when the bar is weak; this is confirmed observationally by Knapen, Pérez-Ramírez, & Laine (2002) and is illustrated for NGC 6782 in Figure 8. As Athanassoula notes, "the resemblance between [the models and the observations] is striking."

The important consequence of this work is that shocks inevitably imply that gas flows toward the center. Because the shocks are nearly radial, gas impacts them at a steep angle. Therefore much of the velocity that is lost in the shock is azimuthal. This robs the gas of energy and forces it to fall toward the center.

Athanassoula estimated that azimuthally averaged gas sinking rates are typically 1 km s^{-1} and in extreme cases up to $\sim$6 km s^{-1}. Viscosity is not an issue in her models, so these estimates are more realistic than earlier ones. Because 1 km s^{-1} = 1 kpc $(10^9$ yr$)^{-1}$, the implication is that most gas in the inner part of the disk—depleted by star formation but augmented by mass loss during stellar evolution—finds its way to the vicinity of the center over the course of several billion years, if the bar lives that long.

In recent years, simulations have continued to concentrate on these inner regions of barred galaxies where dust lanes and star formation are most important (Friedli & Benz 1993, 1995; Piner, Stone & Teuben 1995; Englmaier & Gerhard 1997; Salo et al. 1999; Weiner, Sellwood & Williams 2001a; Regan & Teuben 2003). The conclusions are as follows: (*a*) Gas flows toward the center. (*b*) Star formation fed by the inflow is often concentrated in a narrow nuclear ring. (*c*) The inflow is a

result of gravitational torques produced by the bar, but its immediate cause is the shocks. In essence, these are produced because gas accelerates as it approaches and decelerates as it leaves the potential minimum of the bar. So it tends to pile up near the ridge line of the bar. Incoming gas overshoots a little before it plows into the departing gas, so the shocks are nearly radial but offset from the ridge line of the bar in the forward (rotation) direction. The above simulations confirm Athanassoula's conclusion that offsets happen when the central mass concentration is large enough to allow a "sufficient" range of x_2 orbits. The agreement in morphology between the simulated shocks and the observed dust lanes has continued to improve. But there is an even better reason to think that they are connected. Compelling support is provided by the observation of large velocity jumps across the dust lanes (Pence & Blackman 1984; Lindblad, Lindblad & Athanassoula 1996; Regan, Sheth & Vogel 1999; Weiner et al. 2001b; and especially Regan, Vogel & Teuben 1997).

What happens to the infalling gas? Star formation is almost inevitable. The simulations, expectations from the Schmidt (1959) law, observations of young stars in SB nuclei, and star-formation indicators (Section 5) all point to enhanced star formation, often in substantial starbursts near the center. Examples are shown in Figure 8. NGC 4314 is a barred galaxy whose central star formation is also illustrated in the *Hubble Atlas* (Sandage 1961). NGC 1512 is an SB(rs) galaxy whose outer parts are shown in Figure 2. The dust lane in the bar is best seen in the *Carnegie Atlas of Galaxies* (Sandage & Bedke 1994). NGC 6782 contains an oval disk with an embedded bar. Finally, NGC 4736 is a prototypical unbarred oval galaxy. It is included to illustrate the theme of the next section, namely that barred and oval galaxies evolve similarly.

The examples shown in Figure 8 all have star formation concentrated in tiny rings with mean radii $\sim$0.5 kpc (Buta & Crocker 1993). The physics that determines their radii is complicated and not well understood. It is likely that inflow physics and star-formation physics are both involved. In any case, nuclear star formation rings are quite common; the most prominent examples have been known for a long time (Morgan 1958; Burbidge & Burbidge 1960, 1962; Sandage 1961; Sérsic & Pastoriza 1965, 1967). Kennicutt (1994, 1998a) has reviewed the data, contrasting the global star formation in barred galaxies, which is indistinguishable from that in unbarred galaxies, with the nuclear star formation, which is enhanced over that in unbarred galaxies. As is predicted by simulations, there is plenty of fuel—the central concentration of molecular gas is higher in barred than in unbarred galaxies (Sakamoto et al. 1999). Additional examples of nuclear star-formation rings—and multiple discussions of the best cases—can be found in van der Kruit (1976); Rubin, Ford & Peterson (1975); Hummel, van der Hulst & Keel (1987); Gerin, Nakai & Combes (1988); Benedict et al. (1993, 1996, 2002); Buta (1986a,b, 1988, 1995); Pogge (1989); García-Barreto et al. (1991); Devereux, Kenney & Young (1992); Buta & Crocker (1993); Buta & Combes (1996); Maoz et al. (1996); Elmegreen et al. (1997); Colina et al. (1997); Buta & Purcell (1998); Martini & Pogge (1999); Buta et al. (2000); Pérez-Ramírez et al. (2000); Wong & Blitz (2000); Waller et al. (2001); Knapen, Pérez-Ramírez & Laine (2002); Erwin & Sparke (2003); Eskridge et al. (2003); Martini et al. (2003); and Fathi et al. (2003).

Many of the galaxies discussed in the above papers are barred. Those that are classified as transition objects (SAB) or as unbarred (SA), have created some uncertainty about how much the star formation depends on bars. However, many SAB and some SA objects are prototypical oval galaxies such as NGC 2903, NGC 3504, NGC 4736 (Figures 2 and 8), NGC 5248, and NGC 6951 (see Sandage 1961). We show in Section 3.3 that barred and oval galaxies are essentially equivalent as regards gas inflow, star formation, and pseudobulge building. Section 3.4 suggests that similar evolution happens in unbarred spirals that do not have an ILR.

We argue in later sections, as did some of the above authors, that the nuclear star formation is building pseudobulges. Although the star formation is frequently in a ring, it is not likely to form a ring of stars. If the star-forming ring is associated with ILR, then its radius should change as the central concentration of the galaxy evolves. We expect that the ring of star formation burns its way through the pseudobulge as it grows. Also, the spiral dust lanes interior to the star-formation rings (Figure 8) suggest that gas continues to sink inside ILR (Elmegreen et al. 1998). Finally, we choose to illustrate star-forming rings, because they most clearly establish the connection between star formation and bar-driven secular evolution. However, in many galaxies, the star formation is spread throughout the central region. An example is NGC 1365 (Figure 7; Knapen et al. 1995a,b; Sakamoto et al. 1995; Lindblad 1999).

In summary, a comprehensive picture of the secular evolution of barred galaxies has emerged as simulations of gas response to bars have succeeded with increasing sophistication in matching observations of galaxies. Bars rearrange disk gas to make outer rings, inner rings, and central mass concentrations. SB(s) structure is favored if the bar is weak or rotating rapidly; SB(r) structure is favored if the bar is strong or rotating slowly. Because bars grow stronger and slow down as a result of angular momentum transport to the disk, we conclude that SB(r) galaxies are more mature than SB(s) galaxies. Consistent with this, dust lanes diagnostic of gas inflow are seen in SB(s) galaxies but only rarely in SB(r) galaxies. By the time an inner ring is well developed, the gas inside it has been depleted. Embedded in this larger picture is the most robust conclusion of both the modeling and the observations—that a substantial fraction of the disk gas falls down to small galactocentric radii in not more than a few billion years. Star formation is the expected result, and star formation plausibly associated with bars (concentrated near resonance rings) is seen. These results provide part of the motivation for our conclusion that secular evolution builds pseudobulges.

3. THE SECULAR EVOLUTION OF UNBARRED GALAXIES

How general are the results of the previous section? We reviewed the effects of bars on disks as the most clear-cut example of internal secular evolution. However, we do not mean to create the impression that such evolution is important only in the approximately one third of all disk galaxies that look barred at optical wavelengths.

In this section we first review evidence that many apparently unbarred galaxies clearly show bars in the infrared. With the previous section as a guide, we then argue that similar evolution happens in unbarred but oval galaxies and at slower rates in global-pattern spirals. In fact, any nonaxisymmetry in the gravitational potential can rearrange disk gas.

3.1. Many Apparently Unbarred Galaxies Show Bars in the Infrared

Near-infrared images penetrate dust absorption and are insensitive to the low-M/L frosting of young stars in Sb-Sm disks. We then see the underlying old stars that trace the mass distribution. The most important revelation is that bars are hidden in many galaxies that appear unbarred at optical wavelengths (Block & Wainscoat 1991; Mulchaey & Regan 1997; Mulchaey et al. 1997; Seigar & James 1998; Knapen et al. 2000; Eskridge et al. 2000, 2002; Block et al. 2001; Laurikainen & Salo 2002). Approximately two thirds of all spiral galaxies look barred in the infrared. Quantitative measures of bar strengths based on infrared images (Buta & Block 2001; Block et al. 2001; Laurikainen & Salo 2002) will prove useful in gauging the consequences for secular evolution.

Some bars are weak in amplitude. But secular evolution can be more important than this suggests, because many bars are embedded in oval disks (Section 3.2) that contribute at least as much to the nonaxisymmetric potential as do the bars. NGC 1068 is one example (Scoville et al. 1988; Thronson et al. 1989; Pompea & Rieke 1990); for others, see Hackwell & Schweizer (1983); Block et al. (2002); Jarrett et al. (2003). Hidden bars are the first reason why the results of Section 2 are relevant to more than just the galaxies that look barred at optical wavelengths.

3.2. Oval Galaxies

A strong bar has an axial ratio of $\sim$0.2 and a mass of approximately one third of the disk mass. In this section we discuss unbarred but globally oval galaxies in which the whole inner disk has an axial ratio of $\sim$0.85. Ovals are less elongated than bars, but more of the disk mass participates in the nonaxisymmetry. As a result, barred and oval galaxies evolve similarly.

Strongly oval galaxies can be recognized independently by photometric criteria (Kormendy & Norman 1979; Kormendy 1982a) and by kinematic criteria (Bosma 1981a,b). The diagnostics are illustrated in Figure 9.

3.2.1. BRIGHTNESS DISTRIBUTIONS In prototypical ovals, the disk consists of two nested ovals, each with a shallow surface brightness gradient interior to a sharp outer edge. The inner oval is much brighter than the outer one. The two shelves in the brightness distribution have different axial ratios and position angles, so they must be oval if they are coplanar. But the flatness of edge-on galaxies shows that such disks really are oval. Warped disks are common, but they occur at lower surface brightnesses.

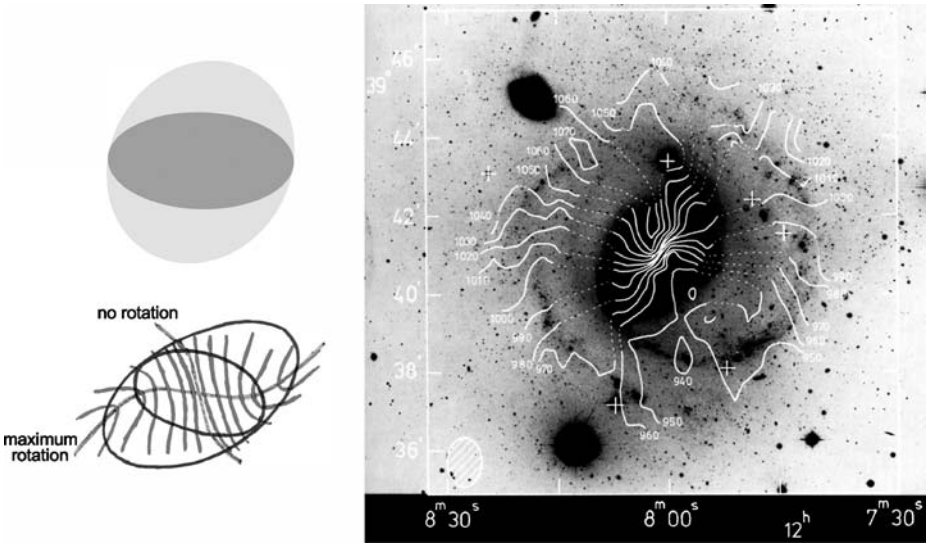

Figure 9 Criteria for recognizing strongly oval but unbarred galaxies shown schematically at left and with observations of NGC 4151 at right. This figure is adapted from Kormendy (1982a). The NGC 4151 HI velocity field is from Bosma, Ekers, & Lequeux (1977a).

Nested ovals in unbarred galaxies are analogous, in barred galaxies, to lenses with embedded bars interior to outer rings. For the purposes of this paper, lenses in early-type galaxies and oval disks in late-type galaxies are functionally equivalent. Both are elliptical shelves in the disk density, and both are nonaxisymmetric enough to drive secular evolution.

Besides NGC 4736 (Figure 2) and NGC 4151 (Figure 9), oval disks illustrated in the *Hubble Atlas* (Sandage 1961) include NGC 4457 (Sa), NGC 3368 (Sa), NGC 4941 (Sa/Sb), NGC 1068 (Sb), NGC 210 (Sb), NGC 4258 (Sb), NGC 5248 (Sc), and NGC 2903 (Sc). Their similarity to barred galaxies can be seen by comparing the two shelves in their brightness distributions with similar ones in NGC 1291 (Figure 2), NGC 3945 and NGC 3081 (Figure 5), and, in the *Hubble Atlas*, NGC 2859 (SB0), NGC 5101 (SB0), NGC 5566 (SBa), NGC 3504 (SBb), and NGC 1097 (SBb).

3.2.2. KINEMATICS Velocity fields in oval disks are symmetric and regular, but (*a*) the kinematic major axis twists with radius, (*b*) the optical and kinematic major axes are different, and (*c*) the kinematic major and minor axes are not perpendicular. Twists in the kinematic principal axes are also seen when disks warp. Warps in HI disks are common, but Bosma (1981a,b) points out that they happen at larger radii and lower surface brightnesses than oval structures, which are obvious in Figures 2 and 9 even at small radii. Also, observations (*b*) and (*c*) imply ovals, not warps.

As pointed out in Kormendy (1982a), the photometric and kinematic criteria for recognizing ovals are in excellent agreement. These strong ovals are expected to evolve similarly to barred galaxies, because the nonaxisymmetry in the potential is similar to that in barred galaxies. In fact, many simulations of the response of gas to bars actually assumed (presumably for computational convenience) that all of the potential is somewhat oval rather than that part of the potential is strongly barred and the rest is not. NGC 4736 is representative of the many unbarred but oval galaxies with strong evidence for secular evolution (see Figure 8 for star formation and Figure 17 for dynamical evidence).

So strongly oval galaxies are readily recognizable. Many are classified SAB; some are SA. However, statistical analyses of large samples of galaxies show that even unbarred disks are slightly oval. The scatter in the Tully-Fisher relation implies that the ellipticity in the potential that controls the disk lies in the range 0–0.06. (Franx & de Zeeuw 1992). The corresponding axial ratio of the density distribution is 0.84–1.0. Analyses of the velocity fields of individual galaxies give similar results (e.g., Andersen et al. 2001). And, in a study of 18 face-on spiral galaxies using K′-band photometry, Rix & Zaritsky (1995) showed that the typical disk has axial ratio 0.91. Not surprisingly, typical disks are more circular than easily recognized ovals. But they are not round. This is plausible, because disks live inside cold dark matter halos that are predicted to be very triaxial (Frenk et al. 1988, Warren et al. 1992, Cole & Lacey 1996). We now need an investigation of how much secular evolution is driven by the above, small nonaxisymmetries.

3.3. The Demise of Bars

Bars destroy themselves if they drive gas inward and build up too large a central mass concentration (Hasan & Norman 1990; Freidli & Pfenniger 1991; Friedli & Benz 1993; Hasan, Pfenniger & Norman 1993; Norman, Sellwood & Hasan 1996; Heller & Shlosman 1996; Berentzen et al. 1998; Sellwood & Moore 1999; Shen & Sellwood 2004). This is another example of an internal secular evolution process. For example, Norman et al. (1996) grew a point mass at the center of an n-body disk that previously had formed a bar. Before they switched on the point mass, they checked that the bar was stable and long-lasting. As they gradually turned on the point mass, the bar amplitude weakened. It weakened more for larger point masses; central masses of 5–7% of the disk mass were enough to dissolve the bar completely. The result was a nearly axisymmetric galaxy.

Why? A heuristic understanding is provided by Section 2.2. Inward gas transport increases the circular-orbit rotation curve and the associated epicyclic frequency $\kappa(r)$ of radial oscillations near the center. As a result, $\Omega - \kappa/2$ increases more rapidly toward small radii. That is, it is less nearly constant. So it is more difficult for self-gravity to persuade x_1 orbits with different radii to precess together at Ω_p and not almost together at $\Omega(r) - \kappa(r)/2$. Furthermore, while $\Omega - \kappa/2$ increases because the central mass concentration increases, the bar slows down because it transfers angular momentum to the outer disk. That is, Ω_p and $\Omega - \kappa/2$ evolve in

opposite directions. This makes it still harder for Ω_p to be approximately equal to $\Omega - \kappa/2$. And as the radius of ILR grows, the radius range of the x_2 orbits that are perpendicular to the bar and that cannot support it also grows. Real bars get nonlinear as their amplitude grows, so the epicyclic approximation on which this discussion is based eventually breaks down.[3] Nevertheless, it provides a plausibility argument for the result found in the simulations, which is that more and more orbits become chaotic and cease to support the bar.

How much central mass is required to destroy the bar differs in different papers. In some simulations, a central mass of 2% of the disk already weakens the bar (Berentzen et al. 1998). Shen & Sellwood (2004) investigated this problem and found that great care is needed to make the time step short enough near the central mass; otherwise, the bar erodes erroneously quickly. They also found that "hard" central masses—ones with small radii, like supermassive black holes—destroy bars more easily than "soft" masses—ones with radii of several hundred parsec, like molecular clouds and pseudobulges. A bar can tolerate a soft central mass of 10% of the disk mass, although its amplitude is reduced by a factor of $\sim$2.

What does a defunct bar look like? Kormendy (1979b, 1981, 1982a) has suggested that some bars evolve into lens components. The suggestion was based partly on the observation (point 7 in Section 2.1) that, when they occur together, the bar almost always fills the lens in its longest dimension. At the time, no reason for such evolution was known. However, the large velocity dispersion observed in the lens of NGC 1553 (Kormendy 1984) is consistent with this idea, as follows. Elmegreen & Elmegreen (1985) found that early-type galaxies tend to have bars with flat brightness profiles, while late-type galaxies tend to have bars with exponential profiles. Therefore azimuthal phase-mixing of an early-type bar would produce a hot disk with a brightness distribution like that of a lens, while azimuthal phase-mixing of a late-type bar would produce a brightness distribution that is indistinguishable from that of a late-type unbarred galaxy. Lenses do occur preferentially in early-type galaxies (Kormendy 1979b). To test whether bars evolve into lenses, we need an n-body simulation in which a bar with a flat profile and a sharp outer edge is destroyed by growing a central mass. The bars in published simulations have steep density profiles.

Therefore secular evolution tends to kill the bar that drives it. The important implication is this: Even if a disk galaxy does not currently have a bar, bar-driven secular evolution may have happened in the past.

3.4. Global Pattern Spirals

Our picture of global spiral structure in galaxies is by now well developed (Toomre 1977b). Global spirals are density waves that propagate through the disk. Like

[3]For example, in Norman et al. (1996), Ω_p increases, late in the simulation, as the internal structure of the dissolving bar changes (Sellwood & Debattista 1996).

water waves in an ocean but unlike bars, they are not always made of the same material. In general, stars and gas revolve around the center faster than the spiral arms, so they catch up to the arms from behind and pass through them. Central to our understanding of why young and bright but short-lived stars are concentrated in the arms is the concept that star formation is triggered when gas passes through the arms. As in the bar case, the gas accelerates as it approaches the arms and decelerates as it leaves them. Again, shocks form where the gas piles up. This time the shocks have a spiral shape. Their observational manifestations are dust lanes located on the concave side of the spiral arms (e.g., NGC 5236 in Figure 7). The strength of the shocks can be predicted from the rotation curve: The mass determines the rotation velocity, and the central concentration determines the arm pitch angle and hence the angle at which the gas enters the arms. The results (Roberts, Roberts & Shu 1975) provide the basis of our understanding of van den Bergh (1960a,b) luminosity classes of galaxies. More massive galaxies tend to have more differential rotation and stronger shocks, so star formation is enhanced and the arms seen in young stars are thinner and more regular.

Gas loses energy at the shocks and sinks toward the center. The effect is weaker than in barred galaxies, because the pitch angles of spiral arms are much less than 90°. The gas meets the shocks obliquely rather than head-on. Nevertheless, it must sink. Where it stalls depends on the mass distribution. In early-type spirals with big classical bulges, the spiral structure has an ILR at a large radius. The spiral arms become azimuthal at ILR and stop there. As the arm pitch angle approaches 0° and as the arm amplitude gets small, the energy loss drops to zero. The gas stalls near ILR. It may form some stars, but the bulge is already large, so the relative contribution of secular evolution is minor.

In contrast, late-type galaxies have no ILR, or the ILR radius is small. The gas reaches small radii and high densities; the result is expected to be star formation. If the process is fast enough, it can build a pseudobulge. Moreover, galaxies with no ILR are late in type. They have little or no classical bulge. Therefore, secular processes can contribute a central mass concentration that we would notice in just those galaxies in which the evolution is most important.

Is the evolution rapid enough to matter? Theoretical timescales are uncertain but look interestingly short. Gnedin, Goodman & Frei (1995) measure spiral arm torques from surface photometry of NGC 4321. They estimate that the timescale for the outward transport of angular momentum is 5–10 Gyr. Thus, even the stellar distribution should have evolved significantly if the spiral structure has consistently been as strong as it is now. NGC 4321 has unusually regular and high-amplitude spiral arms; weak spiral structure can easily imply angular momentum transport timescales that are an order of magnitude longer (Bertin 1983, Carlberg 1987). However, shocks speed up the sinking of gas; Carlberg (1987) estimates that it takes place on a Hubble timescale even for the weak spiral structure in his simulation. Zhang (1996, 1998, 1999, 2003) has derived even shorter timescales. Apart from such disagreements, we do not know how long the spiral structure has been as we observe it, a problem that Gnedin et al. (1995) understood.

Whatever the theoretical uncertainties, observations show that star formation takes place. Timescales are discussed in Section 5. Excellent examples of nuclear star formation in unbarred galaxies can be seen in M51 and NGC 4321 (Kormendy & Cornell 2004 show illustrations). Both galaxies have exceedingly regular global spiral structure. The spiral arms and their dust lanes wind down very close to the center, where both galaxies have bright regions of star formation. NGC 4321 is studied by Arsenault et al. (1988), Knapen et al. (1995a,b), Sakamoto et al. (1995), and García-Burillo et al. (1998). It is classified as Sc in Sandage (1961). In the RC3 (de Vaucouleurs et al. 1991), it is classified as SAB(s)bc; the spiral arms are distorted similar to pseudo-inner and -outer rings. There are signs of a weak bar in the infrared (see the above references and Jarrett et al. 2003). Nevertheless, NGC 4321 suggests that secular evolution can be important even in galaxies that do not show prominent bars at optical wavelengths.

Why doesn't every late-type galaxy have a pseudobulge? Calculations of spiral-arm shock strengths show that the shocks are weak if the rotation curve rises too linearly. The lowest-luminosity galaxies have little shear; it is not surprising that they do not make substantial pseudobulges.

In summary, late-type unbarred but global-pattern spirals are likely to evolve in substantially the same way as barred galaxies, only more slowly.

3.5. Conclusion

Barred galaxies give us a rich picture of secular evolution at work. One robust consequence is the buildup of the central mass concentration via the inward radial transport of gas. Infrared imaging shows that the majority of spiral galaxies have bars. Theoretical arguments and observational evidence suggest that similar processes are at work in many unbarred galaxies, especially in oval galaxies and in late-type, global-pattern spirals. In late-type galaxies, it is relatively easy for the central mass concentration that we see to be caused by secular processes, because the evolution happens most readily if a galaxy does not already have a classical bulge.

4. THE OBSERVED PROPERTIES OF PSEUDOBULGES

The suggestion that some bulge-like components were built by the secular processes discussed in Sections 2 and 3 was first made by Kormendy (1982a,b). A decade later, both the evidence for evolution and the case that it can construct what we now call pseudobulges had grown substantially (Kormendy 1993). Now, after another decade, it is a struggle to review the wealth of new evidence in a single *Annual Review of Astronomy and Astrophysics* article.

Other early papers that focused on the building of pseudobulges by bars include Combes & Sanders (1981) and Pfenniger & Norman (1990). Two processes were discussed. One is the inward transport of gas by bars and ovals. The other involves dissipationless processes that can produce vertically thickened central components when bars suffer buckling instabilities and when disk stars scatter off of bars and

are heated in the axial direction. Both processes can happen in the same galaxy and both make bulge-like components out of disk material. Therefore, we refer to the products of both processes as pseudobulges. In this section, we discuss the observed properties of pseudobulges. As discussed in Section 1.1, we need the context of the above formation mechanisms to make sense of the wealth (or plague) of detail in galactic centers.

How can we tell whether a (pseudo)bulge is like an elliptical or whether it formed secularly? The answer—and the theme of this section—is that pseudobulges retain enough memory of their disky origin so that the best examples are easily recognizable. Before *HST*, the cleanest evidence was dynamical (Kormendy 1993). Pseudobulges are more dominated by rotation and less dominated by random motions than are classical bulges and ellipticals. This evidence remains compelling (Sections 4.6 and 4.7). However, as a result of spectacular progress from *HST* imaging surveys, morphology and surface photometry now provide the best evidence for disk-like bulges. We begin with these surveys.

4.1. Embedded Disks, Spiral Structure, and Star Formation

Central to our image of bulges as elliptical galaxies living in the middle of a disk is their morphological resemblance to ellipticals. Central to our growing awareness that something different is going on in late-type galaxies is the observation that their high-surface-brightness centers look nothing like ellipticals. Instead, they are dominated by young stars and disk structure. This is especially true in barred and oval galaxies, that is, in the objects in which secular evolution should be most rapid.

What are we looking for?

A clear statement that classical bulges are equivalent to ellipticals is provided by Sandage & Bedke (1994) in their description of E/S0 galaxies: "On short-exposure plates showing only the central regions, no evidence of a disk . . . is seen; the morphologies of the central regions are pure E." The section on elliptical galaxies contains this caution: "The presence or absence of dust is not used as a classification criterion. Some E galaxies . . . have dust patches and remain classified as E types." The same is true for bulges; e.g., S0 galaxies range from dustless ($S0_1$) to dusty ($S0_3$), but all have bulges. We need to be careful that what we identify as pseudobulges are not just dust features or the outer disk extending inside a classical bulge all the way to the center. On the other hand, part of the definition of an elliptical, hence also of a bulge, is that "There is no recent star formation, inferred from the absence of luminous blue and red supergiants." Even of Sab galaxies, Sandage & Bedke (1994) say that "the central bulge is . . . nearly always devoid of recently formed stars." Of course, old bulges must have contained young stars in the past; these definitions—and the Hubble sequence—are understood to apply to present-day galaxies and long after major mergers are completed. But ubiquitous ongoing star formation is a pseudobulge signature.

Turning to pseudobulges, Kormendy (1993) noted that the prototypical oval galaxy NGC 4736 has a disk-like bulge: "The central brightness profile . . . is an $r^{1/4}$ law that reaches the high central surface brightness characteristic of a

bulge (Boroson 1981). However, the $r^{1/4}$-law component shows a nuclear bar and spiral structure to within a few arcsec of the center. Bars are disk phenomena. More importantly, it is not possible to make spiral structure in a bulge. Thus the morphology already shows that the $r^{1/4}$-law profile belongs to the disk." This conclusion is consistent with dynamical evidence shown in Figure 17 and with the nuclear star-formation ring shown in Figure 8.

Sandage (1961) commented similarly and presciently about flocculent spirals, including NGC 4736, in his description of NGC 5055: "The curious and significant feature of [these galaxies] is the sharp discontinuity of surface brightness of the spiral pattern between the inner and the outer regions [close to the center]. The spiral structure is as pronounced and well defined in the bright region as in the outer parts. The important point here is that, if the inner arms were to coalesce and to lose their identity as spiral arms, the region would look amorphous, would have a high surface brightness, and would resemble the central regions of NGC 2841 [a classical bulge] . . . and all members of the E and S0 classes." The observation that the spiral structure is as pronounced in the bright region as in the outer parts has important implications. If a high-surface-brightness classical bulge were projected in front of the (relatively faint) inward extrapolation of the outer disk, it would dilute the spiral structure. This is not seen. Therefore it is the high-surface-brightness component that contains the spiral structure. Again, this is a pseudobulge signature.

HST spatial resolution reveals disk structure in the bulge-like central regions of surprisingly many galaxies. Carollo and collaborators carried out a snapshot survey of 75 S0–Sc galaxies with WFPC2 and the F606W filter approximating *V* band (Carollo et al. 1997, 1998; Carollo & Stiavelli 1998; Carollo 1999) and of 78 galaxies with NICMOS F160W approximating *H* band (Carollo et al. 2001, 2002; Seigar et al. 2002). Figures 10–13 show pseudobulges from these papers. What is remarkable about these generally Sb and Sbc galaxies is how often the central structure looks like a smaller version of a normal, late-type disk.

NGC 1353 (Figure 10) is one of the clearest examples. The top-right panel shows the central $18'' \times 18''$ of the PC image (Carollo et al. 1997, 1998). The middle panel is the full WFPC2 field of view, and the bottom image is a *JHK*-band composite from the 2MASS survey (Jarrett et al. 2003). The images show, as Carollo and collaborators concluded, that the central structure in NGC 1353 is a disk with similar flattening and orientation as the outer disk. To make this quantitative, we measured the surface brightness, ellipticity, and position angle profiles in the PC and 2MASS images using the `PROFILE` tool in the image processing system VISTA (Lauer 1985). The left panels show that the apparent flattening at $2'' \lesssim r \lesssim 4''$ is the same as that of the main disk at large radii. The position angle is the same, too. So the part of the galaxy shown in the top-right panel really is a disk. The brightness profile shows that this nuclear disk is responsible for much of the central rise in surface brightness above the inward extrapolation of an exponential fitted to the outer disk. Presented only with the brightness profile or with the bottom two panels of images, we would identify the central rise in surface brightness as a bulge. Given Figure 10, we identify it as a pseudobulge.

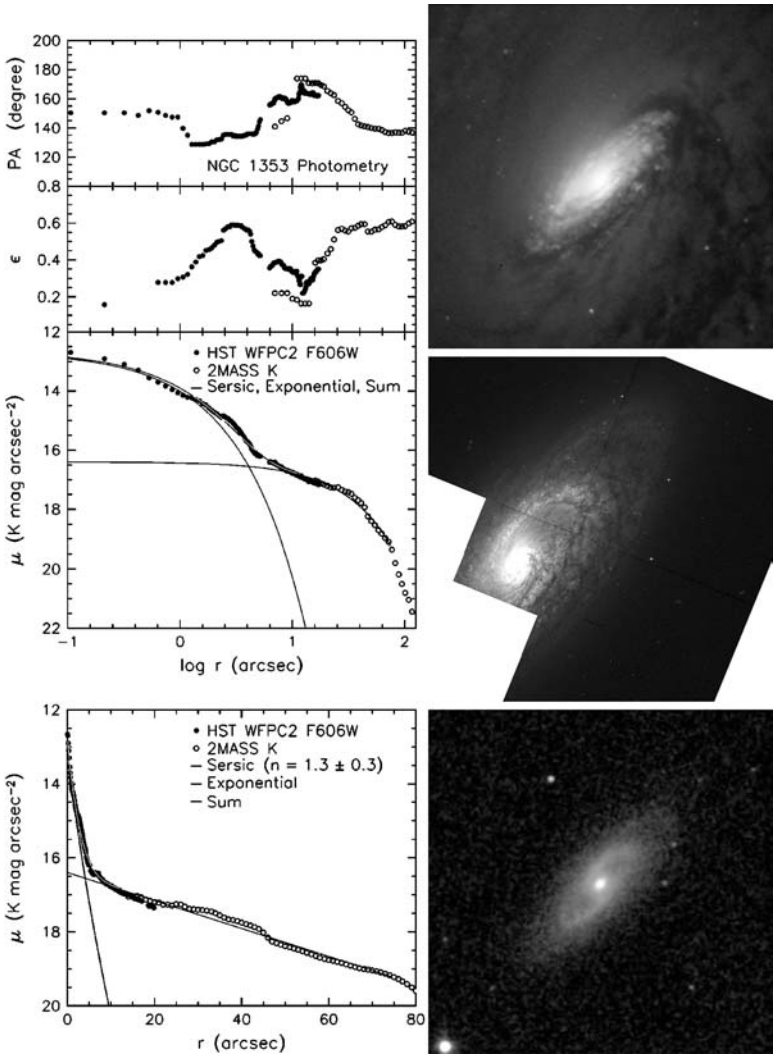

Figure 10 NGC 1353 pseudobulge. Top image: $18'' \times 18''$ zoom; middle: full WFPC2 F606W image taken with *HST* by Carollo et al. (1998). The bottom panel is a 2MASS (Jarrett et al. 2003) $J\,H\,K$ composite image with a field of view of $4'.4 \times 4'.4$. The plots show surface photometry with the *HST* profile shifted to the K-band zeropoint. The lines show a decomposition of the major-axis profile into a Sérsic (1968) function and an exponential disk. The outer part of the pseudobulge has the same apparent flattening as the disk. This nuclear disk produces much of the rapid upturn in surface brightness toward the center.

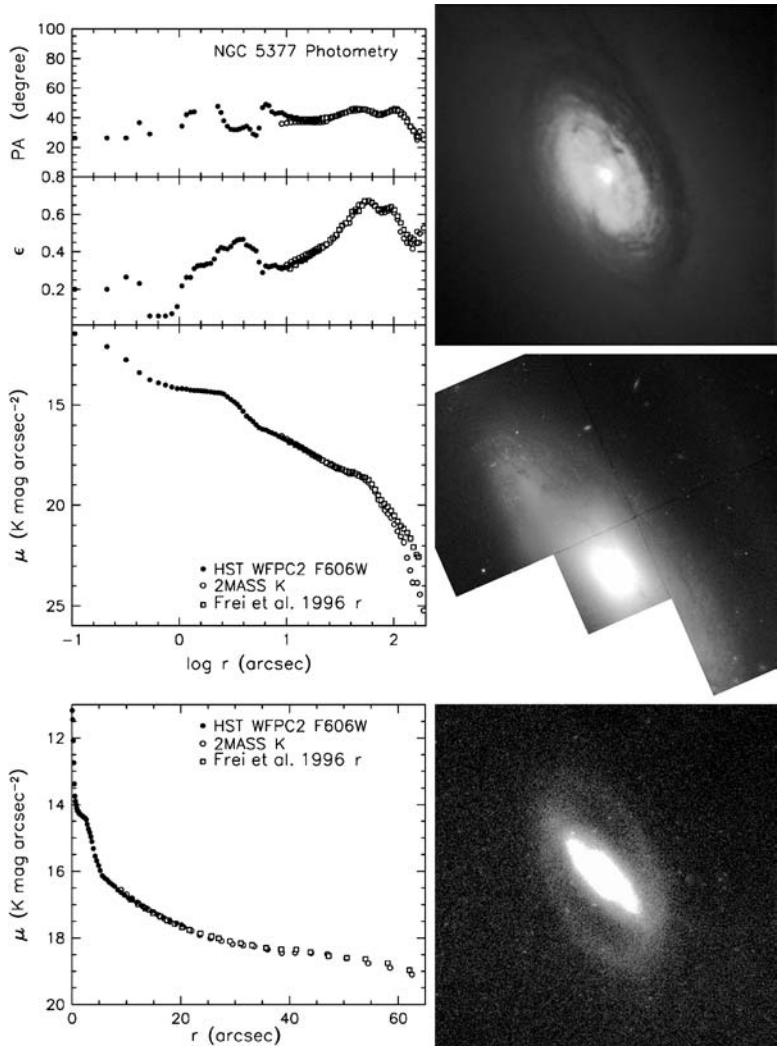

Figure 11 NGC 5377 pseudobulge. Top image: $18'' \times 18''$ zoom; middle: full WFPC2 F606W image taken with *HST* by Carollo et al. (1998). At the bottom is a $7' \times 7'$, r-band image of the outer ring (Frei et al. 1996). The plots show surface photometry of the *HST*, r-band, and 2MASS $J\,H\,K$ composite images, all shifted to the 2MASS, K-band zeropoint. The two shelves in the brightness profile are the nuclear disk and inner oval. The nuclear disk has the same apparent flattening and orientation as the outer ring. It may be embedded in a less obviously disky bulge, but it produces a rapid upturn in surface brightness toward the center.

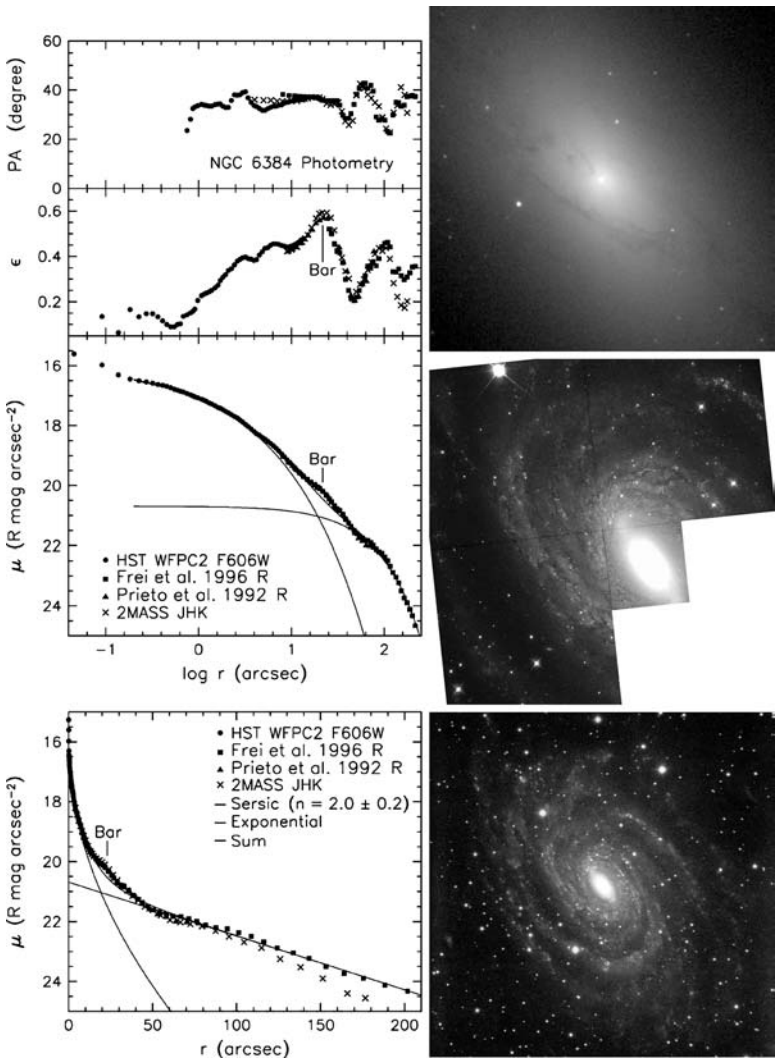

Figure 12 NGC 6384 pseudobulge. Top image: $18'' \times 18''$ zoom; middle: full WFPC2 F606W image taken with *HST* by Carollo et al. (1998). At the bottom is the *B*-band image from the *Carnegie Atlas of Galaxies* (Sandage & Bedke 1994). The top, middle, and bottom panels are shown with logarithmic, square root, and linear stretches. The plots show surface photometry of the *HST* and other images identified in the key, all shifted to the *R*-band zeropoint. The decomposition into a Sérsic function bulge and exponential disk is done over a radius range that omits the region $12'' < r < 40''$ affected by the bar.

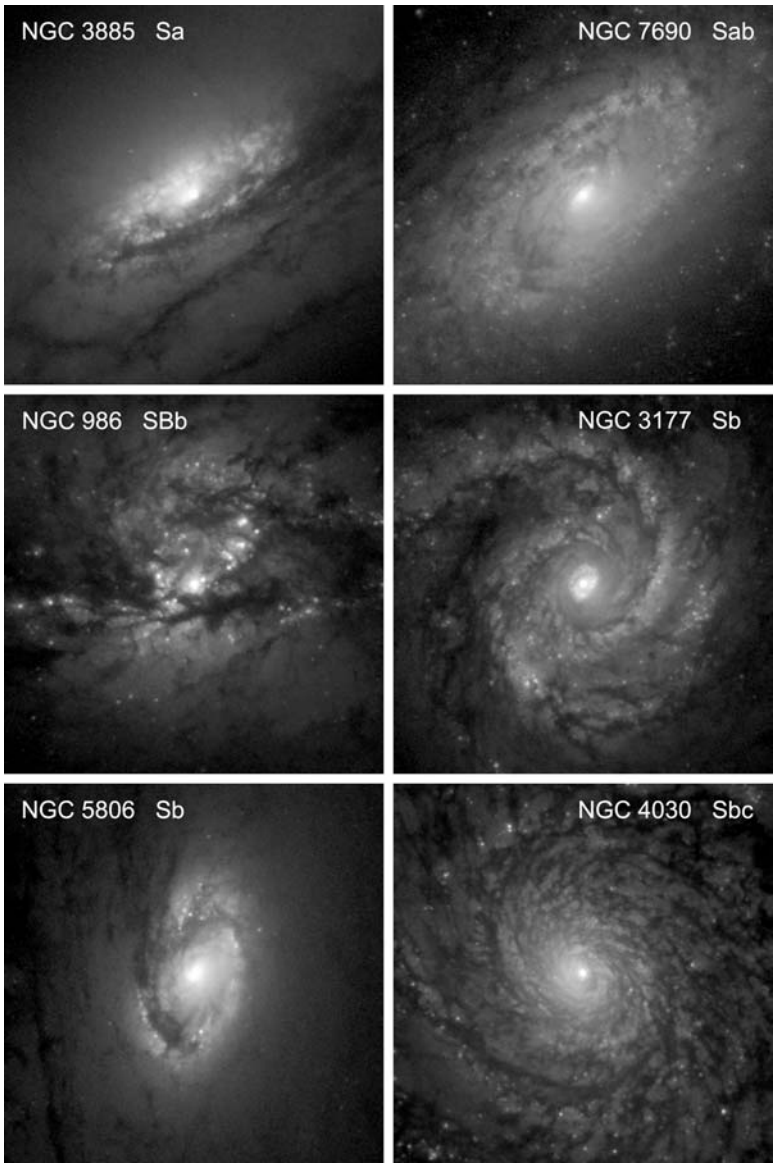

Figure 13 Sa–Sbc galaxies whose "bulges" have disk-like properties. Each panel shows an $18'' \times 18''$ region centered on the galaxy nucleus and extracted from *HST* WFPC2 F606W images taken and kindly provided by Carollo et al. (1998). North is up and east is at left. Displayed intensity is proportional to the logarithm of the galaxy surface brightness. Hubble types are from Sandage & Bedke (1994), except for NGC 4030; its type is from the RC3 and was checked using high-quality images posted on NED.

We have decomposed the major-axis profile into an exponential outer disk plus a Sérsic (1968) function, $I(r) \propto e^{-K[(r/r_e)^{1/n}-1]}$. Here $n = 1$ for an exponential, $n = 4$ for a de Vaucouleurs (1948) $r^{1/4}$ law, and $K(n)$ is chosen so that radius r_e contains half of the light in the Sérsic component. In Section 4.2, we discuss evidence that (pseudo)bulges in late-type galaxies are generally best described by Sérsic functions with $n \sim 1$. That is, they are nearly exponential. This behavior is characteristic of many pseudobulges. Here we note that NGC 1353 is an example. The best fit gives $n = 1.3 \pm 0.3$.

The 2MASS image and the ϵ and PA profiles show that NGC 1353 contains a weak bar with a projected radius of $\sim 15''$ and an approximately NS orientation. This is one example among many of the association between pseudobulges and nonaxisymmetric features that can drive secular evolution. In visible light, the galaxy is classified SBb by de Vaucouleurs et al. (1991) and Sbc by Sandage & Bedke (1994).

Figure 11 shows another example. NGC 5377 is classified SBa or Sa by Sandage and (R)SBa by de Vaucouleurs, and it easily satisfies the photometric criteria for recognizing an oval outer disk. It is one of the earliest-type galaxies discussed in this paper. An Sa should be dominated by a bulge. Indeed, the brightness profile at $r \lesssim 1''$ and at about $6''$ to $10''$ is bulge-like. But the galaxy also contains a high-surface-brightness embedded nuclear disk that is seen as the shelf in the brightness profile at $r \simeq 1''$ to $3''$. Again, this has approximately the same apparent flattening and position angle as the outer disk. If a bulge is defined to be the extra light at small radii above the inward extrapolation of the outer disk profile, then that definition clearly includes the nuclear disk. We prefer not to adopt this definition but rather to identify NGC 5377 as a galaxy with a substantial pseudobulge component. Whether this is embedded in a classical bulge or whether the whole of the central rise in surface brightness is a pseudobulge, we cannot determine from the available data.

Figure 12 shows a third case study, NGC 6384. Its bar is subtle; the galaxy is classified Sb by Sandage and SABbc by de Vaucouleurs. But the bar is clearly visible in the WFPC2 image (middle panel). Sandage & Bedke (1994) note that, "There is a smooth inner bulge . . .". The Carollo et al. (1998) image (top panel in Figure 12) confirms that the central brightness distribution is smooth enough—ignoring dust—that one would ordinarily identify this as a classical bulge. However, photometry of the PC image shows that the PA and apparent flattening are essentially the same at $2'' \lesssim r \lesssim 12''$ as in the outer disk. So the central component is quite flat. Also, it is quite different from a de Vaucouleurs $r^{1/4}$ law. Carollo et al. (1998) concluded that it is exponential. We get $n = 2.2 \pm 0.2$, but this does not take into account the light in the bar. If bar stars that pass through the outer bulge were subtracted from the profile, then n would get smaller. So the flatness of the central component is enough to identify this as a pseudobulge, and its small value of n contributes to the identification of exponential profiles as a pseudobulge characteristic (Section 4.2). NGC 6384 demonstrates that pseudobulges can be subtle enough so that photometry, and not just morphology, is needed to recognize them.

Further examples from Carollo et al. (1997, 1998) of disky centers in Sa–Sbc galaxies are shown in Figure 13. They look like miniature late-type galaxies.

But they occur where the surface brightness rises rapidly above the inward extrapolation of the outer disk profile. This is not obvious in Figure 13 because we use a logarithmic intensity stretch so that we can show the structure over a large range in surface brightness. Spiral structure is a sure sign of a disk. Carollo et al. (1997) conclude that these observations "support scenarios in which a fraction of bulges forms relatively late, in dissipative accretion events driven by the disk."

The statistics of the Carollo sample suggest that pseudobulges are surprisingly common. In the following summary, we distinguish classical bulges that are well described by $r^{1/4}$ laws from pseudobulges that show at least one of the following characteristics: they are flat or are dominated by disk morphology such as spiral structure; they are vigorously forming stars; or they have surface brightness profiles that are best described by Sérsic functions with $n \lesssim 2$. In a few cases, observing $n \simeq 1$ caused us to reclassify a "regular bulge" in Carollo et al. (1997, 1998) as a pseudobulge. Also, we use the mean of the classifications given in the RC3 and in the UGC/ESO-LV (Nilson 1973, Lauberts & Valentijn 1989). Then in the above sample of 75 galaxies, classical bulges are seen in 69% of 13 S0–Sa galaxies, 50% of 10 Sab galaxies, 22% of 23 Sb galaxies, 11% of 19 Sbc galaxies, and 0% of 10 Sc and later-type galaxies. Most of the rest are pseudobulges or have a substantial pseudobulge component added to a classical bulge. In some cases, there is only a compact nuclear star cluster added to a late-type disk; it is not clear whether the same secular evolution processes make these (see Section 4.9). Distinguishing classical bulges from pseudobulges is still an uncertain process. Even the morphological types are sometimes inconsistent between the RC3 and the UGC by several Hubble stages. However, it is unlikely that the conclusions implied by the above statistics are seriously wrong. As noted by Carollo et al. (1997, 1998), most early-type galaxies appear to contain classical bulges; these become uncommon at types Sb and later, and essentially no Sc or later-type galaxy has a classical bulge. Kormendy (1993) reached similar conclusions.

So an *HST* *V*-band survey shows that disky bulges are more common than ground-based data suggested. Clearly it is desirable to check this result. An *H*-band *HST* NICMOS survey by Carollo et al. (2002) and by Seigar et al. (2002) complements the *V*-band survey in several ways. The images are less affected by dust. Classification of nuclear disks is easier. The infrared images are less sensitive to star formation, but Carollo et al. (2002) compensate by including $V - K$ color images. The infrared survey confirms the *V*-band results. Additional imaging studies that reveal central disk structures, dust, or star formation in disk galaxies include van den Bosch, Jaffe & van der Marel (1998); Peletier et al. (1999); Erwin & Sparke (1999, 2002, 2003); Hughes et al. (2003); Martini et al. (2003); Fathi & Peletier (2003), Erwin et al. 2003, and Erwin (2004).

We do not mean to imply that a bulge is always either purely classical or purely pseudo. We cannot tell from available data how much of a classical bulge underlies the pseudobulge component in S0–Sbc galaxies. Indications (e.g., Figure 11) are that the classical bulge component in many early-type galaxies is significant

even when an embedded disky structure is recognized. If our formation picture is correct, then there is every reason to expect that secular evolution often adds disky material to a classical bulge that formed in a prior merger. The relative importance of mergers and secular evolution needs further investigation.

At a more subtle level, some galaxies that are dominated by classical bulges contain nuclear disks that contribute a negligible fraction of the galaxy luminosity. These may be cases in which secular evolution produced only a trace effect. Alternatively, they may be later-type examples of the embedded disks seen in elliptical galaxies. If so, they cannot be a result of disk-driven secular evolution. They are discussed in Section 8.3.

4.2. Exponential Bulges

The pseudobulge galaxies NGC 1353 and NGC 6384 (Figures 10 and 12) have nearly exponential bulge profiles. Andredakis & Sanders (1994) discovered that this is a general phenomenon: The bulges of late-type galaxies are better described by exponentials than by $r^{1/4}$-law surface brightness profiles. Andredakis, Peletier & Balcells (1995) generalized this result and showed that the index n of a Sérsic (1968) function fitted to the central profile varies from $n \simeq 3.7$ (standard deviation = 1.3) in S0 and S0/a bulges to $n \simeq 2.4$ (standard deviation = 0.66) in Sa–Sb galaxies to $n \simeq 1.6$ (standard deviation = 0.52) in Sbc–Sd galaxies. "For Sc and later, the profiles are very close to pure exponentials." An example of an Sbc with an exponential bulge is our Galaxy (Kent, Dame & Fazio 1991). The above trend parallels the trend that pseudobulges get more common in later-type galaxies. Evidently small n values are pseudobulge signatures.

The time was right for Sérsic functions to become the canonical fitting function for bulges and ellipticals. Caon, Capaccioli & D'Onofrio (1993) had recently demonstrated that Sérsic functions fit ellipticals and bulges better than do $r^{1/4}$ laws. They note that this is not a surprise, because $r^{1/n}$ profiles have three parameters, while $r^{1/4}$ laws have only two. The argument that n has physical meaning is the observation that it correlates with the effective radius r_e and total absolute magnitude $M_{B,\mathrm{bulge}}$ of the elliptical or bulge. This was confirmed by D'Onofrio, Capaccioli & Caon (1994); Graham et al. (1996); Binggeli & Jerjen (1998); Graham (2001); Trujillo et al. (2002) and numerous subsequent papers.

The idea that late-type (pseudo)bulges have $n \simeq 1$ to 2 immediately gained acceptance and got simplified in many people's minds (and in our title) to the notion that they are exponential. One reason was that confirmation followed quickly. Courteau, de Jong & Broeils (1996) carried out bulge-disk decompositions for 243 galaxies from Courteau (1996a) and 86 galaxies from de Jong & van der Kruit (1994) and from de Jong (1996a,b). For the Courteau sample, they conclude that "about 85% of [the] Sb's and Sc's are best fitted by the double exponential, while the remainder [are] better fitted with an $r^{1/4}$ bulge profile." For the de Jong sample, they conclude that 60% of the galaxies are best modeled by a double exponential, ∼25% (mostly Sa's and Sb's) are best modeled with $n = 2$ and only ∼15% are

best fitted by an $r^{1/4}$ law. These results are broadly consistent with the statistics in Section 4.1, which refer to a different galaxy sample and which are partly based on morphology and partly on Sérsic function indices.

As a diagnostic of formation processes, Courteau et al. (1996) went on to examine the ratio h_b/h_d of the scale lengths of the inner and outer exponentials. For the combined sample, they found that $h_b/h_d = 0.08 \pm 0.05$, and for the de Jong sample, they found that $h_b/h_d = 0.09 \pm 0.04$. From this, they concluded, "Our measurements of exponential stellar density profiles [in bulges] as well as a restricted range of [bulge-to-disk] scale lengths provide strong observational support for secular evolution models. Self-consistent numerical simulations of disk galaxies evolve toward a double exponential profile with a typical ratio between bulge and disk scale lengths near 0.1 (D. Friedli, private communication) in excellent agreement with our measured values" (see Courteau et al. 1996 for details). MacArthur, Courteau & Holtzman (2003) found that $h_b/h_d = 0.13 \pm 0.06$ for late-type spirals and again noted the connection with secular evolution. We can add one more connection. The above ratios of h_b/h_d, together with the observation that bars are typically about 1 scale length h_d long (e.g., Kormendy 1979b), imply that the scale length of the inner exponential is similar to the radius of star-forming rings (Figure 8) discussed in Section 2.3. We suggested there that these rings are building pseudobulges.

There is a caveat: An examination of the above papers shows that many bulges in late-type galaxies rise above the disk profile by only small amounts. Leverage is limited. Even the conclusion that some bulges are exponential can be uncertain.

HST confirmation of the above results has therefore been very welcome (e.g., Phillips et al. 1996, Balcells et al. 2003, Fathi & Peletier 2003). Carollo et al. (2002) provide the best statistics. Their table 1 classifies central components as "$r^{1/4}$-law," "exponential," or "not fitted" based on the *V*-band images. Galaxies were "not fitted" when the brightness distribution was badly affected by dust, young stars, or patchiness. One galaxy, NGC 2344, is classified as an Sc by the RC3 but has an $r^{1/4}$-law bulge. Images posted on the NASA/IPAC Extragalactic Database (NED) make it clear that this galaxy is not an Sc. We adopt the UGC classification, which is Sb. With this correction, the *V*-band statistics are as follows: $r^{1/4}$-law bulges, exponential pseudobulges, and galaxies not fitted account for the following percentages of the Hubble types indicated. S0 + Sa: 50%, 10%, 40%; Sab: 60%, 0%, 40%; Sb: 17%, 11%, 72%; Sbc: 0%, 28%, 72%; Sc: 0%, 60%, 40%; and Scd to Sm: 0%, 50%, 50% of the galaxies. When we classify the 45 galaxies that were not fitted in *V*-band using the *H*-band images and $V - H$ images, we get 11 classical bulges and 34 pseudobulges. In most cases the classification is clear-cut; when it is not, we try to err equally often in favor of classical bulges and pseudobulges. The statistics on classical and pseudobulges then become as follows: S0 + Sa: 50%, 50%; Sab: 60%, 40%; Sb: 44%, 56%; Sbc: 6%; 94%; and Sc to Sm: 0%, 100%. The $V + H$-band results are in satisfactory agreement with the optical results. The majority of early-type galaxies have classical bulges; there is a sharp transition at Hubble type Sb, and later-type galaxies mostly contain pseudobulges.

Balcells (2001) reviewed implications. Andredakis (1998) commented that "The exponential bulges ... remain essentially unexplained; [the results] suggest that they ... were probably formed, at least in part, by different processes from those of early-type spirals." Even though we do not understand quantitatively how inner exponentials are built, their close association with other disky bulge phenomena supports our tentative conclusion and that of many other authors that Sérsic indices $n \sim 1$ are a signature of secular formation.

4.3. Some Bulges Are As Flat As Disks

In Section 4.1, we repeatedly noted that pseudobulge examples were very flat, based on observed axial ratios or spiral structure. Secular formation out of disks does not require them all to be flat (Section 7.1), but it appears that we are fortunate and that many are flat.

This is seen in the distribution of observed bulge ellipticities derived by Kent (1985, 1987a, 1988). He decomposed major- and minor-axis profiles of disk galaxies into $r^{1/4}$-law bulges and exponential disks. The bulge and disk ellipticities were fit parameters that were allowed to be different. Figure 8 in Kormendy (1993) shows the following:

1. A majority of bulges appear rounder than their associated disks. These include the well-known classical bulges in M31, M81, NGC 2841, NGC 3115, and NGC 4594 (the Sombrero galaxy).
2. Some bulges have apparent flattenings that are similar to those of their associated disks, as Kent noted.
3. Some bulges appear more flattened than their associated disks; these may be nuclear bars (Section 4.4).
4. The median ratio of bulge to disk ellipticity, $\epsilon_{\rm bulge}/\epsilon_{\rm disk}$, is smallest for Sas and increases toward later Hubble types. This agrees with other evidence that pseudobulges are more common in later-type galaxies.
5. However, the median $\epsilon_{\rm bulge}/\epsilon_{\rm disk}$ for S0 galaxies is similar to that for Scs, not Sas. Kinematically disklike bulges also are more common in S0s than in Sas (Sections 4.6 and 4.7). Similar effects led van den Bergh (1976b) to develop his parallel sequence classification.

Bulge-disk decompositions should be interpreted with caution. The bulge and disk parameters are strongly coupled. Even when the bulge ellipticity is a fit parameter, it is assumed to be constant with radius; this is necessary for computational stability. But Figures 10 to 12 and other data show that this is a serious oversimplification. Also, most decompositions in the literature are not suitable. Some have too little leverage on the bulge. Nonparametric decompositions depend on the assumption that the bulge and disk have different flattenings; they force the bulge to be rounder than the disk. So we have few checks of the above results. Those that are available are consistent with points 1 to 5 but show a large dispersion in numbers. Here are two examples:

Fathi & Peletier (2003) carried out bulge-disk decompositions for 35 S0–Sb and 35 Sbc–Sm galaxies based on *HST* NICMOS *H*-band images. The high spatial resolution provides good leverage on small bulges. The results show that $\epsilon_{\rm bulge}/\epsilon_{\rm disk} > 0.9$ in 36% of S0–Sb galaxies and 51% of Sbc–Sm galaxies. This is consistent with Kent's decompositions and confirms that flat pseudobulges are more common in late-type galaxies.

In contrast, Möllenhoff & Heidt (2001) found that only 10% of their decompositions imply $\epsilon_{\rm bulge}/\epsilon_{\rm disk} > 0.9$. These are *K*-band measurements of a sample of S0–Sc galaxies weighted toward late Hubble types. The galaxies are relatively face-on; this reduces sensitivity to the flattening. However, the above results refer to the 39 galaxies that meet the selection criterion used for points 1 to 5, $\epsilon_{\rm disk} < 0.14$. So different authors get substantially different distributions of bulge flattening. Nevertheless, Figures 10–12 clearly show that some pseudobulges are as flat as disks.

4.4. Bars Within Bars

Figure 14 shows galaxies that have a secondary bar interior to the main bar. The inner bar is the component that conventionally would be identified as a bulge—its surface brightness increases rapidly toward the center, far above the inward extrapolation of the disk brightness profile. However, bars are disk phenomena. Seeing a nuclear bar is strong evidence that a galactic center is dominated by a pseudobulge.

The nuclear bar in NGC 1291 was seen as long ago as Evans (1951). de Vaucouleurs (1975) saw nuclear bars in four of the six galaxies illustrated in Figure 14: NGC 1291, NGC 1433 (see also Sandage & Brucato 1979), NGC 1543 (see de Vaucouleurs 1959), and NGC 3081.

Other early examples are NGC 1326 (de Vaucouleurs 1974), NGC 2859, NGC 3945, NGC 7743 (Kormendy 1979b), NGC 1543 (Sandage & Brucato 1979), NGC 1317 (Schweizer 1980), and NGC 2950 (Kormendy 1981, 1982a,b). Kormendy concluded that "*triaxial SB bulges and bars rotate rapidly and are therefore dynamically similar. Both are different from elliptical galaxies, which rotate slowly*" [emphasis in original]. We return to these points in Section 4.6.

The number of known examples grew rapidly as work on barred galaxies accelerated (Jarvis et al. 1988; Buta 1990; Buta & Crocker 1993; Shaw et al. 1993b, 1995; Wozniak et al. 1995; Friedli et al. 1996; Jungwiert, Combes & Axon 1997; Mulchaey et al. 1997; Erwin & Sparke 1999, 2003; Márquez et al. 1999; Martini & Pogge 1999; Greusard et al. 2000; Rest et al. 2001). Erwin (2004) has compiled a catalog, and Friedli (1996) and Erwin (2004) provide reviews.

Recent studies focus on larger and more representative samples and therefore yield better estimates of what fraction of SB galaxies contain nuclear bars. Erwin & Sparke (2002) found nuclear bars in $26 \pm 7\%$ of their sample of 38 SB galaxies. They remarked that the true fraction could be as large as 40%; they could not detect nuclear bars in the (many) objects that have central dust. As in the previous section,

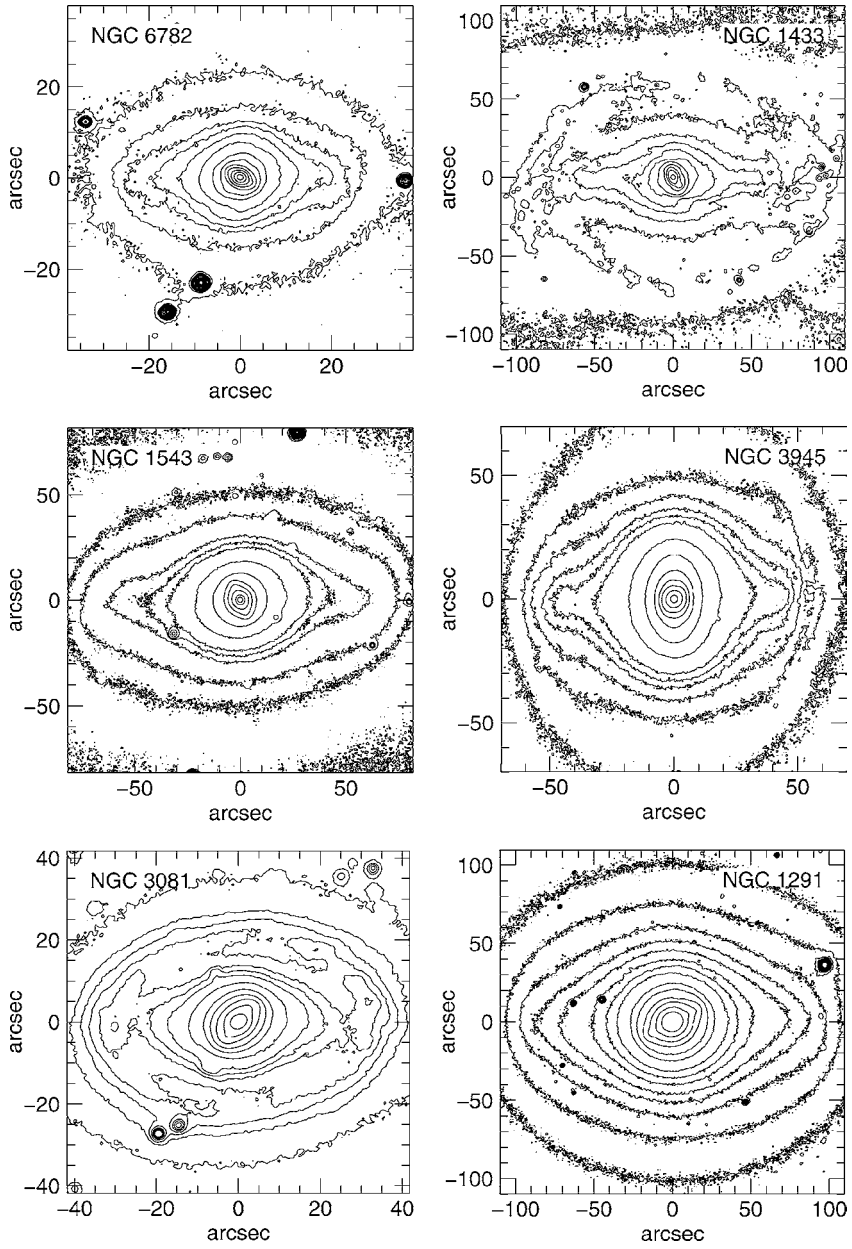

Figure 14 Bars within bars. Each galaxy image is rotated so that the main bar is horizontal. Contour levels are close together at large radii and widely spaced in the nuclear bars. NGC 3081 and NGC 1433 have inner rings. NGC 1291 is also shown in Figure 2, NGC 3081 and NGC 3945 in Figure 5, and NGC 6782 in Figure 8. The images are courtesy of Ron Buta.

pseudobulge features are surprisingly common. The galaxies in the above survey are S0–Sa; these are the Hubble types that are most likely to contain classical bulges.

Laine et al. (2002) analyzed *HST* NICMOS *H*-band images of a matched sample of Seyfert and non-Seyfert galaxies. The sample is slightly biased toward early Hubble types but otherwise is representative. They found that $28 \pm 5\%$ of their barred galaxies have a nuclear bar. They also found several indications that nuclear and main bars have a different origin, most notably that main bar sizes are proportional to the scale length of the disk, while nuclear bar sizes are uncorrelated with the size of the disk and almost always smaller than $\sim$1.6 kpc in radius. Nuclear bars and nuclear star-forming rings have similar size distributions when normalized by the galactic diameter D_{25}. They argued plausibly that this means that nuclear bar radii, like nuclear ring radii, are bounded approximately by ILR (see also Pfenniger & Norman 1990, Friedli & Martinet 1993).

Observations like these support the cononical hypothesis that nuclear bars form when infalling disk gas builds up a central, cold, and disky system that is sufficiently self-gravitating to become barred. How this happens is not known. One possibility is that a cold nuclear disk suffers its own bar instability, independent of that of the main bar (Friedli & Martinet 1993, Combes 1994).

A good sign that we understand the essence of nuclear bar dynamics is the observation (Figure 14) that inner bars are oriented randomly with respect to main bars (Buta & Crocker 1993, Friedli & Martinet 1993, Shaw et al. 1995, Wozniak et al. 1995, Friedli et al. 1996, Erwin & Sparke 2002). This can be understood within the dynamical framework of Section 2.2. At small radii, $\Omega(r) - \kappa(r)/2$ reaches a high peak in galaxies that have such high central mass concentrations. A bar's pattern speed Ω_p seeks out approximately the local angular velocity $\Omega - \kappa/2$ at which closed ILR orbits precess. Therefore, the pattern speeds of inner bars are almost certainly much higher than those of main bars[4] (see Pfenniger & Norman 1990, Friedli & Martinet 1993, Buta & Combes 1996, and Maciejewski & Sparke 2000 for further discussion). Kinematic decoupling of main and nuclear bars is observed by Emsellem et al. (2001) and by Corsini, Debattista & Aguerri (2003).

Shlosman, Frank & Begelman (1989) suggested that bars within bars are a primary way to transport gas farther inward than the gravitational torque of the main bar can achieve. To fuel nuclear activity in galaxies, they envisaged a hierarchy of bars within bars. Triple bars have been seen (Friedli 1996 and Erwin & Sparke 1999 provide reviews).

[4]Similarly, because $\Omega - \kappa/2$ decreases outward, the pattern speeds of spiral arms are likely to be slower than those of bars (Sellwood 1985, Sparke & Sellwood 1987, Sellwood & Sparke 1988, Sellwood & Wilkinson 1993). This accounts for the comment in Section 2.1 that the spiral arms of SB(r) galaxies "often [begin] downstream from the ends of the bar" (Sandage & Bedke 1994).

NGC 4736 is an example of a nuclear bar in an unbarred but oval galaxy (Block et al. 1994; Möllenhoff, Matthias & Gerhard 1995). It emphasizes again the similarity between bars and ovals as engines for secular evolution.

4.5. Box-Shaped Bulges

Bulges with box-shaped isophotes (Figure 15) are well known (Burbidge & Burbidge 1959, Sandage 1961, de Vaucouleurs 1974). Clear examples are seen in approximately one fifth of edge-on galaxies (Jarvis 1986; Shaw 1987; de Souza & dos Anjos 1987; Lütticke, Dettmar & Pohlen 2000a). Numerical simulations universally show that bars heat themselves in the vertical direction; they suggest that box-shaped bulges are edge-on bars. If this is correct, then observing box-shaped isophotes is a sufficient criterion for identifying a pseudobulge. Probably independently of this, boxy bulges also present us with a serious collision between simulations and observations. There are at least two problems. (*a*) Observations imply that bars are flat in the edge-on galaxies in which they can reliably be identified. (*b*) Bars and boxy bulges that are clearly distinct from each other occur together in several galaxies. In these galaxies, the major-axis radii of the boxy bulges are much shorter than the lengths of the bars.

That bars heat themselves in the axial direction was an immediate result of the first three-dimensional *n*-body simulations of unstable disks; it has been a robust theoretical prediction ever since (see Sellwood & Wilkinson 1993 for a review). Combes & Sanders (1981) were the first to point out that *n*-body bars look like boxy bulges (e.g., NGC 7332) when seen end-on and like peanut-shaped bulges (e.g., NGC 128) when seen side-on (both galaxies are illustrated in Sandage 1961 and in Sandage & Bedke 1994). Edge-on *n*-body bars looked boxy in some previous papers (e.g., Miller & Smith 1979), but these resulted from the collapse of spherical stellar systems, so it was not clear that their vertical structure was relevant to the evolution of disks. The Combes & Sanders (1981) results have been confirmed and extended by many authors (e.g., Combes et al. 1990, Pfenniger & Friedli 1991, Berentzen et al. 1998, Athanassoula & Misiriotis 2002, Athanassoula 2003). Early papers concluded that the orbits that contribute most to the boxy structure are in vertical ILR with the bar. With two vertical oscillations for each revolution, it is easy to arrange that a star be at its maximum height above the disk plane when it is near apocenter. Then it contributes naturally to a box-shaped structure. The importance of vertical resonant heating was emphasized by Pfenniger (1984, 1985) and especially by Pfenniger & Norman (1990). From sticky-particle simulations, Pfenniger & Norman (1990) found both the mass inflow discussed earlier and vertical heating that fed stars into a component with the scale height of a bulge. Timescales were short, on the order of one tenth of a Hubble time.

In contrast, Raha et al. (1991) showed that buckling instabilities thicken bars in the axial direction. These are collective phenomena, so they are different from resonant heating. Raha et al. (1991) suggested that buckling instabilities also occurred in the above simulations; Pfenniger & Friedli (1991) acknowledged this possibility.

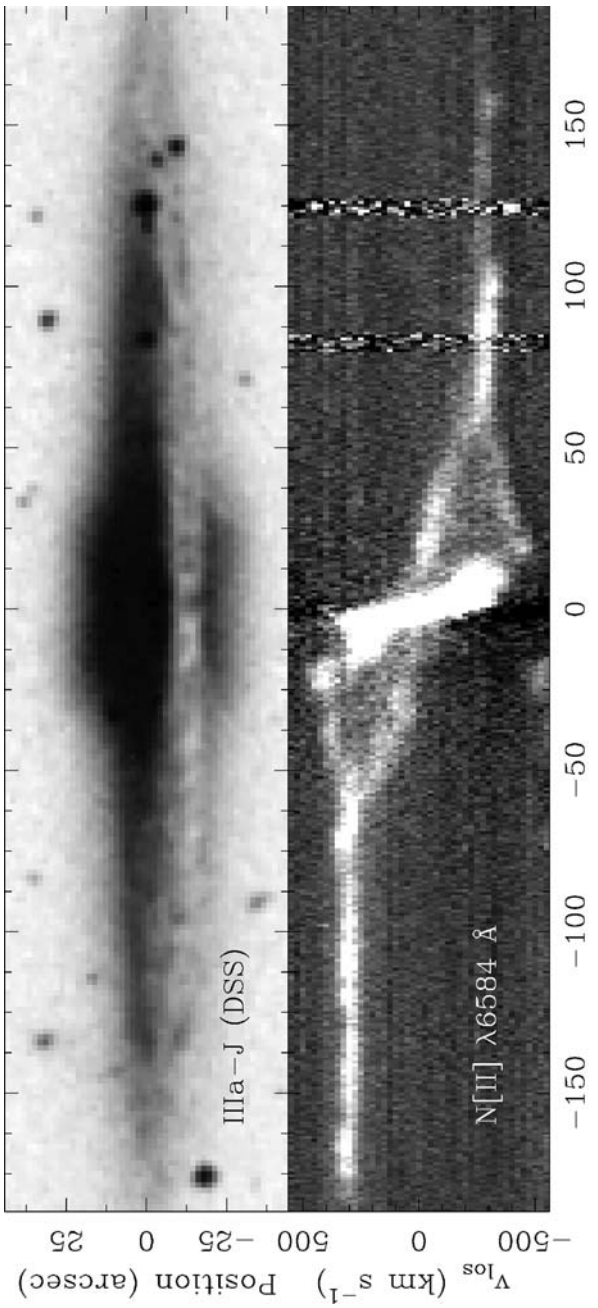

Figure 15 (*Top*) NGC 5746 (Sb) has a prominently box-shaped bulge (see also Sandage & Bedke 1994). (*Bottom*) Position-velocity diagram of the [NII] λ6584 Å emission line along the major axis registered in position with the image. The "figure 8" pattern is interpreted as the signature of a barred galaxy by Bureau & Freeman (1999), who kindly supplied this figure, and by Kuijken & Merrifield (1995).

Additional examples of buckling instabilities are in Sellwood (1993b), Kalnajs (1996), and Griv & Chiueh (1998). Further discussion is provided by Toomre (1966), Merritt & Sellwood (1994), Pfenniger (1996a), and Merrifield (1996).

However the heating happens, all of the simulators agree that bars and boxy bulges are connected. A few papers suggest only that disk stars are heated vertically and fed into the bulge (pre-existing or not), giving it a box-shaped appearance. But most authors advocate a stronger conclusion, namely that boxy bulges are nothing more nor less than bars seen edge-on.

What do the observations say? Persuasive observations show that boxy bulges occur in SB galaxies. However, they also suggest that box bulges are not identical to edge-on bars.

The obvious sanity check—that boxy bulges are seen in edge-on galaxies as frequently as well-developed bars are seen in face-on galaxies—is passed with flying colors. References are in the first paragraph of this subsection.

A link between *n*-body bars and boxy bulges is the observation in both of cylindrical rotation to substantial heights above the equatorial plane (see Bertola & Capaccioli 1977; Kormendy & Illingworth 1982; Jarvis 1990; Shaw, Wilkinson & Carter 1993a; Shaw 1993; Bettoni & Galletta 1994; Fisher, Illingworth & Franx 1994; D'Onofrio et al. 1999; and Falcón-Barroso et al. 2004 for the observations and Combes et al. 1990; Sellwood 1993a; Athanassoula & Misiriotis 2002 for simulations). Classical bulges and ellipticals do not rotate cylindrically, as evident from early long-slit spectroscopy (Illingworth & Schechter 1982; Kormendy & Illingworth 1982; Binney, Davies & Illingworth 1990) and now beautifully shown by integral-field spectroscopy (de Zeeuw et al. 2002; Verolme et al. 2002, Bacon et al. 2002; Copin, Cretton & Emsellem 2004; Falcón-Barroso et al. 2004).

Kuijken & Merrifield (1995) and Merrifield (1996) suggest that a kinematic signature of edge-on bars is a splitting in the gas velocities just interior to corotation because the gas there is depleted by radial transport. They observe such velocity splitting in NGC 5746 and NGC 5965 and argue that both galaxies are barred. Merrifield & Kuijken (1999) and Bureau & Freeman (1999) show additional examples. NGC 5746 from the latter paper is shown in Figure 15. The "figure 8" pattern in the emission line is the bar signature. The rapidly rotating gas is identified with a nuclear disk of x_2 orbits, and the slowly rotating component shows the line-of-sight velocities in the disk beyond the end of the bar. The lobes of the "figure 8" are empty because an annulus between the nuclear disk and the end of the bar contains little gas. The idea is that the missing gas has been transported to the center or to an inner ring at the end of the bar. This is an interpretation: an axisymmetric disk containing an annulus devoid of gas would also show the "figure 8." The connection with bars is indirect: (*a*) in face-on galaxies, gasless annuli are seen only in mature SB(r) galaxies, and (*b*) [NII] λ6584 Å emission is much stronger than Hα in the steep-rotation-curve central disk; this is a possible diagnostic of the shocks expected in the inner parts of the bar (Bureau & Freeman 1999). On the other hand, we noted in Section 2.1

that mature SB(r) galaxies—the ones in which an annulus interior to the inner ring has been cleared of gas—do not have the radial dust lanes that are characteristic of shocks. Despite these uncertainties, the almost universal detection of figure-8-like line splitting in boxy bulges and (equally important) the lack of such splitting in elliptical bulges argues that the former are found in barred galaxies.

A third observation that connects boxy bulges with bars is the detection in the disks of a few edge-on examples of density enhancements that plausibly are inner rings (Aronica et al. 2003).

Galaxy mergers probably create a minority of boxy bulges (Jarvis 1987). Also, Patsis et al. (2002) illustrated a simulation that makes a boxy-bulge-like structure in the absence of a bar. However, the conclusion that galaxies with boxy bulges generally contain bars seems reasonably secure.

This is not proof that they are the same things. There are two problems with the simple, well-motivated, and almost universally accepted notion that boxy bulges are edge-on bars.

First is the observation that at least some edge-on bars are flat. The "Rosetta stone" object for this subject is NGC 4762. It is studied in an important paper by Wakamatsu & Hamabe (1984) and is illustrated in Figure 16.

NGC 4762 is unique among edge-on galaxies studied so far because it has, in addition to a bulge, three clear-cut shelves in its major-axis brightness distribution. All three shelves are visible in the *Hubble Atlas* images (Sandage 1961), which also show that the bulge is slightly boxy. More face-on galaxies show us that three shelves in the surface brightness profile are common in early-type galaxies that contain a bar, a lens, and an outer ring (see NGC 1291 in Figure 2, NGC 3945 in Figure 5, and NGC 2217 and NGC 2859 in the *Hubble Atlas*). Lenses and outer rings have shallow brightness gradients interior to a sharp outer edge; their two nested ovals are exactly analogous to those in later-type oval galaxies (Figure 9). Kormendy (1979b) emphasized that the bar almost always fills the lens in its longest dimension. Because SB(lens)0 galaxies are common and because they are the only S0s with three prominent shelves in the brightness profile, interpreting NGC 4762 is reasonably straightforward. Wakamatsu & Hamabe (1984) suggested that the outer shelf is an outer ring, that the middle shelf is a lens, and that the inner shelf is a bar. Because the inner shelf has a smaller radius than the middle shelf, the bar must be seen at a skew orientation ϕ (Figure 16). Wakamatsu and Hamabe pointed out that their interpretation is supported by four observations: (*a*) The deprojected profile of the outer shelf is that of a ring: It has a minimum interior to an outer maximum. (*b*) The radius of the outer shelf satisfies the correlation between outer ring radii and galaxy luminosity. (*c*) The radius of the inner shelf satisfies the correlation between lens radii and galaxy luminosity; both correlations are from Kormendy (1979b). (*d*) The ratio of the radius of the outer shelf to the radius of the inner shelf is 2.4 ± 0.2, consistent with the average ratio of outer ring to lens radii, 2.21 ± 0.12 (Kormendy 1979b; Buta & Combes 1996 and references therein).

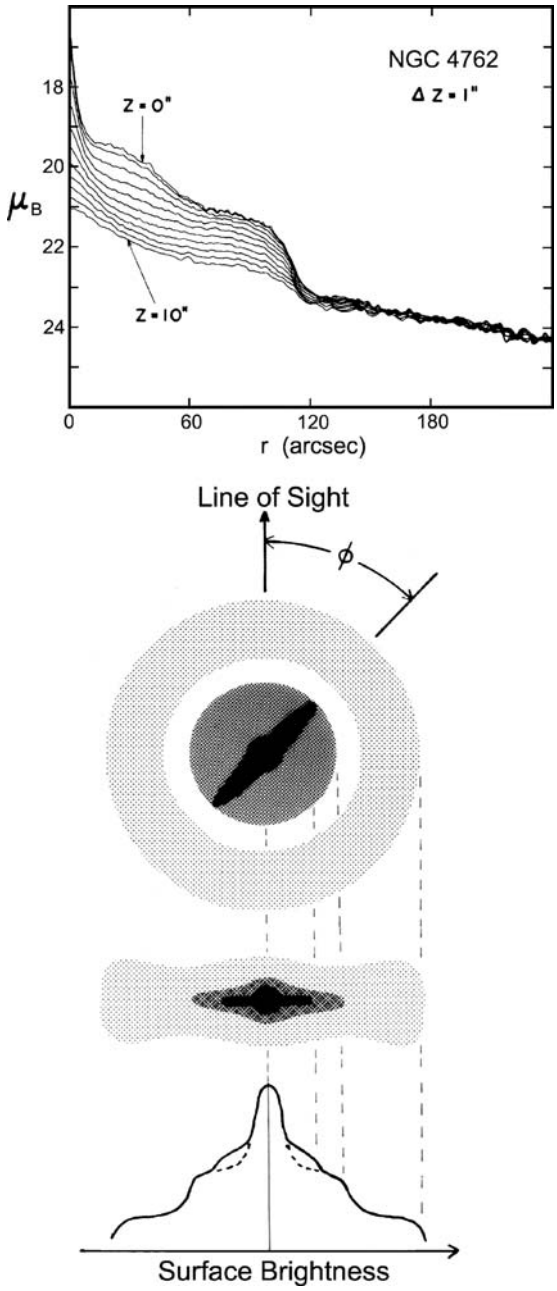

Figure 16 (*Top*) Brightness cuts parallel to the major axis of NGC 4762 and displaced from it by Δz along the minor axis. (*Bottom*) Assumed viewing geometry: face-on (*upper diagram*) and as seen by us (middle sketch and major-axis brightness cut). Figure is from Wakamatsu & Hamabe (1984).

We belabor these points because it is critically important to know that the inner shelf is the bar. The reason is illustrated in the top panel of Figure 16. Wakamatsu & Hamabe (1984) show convincingly that the bar is flat. In the series of brightness cuts parallel to the disk major axis and displaced from it by $\Delta z = 0''$, $1''$, $2''$, $\ldots 10''$, the bar disappears as a feature distinct from the lens by $\Delta z \simeq 5''$. That is, its scale height is less than that of the lens and much less than that of the bulge. The bar is the flattest component in the galaxy.

Also, the bar and the bulge are photometrically distinct. The boxy outer part of the bulge (which is not evident in the brightness cuts in Figure 16) has a radius about half as big as the projected radius of the bar. If the bar fills the lens, then this is about one-fifth of the true radius of the bar.

Similar evidence for flat bars is presented in de Carvalho & da Costa (1987); Lütticke, Dettmar & Pohlen (2000b); and Quillen et al. (1997).

The second problem with the assumption that boxy bulges are edge-on bars is the observation that both occur together but are distinct from each other in NGC 7582 (Quillen et al. 1997). We see this galaxy at an inclination $i \simeq 65^\circ$ that is close enough to edge-on so that the boxy bulge is visible in the infrared but far enough from edge-on so that the bar can be recognized (Sandage & Bedke 1994). In fact, the galaxy has the morphology of a typical oval disk with the bar filling the inner oval along its apparent major axis. Therefore the bar is seen essentially side-on. However, the bar is very flat, the boxy bulge is clearly distinct from it, and the maximum radius of the boxy structure along the disk major axis is about one-third of the radius of the bar.

These observations suggest that boxy bulges and edge-on bars are not exactly equivalent.

An interesting alternative not previously considered is this: Observations and theory are consistent with the hypothesis that at least some and possibly most box-shaped bulges are edge-on *nuclear* bars. For example, the two nested triaxial components in our Galaxy proposed by Blitz & Spergel (1991, see their figure 1) are similar to the bar-within-bar structure in Section 4.4. If the inner bar has a radius of 1–2 kpc (Binney et al. 1991; Blitz & Spergel 1991; Binney & Gerhard 1993; Sellwood 1993b; Dwek et al. 1995), then it is more nearly the length of typical nuclear bars than of typical main bars. (Scaling our Galaxy to other Sbcs, a normal bar should be $\sim$3.5 kpc in radius.) It is the inner bar that looks boxy in *COBE* images (Weiland et al. 1994; Dwek et al. 1995). We may live in a weakly barred or oval galaxy with a boxy nuclear bar. However, only one-quarter of strongly barred galaxies contain nuclear bars. There may be too few of them to account for all boxy bulges.

Another solution may be the indication noted in figure 1.1b of Shen & Sellwood (2004) that the boxy part of their *n*-body bar is smaller than the bar as a whole. We are indebted to Jerry Sellwood for pointing this out.

The safest conclusion—and one that is sufficient for our purposes—is that boxy bulges are connected with bars and owe their origin to them. All mechanisms

under discussion build the box structure out of disk material. We therefore conclude that detection of boxy bulge isophotes is sufficient for the identification of a pseudobulge. However, the disagreement between the bar simulations and the above observations needs attention.

4.6. Bulges with the Dynamics of Disks: The V/σ $-$ ϵ Diagram

Figure 17, the $V_{\max}/\sigma - \epsilon$ diagram (Illingworth 1977; Binney 1978a,b), shows that pseudobulges (filled symbols) are more rotation dominated than are classical bulges (open circles), which are more rotation dominated than are giant elliptical galaxies (crosses). This is disky behavior.

The essential features of the $V_{\max}/\sigma - \epsilon$ diagram are as follows:

1. The virial theorem relates the gravitational potential and kinetic energy tensors; the former involves the shape of the stellar system; the latter involves the balance between rotational and random kinetic energies (Binney 1978a, Binney & Tremaine 1987). In Figure 17, $V_{\max}/\sigma$ is a surrogate for the (square root of) the ratio of ordered to random kinetic energies and ϵ is the apparent flattening.
2. If rotation is dynamically unimportant ($V_{\max}/\sigma \ll 1$) and if the system is flattened, then it must be anisotropic (Binney 1976; 1978a,b; 1980; 1982). Stars climb farthest out of their mutual gravitational potential well in the direction in which the velocity dispersion is largest.
3. Rotation adds extra flattening regardless of velocity anisotropy, because rotation plus random motions allow stars to climb farther out of their mutual gravitational potential well than do random motions alone. Isotropic systems that are flattened into spheroids by rotation have a simple relationship between flattening and $V_{\max}/\sigma$ that is shown by the line labeled "oblate" in Figure 17. Binney (1978a) gave it implicitly; Fall (1981) provided an explicit equation for the projected configuration seen edge-on, and Kormendy (1982a) gave an approximation formula, $V_{\max}/\sigma \simeq [\epsilon/(1-\epsilon)]^{1/2}$, that is good to 1% for $0 \leq \epsilon \leq 0.95$.
4. For $0.1 \lesssim \epsilon \lesssim 0.5$, projection moves an isotropic oblate spheroid almost parallel to the oblate line. If an isotropic spheroid with $\epsilon = 0.5$ is seen at a skew orientation so that it looks like an $\epsilon = 0.3$ system seen edge-on, then both systems have approximately the same value of $V_{\max}/\sigma$. However, an edge-on disk that is near the oblate line at $\epsilon \sim 0.9 \pm 0.1$ projects well above the oblate line when it is seen other than edge-on.
5. Most giant ellipticals have insignificant rotation and are dominated by velocity anisotropy (Bertola & Capaccioli 1975, Illingworth 1977) (crosses in Figure 17). Low-luminosity ellipticals are more nearly isotropic and consistent with the oblate line (Davies et al. 1983). And classical bulges are consistent with being isotropic oblate rotators (Illingworth & Schechter

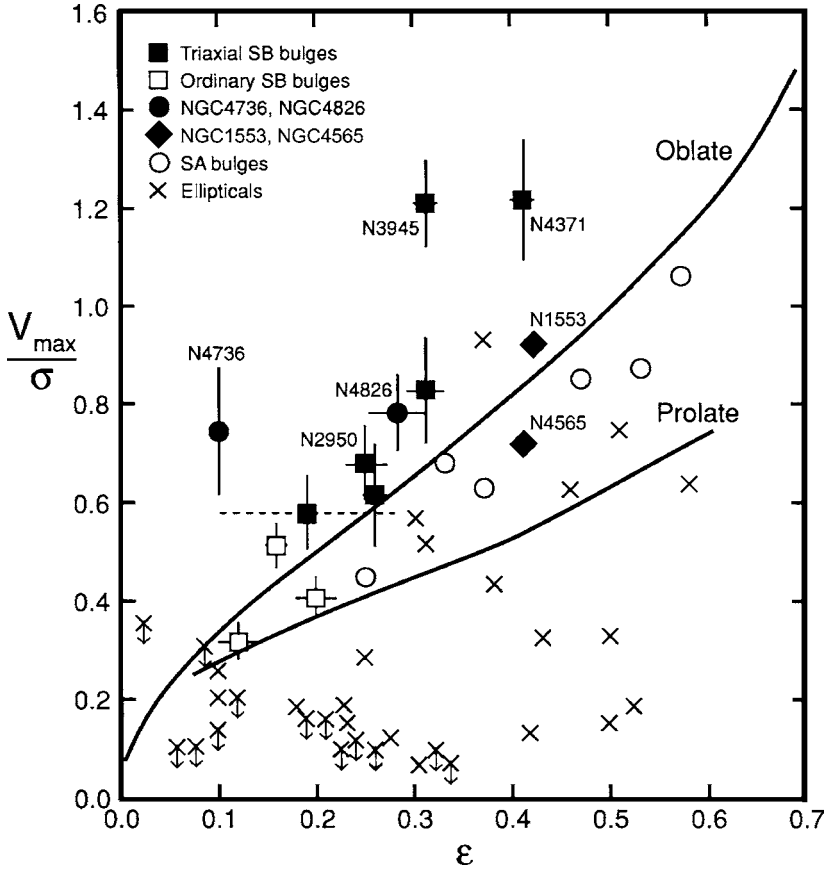

Figure 17 The relative dynamical importance of rotation and random motions as a function of observed ellipticity for various kinds of stellar systems. Here $V_{\max}/\sigma$ is the ratio of maximum rotation velocity to mean velocity dispersion interior to the half-light radius and $\epsilon = 1 -$ axial ratio. The "oblate" line describes oblate-spheroidal systems that have isotropic velocity dispersions and that are flattened only by rotation; it is a consequence of the tensor virial theorem (Binney & Tremaine 1987). The "prolate" line is one example of how prolate spheroids can rotate more slowly for a given ϵ because they are flattened partly by velocity dispersion anisotropy. This figure is updated from Kormendy (1993).

1982, %Kormendy & Illingworth 1982, Kormendy 1982b) (open circles in Figure 17). Classical bulges fall slightly to the right of the oblate line, but the extra flattening is provided by the disk potential (Jarvis & Freeman 1985).

The above papers show that anisotropic giant ellipticals are triaxial. We emphasize that this triaxiality is different from that of bars. Ellipticals are triaxial because they have little angular momentum. They are made largely out of "box orbits" that have no net angular momentum (see Binney & Tremaine 1987 for a review). Rotation is provided by "z-axis tube orbits" that encircle the z = rotation axis; in a triaxial elliptical, these are somewhat elongated in the direction of the longest axis. Other orbits, including chaotic ones, are present as well. But the essential character of an elliptical is defined by its box orbits.

In contrast, a barred galaxy is barred not because it has little angular momentum but rather because it has too much for the combination of its velocity dispersion and its central concentration. This is why the disk made a bar. Bars are not made of box orbits; they are made of x_1 orbits. These are very elongated z-axis tubes that, in some cases, include baroque decorations such as loops. They have lots of angular momentum. It is important to keep in mind the distinction between bars and ellipticals. They are not different versions of each other, and they virtually never occur together. A bar is fundamentally a disk phenomenon.

Contrast now the behavior of the bulges that are plotted in Figure 17 as filled symbols. They are above the oblate line and even more above the distribution of classical bulges plotted with open symbols. Rotation is more important in these objects than it is in classical bulges and ellipticals. Point 4, above, shows why this is disk-like behavior. It indicates an admixture of stars that are flattened, dynamically cold, and rapidly revolving around the galactic center—that is, a disk contribution that would appear near the oblate line if seen edge-on but that lies well above the oblate line when the galaxies are viewed at skew inclinations. The filled symbols include barred galaxies and the prototypical unbarred oval galaxy NGC 4736 (Figures 2 and 8). These are objects in which we argued that secular evolution has been important. Another prominent example is NGC 3945; its rapidly rotating bulge is the nuclear bar shown in Figure 14 (see Erwin et al. 2003 for a detailed discussion). Another is NGC 2950, which also contains a nuclear bar. Thus the dynamical evidence agrees with other evidence that these are pseudobulges.

Two pseudobulges from Kormendy & Illingworth (1982) deserve comment. They are plotted as filled diamonds in Figure 17. NGC 1553 contains the prototypical lens in an unbarred galaxy (point 7 of Section 2.1). Figure 17 shows that it has an unusually high value of $(V_{\rm max}/\sigma)^*$ for an unbarred galaxy. Consistent with the suggestion that the lens is a defunct bar (Kormendy 1979b, 1984) (Section 3.3), the hint is that the galaxy grew a pseudobulge while it was still barred. In contrast, the boxy bulge of NGC 4565 has $(V_{\rm max}/\sigma)^* = 0.86 \pm 0.16$. This is smaller than $(V_{\rm max}/\sigma)^*$ values for other pseudobulges. However, a box-shaped pseudobulge rotates cylindrically, so $(V_{\rm max}/\sigma)^*$ underestimates the dynamical importance of rotational kinetic energy compared with ellipsoidal bulges.

The difference between classical and pseudobulges need not always be large. It is entirely implausible that secular evolution sometimes augments a classical bulge with new, disky material. We also point out in Section 7.1 that pseudobulges

can heat themselves in the vertical direction, thereby decreasing their dynamical difference from classical bulges. Therefore, large $(V_{\max}/\sigma)$ is evidence for a pseudobulge, but values comparable to those on the oblate line do not guarantee that the bulge is classical.

4.7. Velocity Dispersions and the Faber-Jackson Relation

Figure 18 shows the correlation between the velocity dispersion and absolute magnitude for elliptical galaxies and for bulges of disk galaxies. Most early-type galaxy bulges are consistent with the well-known correlation $L_B \propto \sigma^4$ (Faber & Jackson 1976; see Minkowski 1962 for an early hint). But a few early-type (pseudo)bulges and a large majority of Sbc–Sm (pseudo)bulges fall well below the correlation. One possible interpretation is that these have small velocity dispersions and are similar to disks. Alternatively, the centers of late-type galaxies may actively be forming stars and therefore have small mass-to-light ratios. Figure 18 would then imply that the central parts of most late-type galaxies have young stellar

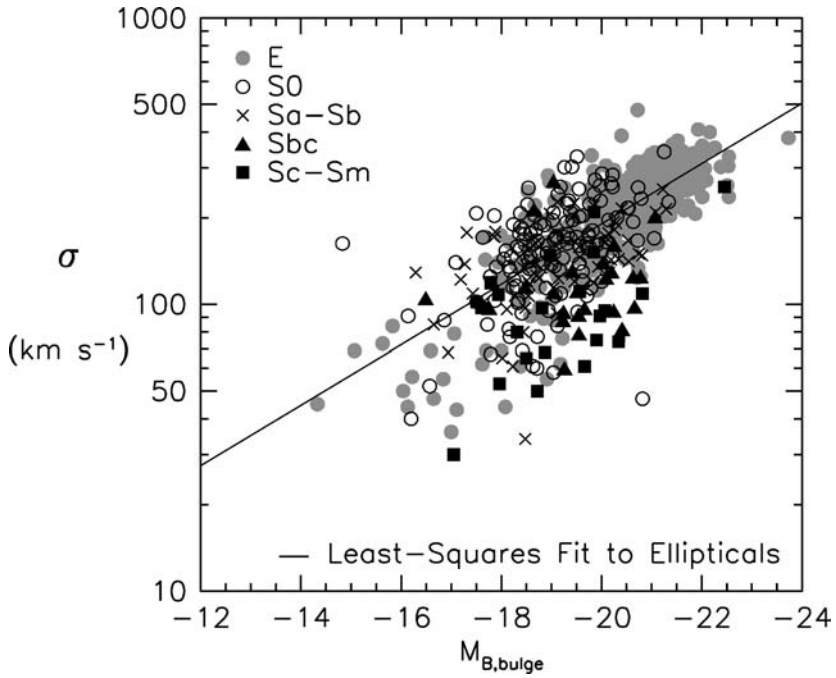

Figure 18 Correlation between central velocity dispersion and bulge absolute magnitude for all galaxies of the indicated Hubble types that have velocity dispersions tabulated in Hypercat. The straight line is a least-squares fit to the ellipticals. Updated from Kormendy & Illingworth (1983), this figure is from Kormendy & Cornell (2004).

populations. Therefore, star formation must be secular, not episodic. In either case, Figure 18 suggests that most late-type galaxies contain pseudobulges. In contrast, most early-type bulges are similar to elliptical galaxies.

4.8. Pseudobulges and the Fundamental Plane Correlations

If pseudobulges have Sérsic indices ($n \sim 1$) that are smaller than those of elliptical galaxies ($n \sim 4$), then this signals a breakdown in the homology that, together with the virial theorem, is the reason why classical bulges and ellipticals satisfy the Fundamental Plane (FP) correlations (e.g., Djorgovski & Davis 1987; Dressler et al. 1987; Faber et al. 1987; Lauer 1987; Djorgovski, de Carvalho & Han 1988; Kormendy & Djorgovski 1989; Bender, Burstein & Faber 1992, 1993; Burstein et al. 1997); that is, bulges and ellipticals lie in an inclined plane, $R \propto \sigma^{1.4\pm0.15} I^{-0.9\pm0.1}$ in the space of observed radius R, surface brightness I, and velocity dispersion σ. The scatter of ellipticals around the FP is small (Saglia, Bender & Dressler 1993). Therefore deviations from the FP are a sensitive test of whether the structure of a bulge-like component is or is not similar to that of an elliptical. Carollo (1999) found that pseudobulges deviate from the FP of classical bulges and elliptical galaxies in the direction of having lower densities (see also Kent 1985; Andredakis, Peletier & Balcells 1995). They lie closer to the locus of disks than to that of hot stellar systems. Similar studies of larger samples may provide an additional quantitative way to recognize pseudobulges.

4.9. Nuclei

Nuclei are compact star clusters[5] at galactic centers (see Kormendy & Djorgovski 1989 for a review). They should not be confused with steep density cusps that are the central parts of nearly featureless power-law profiles (Lauer et al. 1995). For example, M32 does not have a nucleus (Lauer et al. 1992, 1998). Rather, nuclei are clearly differentiated from the surrounding (pseudo)bulge and disk in the sense that they have much smaller effective radii r_e and much higher effective surface brightnesses $\mu(r_e)$ than their surroundings. Figure 20 illustrates the prototypical example in M33 (Kormendy & McClure 1993). Tremaine & Ostriker (1982) have shown that the nucleus and bulge of M31 are dynamically independent; we assume that the same is true for other nuclei. Local Group examples are found in M31 (e.g., Lauer et al. 1993, 1998), M33, and NGC 205 (Jones et al. 1996). Not much farther away are the nuclei in IC 342 (Böker et al. 1997, 1999a) and in NGC 7793 (Díaz et al. 2002).

[5]Many galaxies have active centers that are dominated by nonthermal radiation and by emission from hot gas. These are universally called active galactic nuclei. They are quite distinct from star clusters. When we speak of nuclei, we expressly exclude radiation from active galactic nuclei. Caution: Not all authors do this.

Late-type disk galaxies usually contain nuclei. Many of these have young stellar populations. They imply episodic star formation over long periods of time and so are consistent with secular growth in a manner that is similar to the proposed formation of pseudobulges. But the "smoking gun" that is most compelling is not the one that points at secular evolution. Rather, the observations are screaming that there is another physical process taking place that we do not understand. This is clear because nuclei are not just the low-luminosity limit of pseudobulges. Also, compact nuclei and fluffy pseudobulges often occur in the same galaxy. If they form similarly, why are they so different? Our review highlights a remarkable list of enigmas.

Surveys of late-type galaxies and detailed studies of individual objects provide the following list of properties:

1. Nuclei are very common in late-type spirals. Böker et al. (2002) found them in 75% of 77 Scd–Sm galaxies in an *I*-band *HST* survey. Carollo et al. (2002) found nuclei in 30% of S0–Sa galaxies, 59% of Sab–Sb galaxies, and 77% of Sbc–Sm galaxies. Nuclei are also common in spheroidal galaxies (Binggeli et al. 1984, 1985; van den Bergh 1986).
2. Nuclei are rare in irregulars (van den Bergh 1995).
3. Nuclei are fairly homogeneous in their properties. Typical luminosities are 10^6 to 10^7 $L_\odot$ (Kormendy & McClure 1993, Matthews et al. 1999a, Carollo et al. 2001, Matthews & Gallagher 2002, Böker et al. 2002). Effective radii are typically $10^{1\pm0.5}$ pc (Carollo et al. 1999, Böker et al. 2003b). Observed central densities are high and are limited by the spatial resolution of the images; they are 10^4 to 10^5 $L_\odot$ pc^{-3} in examples in Matthews et al. (1999a) and are even higher, at least 10^7 $L_\odot$ pc^{-3}, in M33 (Lauer et al. 1998). These values are enormously higher than the surrounding disk densities.
4. Most nuclei are at the centers of their galaxies to within measurement errors (Böker et al. 2002). Exceptions are rare (Matthews et al. 1999a; Binggeli, Barazza & Jerjen 2000; Carollo et al. 2002). This is hard to understand. In their absence, the center does not look like a special place. The gravitational potential gradient of the visible matter is shallow (Kormendy & McClure 1993, Matthews et al. 1999a, Böker et al. 2002). Why does a nucleus form at the center, and why is its scale length so short compared with that of the rest of the galaxy (Figure 19; Böker, Stanek & van der Marel 2003c)? Could the reason be that cold dark matter halos are cuspier than the baryons (Navarro, Frenk & White 1996, 1997), or, if they are not so now (Moore 1994), could they have been so in the past, before baryonic physics intervened (Navarro, Eke & Frenk 1996)? Could nuclei be compact not because the galactic center is a special place but rather because galaxies know how to make compact clusters and they can sink to the center by dynamical friction (Tremaine, Ostriker & Spitzer 1975)? Carollo (1999) argues that the timescale for dynamical friction against dark matter is interestingly short.

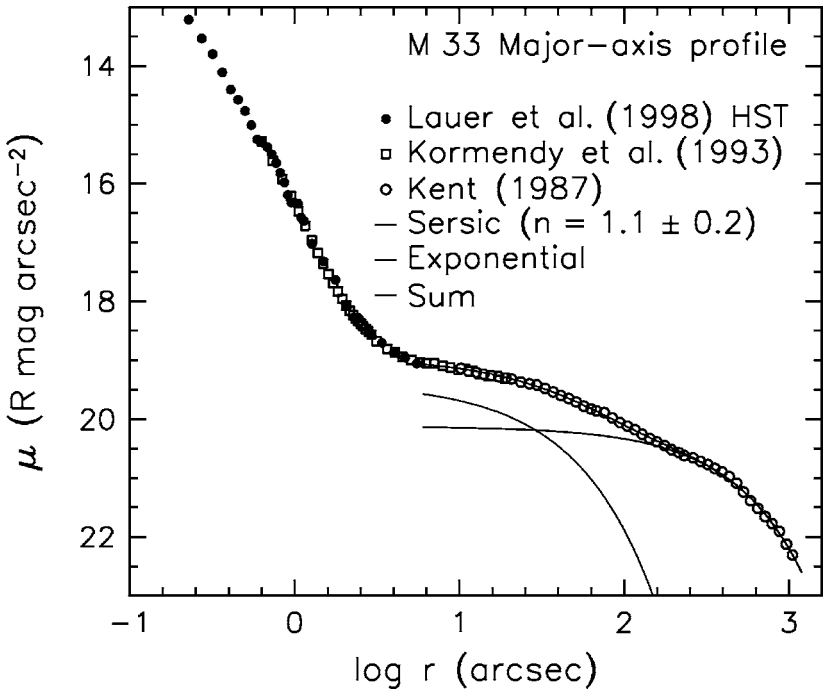

Figure 19 Major-axis surface brightness profile of M33. The steep rise in surface brightness near the center is the nucleus. The rest of the profile has been decomposed into an inner Sérsic function plus an exponential. We thank S. Faber and the Nuker team for suggesting a discussion of M33.

This may explain the seeds of the observed nuclei, but it remains remarkable that subsequent star formation keeps them so compact.

5. Stellar populations often imply young ages for the stars that contribute most of the light. The M33 nucleus is typical. It has a composite, late-A to early-F spectrum dominated by younger stars at bluer wavelengths (e.g., van den Bergh 1976a, 1991; Gallagher, Goad & Mould 1982; O'Connell 1983; Schmidt, Bica & Alloin 1990; Gordon et al. 1999). Population synthesis by Long, Charles & Dubus (2002) gives a best fit to the spectrum between 1150 Å and 5700 Å for two starbursts, one with a mass of 9000 $M_\odot$, 40 Myr ago and the other with a mass of 76,000 $M_\odot$, 1 Gyr ago. [The total nuclear mass is 2×10^6 $M_\odot$ (Kormendy & McClure 1993)]. The spectra are insensitive to still older starbursts.

   Additional examples of nuclei with blue colors indicative of young stars are discussed in Díaz et al. (1982); Bica, Alloin & Schmidt (1990); Shields & Filippenko (1992); Böker et al. (1997, 1999a); Matthews et al. (1999a); Davidge & Courteau (2002); Böker et al. (2001, 2003b); see also Ho,

Filippenko & Sargent (1997). Carollo et al. (2001) observe colors that are consistent with a range of ages; there is some tendency for bluer nuclei to be associated with bluer surrounding disks. In fact, "brighter nuclei ($M_V \lesssim -12$) are typically found ... in the centers of galaxies with circumnuclear rings/arms of star formation or dust and an active, i.e., H II or AGN-type ... spectrum" (Carollo 1999, consistent with Ho, Filippenko & Sargent 1997). Since so many nuclei contain young stars, star formation does not happen over only a small fraction of the life of the cluster but rather is secular.

6. Nuclei are not more common in barred galaxies than in unbarred galaxies (Carollo et al. 2002, Böker et al. 2003b). Evidently, supplying gas to feed their star formation does not require a bar.
7. In the FP parameter correlations, nuclei are more similar to large Galactic globular clusters and to compact young clusters in interacting and merging galaxies than they are to (pseudo)bulges (Carollo 1999; Geha, Guhathakurta & van der Marel 2002; Böker et al. 2003b). There is no sign that nuclei form the faint end of the sequence of (pseudo)bulge properties (see also Section 4.10).
8. The luminosities of nuclei correlate with the luminosities and central surface brightnesses of their host galaxies (Böker et al. 2003b).

What does all of this mean? Point 5 provides the strongest evidence that nuclei are built by secular processes like those that we suggest make pseudobulges. Point 8 also seems consistent. So is observation 1 that nuclei are more common in later-type galaxies; they are approximately as common as pseudobulges. However, points 2, 3, 4, 6, and 7 either are major puzzles or suggest that nuclei and pseudobulges are fundamentally different.

The prudent conclusions are these: Nuclei are not a problem for our picture of pseudobulge formation by inward secular transport of gas. In fact, many authors have argued that this is how they grow. But nuclei are not a secure argument for secular evolution, either. We find it compelling that nuclei and pseudobulges are very different in their parameters but occur together in the same galaxies. Nuclei appear to be related to globular clusters and to young clusters in merger starbursts. Several mysteries would be easier to understand if they got their start as such clusters and then sank to the center by dynamical friction. In particular, our problem with points 3 and 4—that nuclei are tiny and dense compared with pseudobulges and disks—would vanish.

4.10. In Which Pseudobulges Fade Out into Disks

Böker, Stanek & van der Marel (2003c) have investigated how pseudobulges fade out into disks. Their most subtle examples of pseudobulges also highlight fundamental uncertainties about the meaning of profile decomposition. M33 (Figure 19) provides an example. The disk has somewhat irregular but global-pattern spiral structure (Sandage 1961, Sandage & Bedke 1994). There is no sign of an ILR,

i.e., the spiral arms become radial near the center and pass through it. At the center, a very distinct nucleus (Kormendy & McClure 1993) is representative of the ones discussed in Section 4.9. Figure 19 shows that the disk surface brightness profile has a subtly two-component look; it is well fitted by the sum of two exponentials. The figure shows a decomposition into a Sérsic function plus an outer exponential; it confirms that $n = 1.09 \pm 0.18$ for the inner component. This inner component is essentially the bulge discussed by Minniti, Olszewski & Rieke (1993). It is also visible as a subtle upturn in surface brightness at $r < 150''$ in the *JHK* profiles posted at the 2MASS Web site. What does this mean? Does M33 contain a pseudobulge?

The inner component is consistent with, although on the low-density side of, the parameter distribution for exponential bulges given in Carollo (1999). The effective radius of the inner component is $r_e = 0.31 \pm 0.05$ kpc, and the mean surface brightness within r_e is 20.7 ± 0.2 R mag arcsec^{-2}. (All errors quoted take account of parameter coupling in the decomposition.) If one applies profile decomposition in the canonical way, then one could reasonably conclude that this is a pseudobulge not unlike the fluffiest ones discussed in the literature.

On the other hand, we are uneasy about the decomposition in Figure 19. The distinction between the components is subtle. The inner one is at most a factor of 2 brighter than the outer one, and it is so only at $r < 10''$ where the outer exponential has already been extrapolated far inward. The stars in both components are presumably in nearly circular orbits; stars that define the outer exponential do not, by and large, visit the inner exponential and vice versa. Does it really make sense to say that half of the disk stars at $r \simeq 25''$ belong to the main disk and half belong to a pseudobulge? If we could observe each star, how would we decide which ones belong to the bulge and which to the disk? It is difficult to believe, given substantial spread in kinematic and composition properties, that there would be such a clean separation into two components that we could label each star correctly. Another way to put it is this: Given that the fitting functions used for each component are not physically motivated or explained, is there any reason to believe that each one extrapolates without change into the part of the galaxy that is dominated by the other? And still another way: No theory of the formation of exponential disks explains why an exponential is so magic and so required that modest departures from it cry out for explanation. We already accept Freeman (1970a) "Type II profiles" as canonical disk behavior, even though we can explain it in only a few cases (e.g., Talbot, Jensen & Dufour 1979). We accept outer cutoffs (e.g., van der Kruit & Searle 1981a,b; 1982). Oval disks are only piecewise exponential (Section 3.2). Would it be a surprise if disks also knew how to deviate above an inward extrapolation to small radii?

We believe that it is not possible, given the available information, to distinguish between the following possibilities: It is entirely plausible that the inner exponential is a protopseudobulge. Alternatively, disk profiles can have a variety of wiggles and this is one of them. Interestingly, the inner component is significant out to a radius that is comparable to the width of the spiral arms. Spiral arms pass through the center when there is no ILR. This means that the profile near the center measures

light only from a spiral arm crest, while the profile farther out is an average over arm crests and arm troughs. This could be part of the explanation of the inner component.

This discussion highlights a fundamental conceptual uncertainty with the blind application of profile decomposition. In the case of a big, classical bulge plus an obvious disk, we can be confident that a decomposition has physical meaning. We know this from edge-on galaxies. The bulge in the Sombrero galaxy clearly extends into and beyond the radii where we would see the disk if the galaxy were face-on; at these radii, we would see bulge stars in front of and behind the disk. Bulge formation via mergers guarantees that this be so, because some stars in a merger always splash out to large radii. But secular evolution involves the slow transport of gas that is never far from dynamical equilibrium. No substantial splashing occurs. The concept that a pseudobulge coexists, at some radius of interest, with a disk that was already in place has much less physical meaning than it does in the case of a classical bulge. It is not clear to us that decomposition has any meaning at all in distinguishing pseudobulges from disks. It may be more meaningful to fit the profile piecewise.

Decomposition remains a useful way to derive diagnostic parameters. We should not overinterpret the results. Further work is needed to define the boundaries between what deserves interpretation and what does not.

What are the implications? We believe that the conclusions about well-developed pseudobulges—the ones whose profiles rise well above the inward extrapolation of the disk profile, as in Figures 10 to 12—are unchanged. The FP correlations then tell us that the dividing line between pseudobulges and disks is just as fuzzy as the one between classical bulges and pseudobulges. The reason is not that our machinery is inadequate. The reason is that there is a physical continuum between disks and pseudobulges, as suggested by Kormendy (1993) and by Böker, Stanek & van der Marel (2003c). The sequence of pseudobulges fades out not where they become tiny, like nuclei, but where they become large, low in surface brightness, and indistinguishable from disks.

5. CENTRAL STAR FORMATION AND PSEUDOBULGE GROWTH

What is the rate at which star formation is building stellar mass density in pseudobulges? Is the picture of secular evolution in Sections 2 and 3 consistent via plausible formation timescales with the properties of pseudobulges in Section 4?

Figure 8 shows central gas disks in barred and oval galaxies that have radii and masses comparable to those of pseudobulges and that are intensely forming stars. They are a window on pseudobulge formation. We begin by discussing well-studied systems in which star-formation rates (SFRs), gas masses, stellar mass deposition rates, and hence, evolution timescales can be constrained accurately.

We then review the broader body of observations of circumnuclear gas disks and SFRs. Star formation is ubiquitous in late-type galaxies. This means that it cannot be driven by episodic events such as mergers. It must be secular.

5.1. Case Studies: NGC 1326, NGC 1512, NGC 4314, and NGC 5248

These galaxies are excellent prototypes for studying circumnuclear disks, because each has been studied in depth using a combination of *HST* and ground-based imaging (Buta et al. 2000, Maoz et al. 2001, Benedict et al. 2002, Jogee et al. 2002). Also, the four objects span a representative range of host galaxy properties. They are all barred, and they all have similar luminosities ($-19.0 \geq M_B^0 \geq -20.3$), but they cover a wide range of morphological types (SB0/a–SBbc) and environments. NGC 1326 is in the Fornax cluster, NGC 1512 is in an interacting pair with NGC 1510, and NGC 4314 and NGC 5248 are relatively isolated field galaxies located in loose groups. Nearly all (>80%) of the star formation in NGC 1326 and NGC 4314 is contained in the circumnuclear rings, whereas NGC 1512 and NGC 5248 have actively star-forming outer disks, with less than 40% of the total SFR near the center. The diversity in galaxy properties and environments already suggests that internal structure (e.g., bars) is more important than external influences in feeding the central star formation.

The central star-forming rings of NGC 1512, NGC 1326, and NGC 4314 are illustrated in Figure 8. At high spatial resolution, the rings of H II regions and young star clusters often are revealed to be pairs of tightly wound spiral arms. This is shown for NGC 1512 in Figure 3. The spiral structure is seen most clearly in red continuum images, where networks of dust features spiraling toward the center from within the star-forming rings can be seen. The continuum images also reveal large numbers of bright stellar knots (>70 in NGC 4314; 500–1000 in the others). The luminosities and de-reddened colors of these knots indicate that they are not single stars but instead are luminous associations or star clusters. The brightest of these have stellar masses of order $10^5\ M_\odot$, placing them in the class of populous blue clusters observed in the Magellanic Clouds (MCs) and other gas-rich galaxies. Some may be young progenitors of globular clusters. Many of the clusters are coincident with H II regions, but most are free of surrounding nebulosity, and these are probably older than the 5–10-Myr lifetimes of typical H II regions.

Current SFRs in these regions can be estimated from extinction-corrected Hα or Paα measurements converted using the SFR calibrations of Kennicutt (1998a). The resulting SFRs range from $\sim$0.13 $M_\odot\ \mathrm{yr}^{-1}$ in NGC 4314 (Benedict et al. 2002) to 1 $M_\odot\ \mathrm{yr}^{-1}$ in NGC 1326 and NGC 1512 (Buta et al. 2000, Maoz et al. 2001) and $\sim$2 $M_\odot\ \mathrm{yr}^{-1}$ in NGC 5248 (Maoz et al. 2001 corrected to a distance of 15 Mpc). These values are probably accurate to within $\pm$50%, given uncertainties in the amounts and patchiness of the extinction and in the assumed distances to the galaxies. This is sufficient to characterize the evolutionary properties and physical conditions in these regions.

These rates are modest when compared with the total SFRs in giant spiral galaxies, which typically range from 0.1–1 $M_\odot\,\mathrm{yr}^{-1}$ in normal Sa galaxies to 1–10 $M_\odot\,\mathrm{yr}^{-1}$ in Sb–Sc galaxies (Kennicutt 1983, 1998a). However, they are quite exceptional considering the physical compactness of the star-forming regions. The star-forming rings have radii of 500–700 pc, so the surface densities of star formation are of order 0.1 to 1 $M_\odot\,\mathrm{yr}^{-1}\,\mathrm{kpc}^{-2}$. This is 1 to 3 orders of magnitude larger than the typical disk-averaged SFR densities in normal galaxies, and it approaches the SFR densities seen in some infrared starburst galaxies (Kennicutt 1998a,b). If these rates were to persist over a Hubble time, they would produce bulges with stellar masses of 10^9–$10^{10}\ M_\odot$. Thus, while the total amounts of star formation in these regions are not unusual by galactic standards, the character of the star formation is quite distinct.

The distinctive character of the star formation is underscored by the large populations of luminous young star clusters. Their extinction-corrected absolute magnitudes range from $M_V^0 = -13$ to $M_V^0 \sim -8$. For clusters fainter than this, *HST* photometry becomes very incomplete. The corresponding masses, corrected for the ages of the clusters, are $\sim 10^3$ to $10^5\ M_\odot$. These are similar to the masses of giant OB associations such as those in supergiant H II regions like 30 Doradus in the Large Magellanic Cloud (LMC) and to the masses of the populous blue star clusters found in the LMC and other gas-rich galaxies (e.g., Kennicutt & Chu 1988). The luminosity functions of the knots are well fitted by a power law with slope $dN/dm \sim -2$. They are consistent with the luminosity functions of H II regions and their embedded OB associations (e.g., Kennicutt, Edgar & Hodge 1989, Bresolin & Kennicutt 1997). They are also similar to the young star cluster populations in merger remnants such as NGC 4038-39 (e.g., Zhang & Fall 1999). However, no examples are found in these galaxies of the so-called super star clusters (SSCs) with $M_V < -15$ that are often seen in merger remnants and luminous starburst galaxies. This may be a reflection of the lower total amounts of star formation in these rings rather than any sign of a different cluster mass spectrum. Even if the power-law cluster mass spectra extend to the realm of the SSCs in these objects, the number of SSCs that we expect to observe at any one moment is less than one, based on the total size of the populations observed. We need to observe more central star-forming rings to determine whether they can form SSCs.

The star clusters can be age-dated using multicolor photometry and synthesis models (e.g., Leitherer et al. 1999). These measurements provide a powerful probe of the star-formation histories in the circumnuclear regions. In all four of these galaxies, multiband *HST* imaging in different combinations of *U*, *B*, *V*, *I*, *H*, and Hα have been used to derive reddening-corrected colors, luminosities, and hence age distributions. The galaxies all show a spread in cluster ages from zero to 200–300 Myr. The age distributions are heavily weighted toward younger clusters, but this is readily accounted for by dimming with age and by dynamical disruption effects. When corrections are applied for these processes, the age distributions are generally consistent with a roughly constant cluster formation rate over the past

200–300 Myr (Maoz et al. 2001). However, more sporadic histories cannot be ruled out.

If the rings have been forming stars at the current rate for 0.2 to 0.3 Gyr, the total mass of stars formed is (2–6) $\times 10^8\ M_\odot$ in NGC 1326, NGC 1512, and NGC 5248 and about $2 \times 10^7\ M_\odot$ in NGC 4314. We can check the consistency of these results by comparing the SFRs with the masses of the circumnuclear gas disks. Millimeter measurements of CO emission in the centers of NGC 1326, NGC 4314, and NGC 5248 have been reported by Garcia-Barreto et al. (1991), Combes et al. (1992), Benedict et al. (1996), Sakamoto et al. (1999), Jogee et al. (2002), and Helfer et al. (2003). The corresponding molecular gas masses range from $0.7 \times 10^8\ M_\odot$ in NGC 4314 to (5–12) $\times 10^8\ M_\odot$ in NGC 1326 and NGC 5248. Several authors (e.g., Wilson 1995, Paglione et al. 2001, Regan 2000) have advocated using a lower conversion factor of CO intensity and H_2 column density for these metal-rich environments; if these were used this would reduce the masses by factors of up to 2–3. The gas masses are comparable to the masses of stars already formed in the central disks during the current star-formation burst. This is what one would expect if observations are made at random times during the burst. Combining the gas masses with the SFRs also shows that there is sufficient fuel to feed the current circumnuclear SFRs for another 0.2–1 Gyr. By the time the gas is exhausted, central stellar disks with masses of 10^8 to $10^9\ M_\odot$ will have formed. Of course, the masses are even larger if gas from the galaxies' bars continues to feed the star formation. In the cases of NGC 1326, NGC 1512, and NGC 5248, these masses are several times higher than the mass in stars ($\sim 10^8 M_\odot$, see below) formed in the main exponential disks if the parameters of these disks are extrapolated to the center. In fact, the stellar disks being formed by the star-forming rings have characteristic masses and sizes that are comparable to those of pseudobulges. Thus in these four galaxies, we are almost certainly observing the formation of pseudobulges, or the continued growth of pre-existing pseudobulges.

5.2. General Properties of Circumnuclear Regions

The circumnuclear star-forming rings discussed above are not extreme cases; even higher SFRs are observed at the centers of NGC 1097 and some other nearby galaxies. Nevertheless, before we attempt to characterize the global rates of star formation in these objects, it is important to review the properties of circumnuclear star-forming rings and disks in general. This subject was reviewed by Kennicutt (1998a), with emphasis on the most luminous starburst galaxies. These are nearly always associated with major mergers of gas-rich galaxies that are forming high-mass bulges and elliptical galaxies (Sanders & Mirabel 1996; Kennicutt, Schweizer & Barnes 1998, and references therein). Here, we focus exclusively on the central regions of normal spiral galaxies, where the circumnuclear activity is fed by the kinds of secular processes discussed in this review.

The frequency of occurrence of dense central gas disks and vigorous star formation can be estimated from two independent lines of evidence, surveys of

central star formation in the ultraviolet, visible, or mid-infrared, and CO surveys of central molecular gas. Prominent circumnuclear rings like those in Figure 8 are easily identified. From an ultraviolet imaging survey of 110 nearby spirals, Maoz et al. (1996) estimate that approximately 10% of Sc and earlier-type spirals contain such strong circumnuclear star-forming regions. This is roughly consistent with the frequency of circumnuclear hot-spot galaxies in the survey of Sérsic (1973), which was based on blue photographic plates. Most of these galaxies are barred. This includes all of the galaxies that have ultraviolet-bright rings identified by Maoz et al. (1996), 88% of the hotspot galaxies in the Sérsic (1973) compilation, and 81% of all galaxies with peculiar nuclei identified by Sérsic. Galaxies with strong circumnuclear star formation tend to have Hubble types between Sa and Sbc (Devereux 1987, Pogge 1989, Ho et al. 1997), although there are examples outside of this type range. Altogether, the frequency of circumnuclear rings among the core population of massive, intermediate-type barred galaxies is of order 20%.

Quantifying the star-formation statistics in less spectacularly star-forming galaxy centers is more difficult. In early-type galaxies, the typical levels of extended disk star formation are relatively low (Kennicutt 1998a and references therein). Any nuclear star formation stands out. However, in the gas-rich, late-type spirals that dominate the total star formation in the local universe, it can be difficult to distinguish central star formation that might be associated with pseudobulge growth from the background of general disk star formation.

CO interferometer surveys give a clearer picture. Some of the more comprehensive aperture synthesis CO surveys include studies by Sakamoto et al. (1999), the BIMA Survey of Nearby Galaxies (SONG), (Regan et al. 2001, Helfer et al. 2003, Jogee 1998, Jogee et al. 2004). Studies have also been made by Kenney et al. (1992), Schinnerer et al. (2002, 2003) and many others. Larger samples of galaxies have been observed in the ^{12}CO (1–0) and (2–1) rotational lines using single-dish telescopes, with typical beam diameters of 11–50″ (Young & Devereux 1991; Braine et al. 1993; Böker, Lisenfeld & Schinnerer 2003a). A survey in HCN that includes a large subsample of normal galaxies is given in Gao & Solomon (2004).

These surveys show that central molecular disks are common but not universal. The disks are found more frequently in barred spirals, and their masses tend to be higher in barred systems (Sakamoto et al. 1999, Helfer et al. 2003). Although a few systems show centrally peaked distributions that might be similar to the exponential profiles of stellar disks or pseudobulges, the predominant structures are barlike distributions, bipolar twin-peak distributions (Kenney et al. 1992), circumnuclear rings, spiral arms, or combinations of these structures. In many of these, the gas is unlikely to be in steady-state equilibrium, and the interpretation is complicated by the likelihood that variations in temperature influence the CO emission distributions. We can conclude only that the gas disks have radii that are characteristic of central bars, bulges, and pseudobulges.

The first CO observations that spatially resolved galaxies showed that the distribution of molecular gas often follows the starlight (e.g., Young & Scoville 1991).

Recent observations confirm this result (Regan et al. 2001, Böker et al. 2003a). This occurs even when the stellar brightness rises steeply toward the center, above the extrapolated profile of the outer exponential disk. Five examples are shown in Figure 20. They are all excellent examples of objects in which a bar (top row), oval (middle row), or global spiral structure that reaches the center (NGC 4321 in the bottom row) provides an engine for inward gas transport. For all of these, the molecular gas is very centrally concentrated. Because star formation rates increase faster than linearly with gas density (Figure 21), the observation that the molecular gas density follows the starlight guarantees that star formation will further enhance the density contrast between the (pseudo)bulge and the outer disk. We have discussed several of these objects as typical pseudobulges. The exception in Figure 20 is NGC 7331, a galaxy that contains a probable classical bulge.

When the data from the aperture synthesis surveys are combined with small-beam, single dish measurements (Braine et al. 1993, Böker et al. 2003), the gas masses show a large range, from $\sim 10^6\ M_\odot$ to $2\ \times 10^9\ M_\odot$. Here a standard CO-to-H_2 conversion factor, $X_{CO} = 2.8 \times 10^{20}$ cm^{-2} (K km s^{-1})$^{-1}$, has been used. If instead we use a variable, metallicity-dependent conversion factor (e.g., Wilson 1995, Paglione et al. 2001, Boselli et al. 2002), then this range narrows to $\sim 10^7$–$10^9\ M_\odot$ (Böker et al. 2003a). Pseudobulges are expected to grow to masses at least as large as these. More massive pseudobulges would result if gas continues to be added to the nuclear disks.

Studies of the SFRs in individual systems are too numerous to be listed here, but representative studies include Kennicutt, Keel & Blaha (1989), Pogge (1989), Phillips (1993), Maoz et al. (1996, 2001), Elmegreen et al. (1997, 2002), Usui et al. (1998, 2001), Buta et al. (2000), Colina & Wada (2000), Inoue et al. (2000), Alonso-Herrero & Knapen (2001), Ryder et al. (2001), Benedict et al. (2002), and Knapen et al. (2002). In these studies a variety of star-formation tracers have been used, including measurements of ultraviolet and infrared continua, and Hα, Pα, Brγ, and other hydrogen recombination lines (see Kennicutt 1998a). The Spitzer Space Telescope will have a strong impact on this subject by providing spatially resolved maps of the thermal-infrared dust emission from these regions.

SFRs measured by different authors are generally consistent at the factor-of-two level; this is comparable to the uncertainties that are typically quoted for these highly dust-attenuated regions. Although this limits the reliability of SFRs for any individual object, good measurements are available for $\sim$40 galaxies, and this is sufficient to characterize the range of star-formation properties. The absolute SFRs within circumnuclear rings and disks range over a factor of about a thousand, from 0.01 to 10 $M_\odot$ yr^{-1}. This covers the range of SFRs observed in our case studies and is comparable to the range observed in the integrated SFRs of normal spiral galaxies (Kennicutt 1998a and references therein). The central star formation accounts for 10–100% of the total SFR of spiral galaxies. The highest fractions occur in early-type galaxies, which typically have low SFRs in their outer disks (Kennicutt 1983, 1998a).

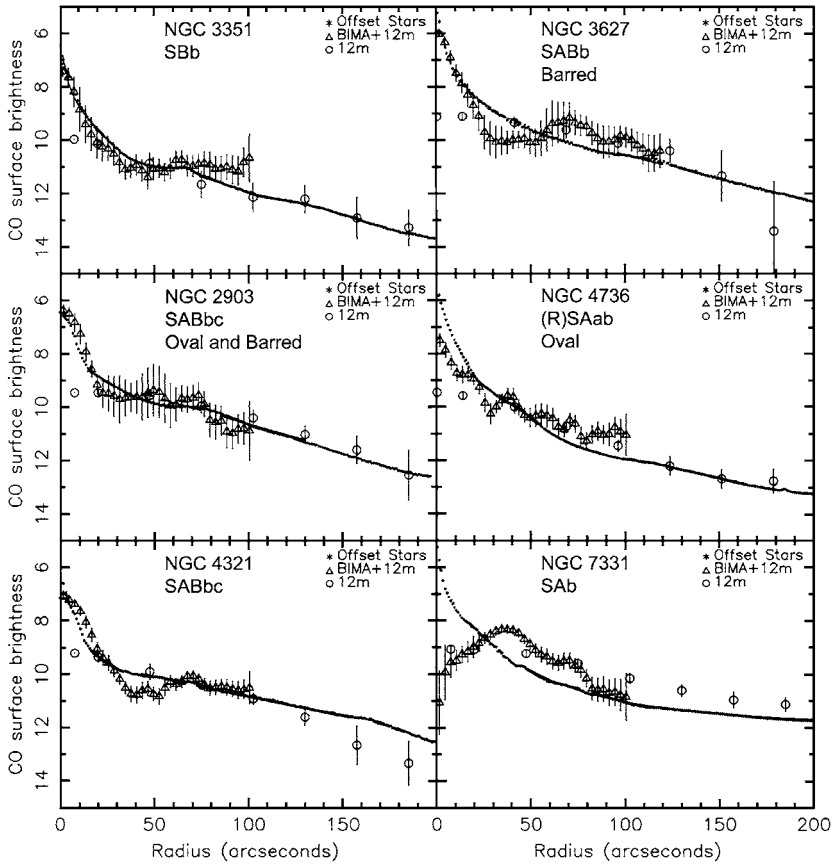

Figure 20 Radial profiles of CO and stellar K-band surface brightness from the BIMA SONG (adapted from Regan et al. 2001). CO surface brightness is in magnitudes of Jy km s^{-1} $arcsec^{-2}$ with zeropoint at 1000 Jy km s^{-1} $arcsec^{-2}$. The stellar surface brightness profiles have been shifted vertically to the CO profiles. Morphological types are from the RC3. NGC 2903 and 3627 are clearly barred in the K-band images shown in Regan et al. (2001). NGC 2903 and 4736 are oval galaxies (Section 3.2). NGC 4736 contains a prototypical pseudobulge; it is also illustrated in Figures 2, 8, and 17. NGC 4321 is an unbarred galaxy with no ILR (discussed in Section 3.4). All galaxies in this figure except NGC 7331 have structures that are expected to cause gas to flow toward the center. NGC 7331 is included to show the very different CO profile in a galaxy with a probable classical bulge.

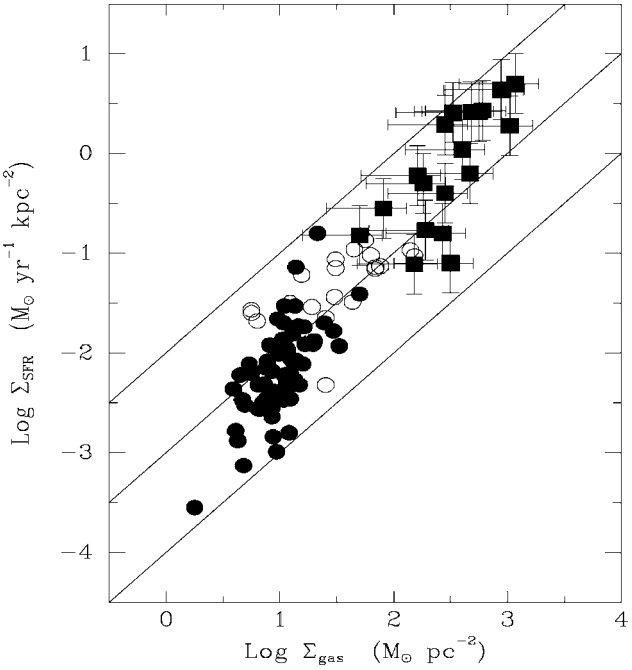

Figure 21 Correlation between SFR surface density and total gas surface density for 20 circumnuclear star-forming rings (*filled squares with error bars*) compared to disk-averaged values for 61 spiral galaxies (*filled circles*) and the centers of these galaxies (*open circles*). The circumnuclear data are compiled in this paper, and the comparison data are from Kennicutt (1998b). The solid diagonal lines show constant gas consumption timescales (increasing downward) of 0.1, 1, and 10 Gyr.

5.3. Constraining Evolution Timescales and Pseudobulge Growth

The data on SFRs and gas contents of the central regions of galaxies can be combined to constrain the evolutionary timescales and formation rates of pseudobulges. We first consider the prominent circumnuclear star-forming rings, which represent only the high-luminosity extreme of this activity, but for which we can derive relatively hard constraints. A search of the literature reveals 20 galaxies with circumnuclear star formation and reliable data on the SFRs, central gas masses, and sizes of the star-forming regions. For each galaxy, we derived the mean molecular gas surface density (using standard CO−H_2 conversion factors) and the mean SFR surface density within the circumnuclear regions. These are plotted as filled squares with error bars in Figure 21. The large error bars reflect considerable uncertainties in the SFRs owing to dust extinction and possible AGN contamination and uncertainties in the CO−H_2 conversions that provide the gas masses. Ignoring atomic gas introduces another uncertainty, but this is expected to be of order 10%

or less. Figure 21 also shows the disk-averaged SFR and total gas densities for 61 spiral galaxies (solid circles), and the same data for the centers of those galaxies when spatially resolved data are available (open circles).

Figure 21 clearly shows that the circumnuclear rings populate a unique regime of molecular gas density and SFR. They extend the Schmidt SFR power law that is seen in the other galaxies (Kennicutt 1998b). For the sake of consistency, we adopted the same standard CO–H_2 conversion factor for all of the points; adopting a lower conversion factor for the centers would move the filled squares and open circles to the left by as much as 0.3 to 0.5 dex. This would increase the best-fitting Schmidt-law slope from $N \sim 1.4$ to $N \sim 1.5$.

The same diagram can be used to constrain the timescale on which the circumnuclear gas disks turn into stellar disks. Figure 21 shows lines of constant gas consumption times of 0.1, 1, and 10 Gyr. The outer star-forming disks of these galaxies are characterized by mean star-formation efficiencies of approximately 5% per 10^8 yr and gas depletion times of $\sim$2 Gyr on average. However, the star-formation efficiencies in most of the circumnuclear disks are much higher, of order 10–50% per 10^8 years. Gas consumption timescales are $0.2-1$ Gyr. If we assume that we observe the average disk at the midpoint of a gas accretion and starburst episode, this means that the typical formation timescales for these pseudobulges is approximately 0.4–2 Gyr, consistent with the (luminosity-averaged) star cluster ages of 0.0–0.3 Gyr inferred in the *HST* studies cited earlier. If a lower CO$-H_2$ conversion factor is appropriate in these regions, we overestimate the molecular masses, and the inferred timescales would be lowered by a comparable amount.

We can now construct a rough picture of the growth rates of pseudobulges in present-day spirals. The results above imply a typical formation timescale for the central disks of $\sim$1 Gyr. When we combine this with a typical SFR range of $0.1-10\ M_\odot\ \mathrm{yr}^{-1}$, gas accretion episodes will form pseudobulges with masses of order 10^7–$10^{10}\ M_\odot$. Typical systems like the examples in Figure 8 fall in the 10^8 to $3\ \times 10^9\ M_\odot$ range. Circumnuclear star-forming rings of this type are seen in $\sim$10% of intermediate-type spiral galaxies (Sérsic 1973, Maoz et al. 1996). As discussed above, lookback studies suggest that strong bars first formed at least 5 Gyr ago. Combining these numbers suggests that about half of unbarred spirals and nearly all barred spirals may have formed pseudobulges in this mass range. Of course, this rough calculation is subject to a chain of possible systematic errors. However, it demonstrates the plausibility of a scenario in which pseudobulges are a common or even ubiquitous constituent of intermediate Hubble-type, massive spiral galaxies.

So far, our results are based solely on the occurrence of the most prominent circumnuclear star-forming rings in barred galaxies. Is there independent evidence based on the statistics of central molecular gas disks for lower levels of star formation in central pseudobulge disks? To make such an estimate, we used the BIMA SONG survey (Helfer et al. 2003) to derive the median central molecular gas surface density in their unbiased sample of 44 nearby spiral galaxies. This is

$\sim$200 $M_\odot$ pc^{-2}, for a standard CO—H_2 conversion factor. This gas density already exceeds the central stellar surface density in most local spiral disks, which, from surface brightness measurements and M/L$_B$ $\simeq$ 1, is $\sim$130 $M_\odot$ pc^{-2}. Consequently, if the current gas disks are converted into stars, the central surface brightness of the disk more than doubles. If the gas infall continues for a few Gyr, a still brighter stellar component should form.

We can make a similar calculation by using Figure 21 to estimate the typical SFR densities in the centers of barred galaxies, and combine it with the typical star-formation timescales derived earlier to estimate the total surface density of stars formed. This calculation is not entirely independent, because the star-formation timescales are partly derived from the measured molecular gas densities. However, there are independent constraints on the star-formation timescales from *HST* studies of star clusters in circumnuclear starbursts and from photometric constraints derived from integrated light. For a typical SFR density of 0.1–1 $M_\odot$ yr^{-1} kpc^{-2} (Figure 21), we expect to build up central stellar densities of 50$-$500 $M_\odot$ pc^{-2} for star-formation lifetimes of 0.5 Gyr, and 500$-$5000 $M_\odot$ pc^{-2} if the feeding of gas from the bar persists for 5 Gyr. This compares to Freeman (1970a) disk central densities of $\sim$100–250 $M_\odot$ pc^{-2} for $M/L_B = 1-2$. The total masses in these components are of the same order as the observed molecular gas disks in the centers of these galaxies, 10^7–10^9 $M_\odot$, if there is no continued feeding of the nuclear disks, and may be up to 5 times larger if the gas feeding persists for 5 Gyr at a rate that is sufficient to replace the mass lost from star formation.

We reiterate that there are large uncertainties in these numbers. The most important uncertainties are the total duration of the inward gas transport in the bars, the CO—H_2 conversion factors used to estimate the molecular gas masses, and uncertainty in separating psudobulge star formation from steady-state disk and/or nuclear star formation. However, we believe that in a typical barred spiral, the total central star formation that results from secular gas inflow can easily exceed that in the underlying disk. By the same token, even the high end of the mass ranges described here falls 1 to 2 orders of magnitude short of the massive bulges that are typical of giant S0–Sab and elliptical galaxies.

6. COSMOLOGICAL IMPLICATIONS OF SECULAR EVOLUTION

6.1. Evolution Along the Hubble Sequence

The qualitative arguments in Sections 2–4 and the star-formation measures in Section 5 imply that secular evolution increases bulge-to-total luminosity ratios B/T. How much evolution along the Hubble sequence is plausible?

This question is too important to be postponed, but we warn readers that the results of this section are very uncertain. To address the question, we compare predicted B/T ratios with the distribution of values observed by Simien & de

Vaucouleurs (1986). They decomposed the *B*-band surface brightness profiles of 98 galaxies to measure B/T as a function of RC2 type. They added up all of the central light in excess of the inward extrapolation of exponentials fitted to the outer disks, so B/T measures the sum of bulge and pseudobulge light. They found that B/T is typically 2% in Sd galaxies, 9% in Sc galaxies, 16% in Sbc galaxies, 24% in Sb galaxies, and 41% in Sa galaxies. The scatter around these values is large. In Sections 5.1 and 5.2, we estimate that circumnuclear star-forming rings grow pseudobulges with masses of $\sim 10^9\ M_\odot$. The plausible range of these masses is also large, from $\sim 10^7$ to $10^{10}\ M_\odot$. The total stellar masses of these galaxies are of order (1 to 5) $\times\ 10^{10}\ M_\odot$. Therefore secular evolution can reasonably have produced pseudobulges with masses ranging from 0% to >10% of the total stellar masses of the systems. This is comparable to the B/T value in Sc galaxies, consistent with our conclusion that Scs contain pseudobulges. Evolution of one Hubble stage—e.g., from Sd to Sc—is plausible at the late end of the Hubble sequence. Evolution from Sc to Sbc is also plausible.

However, it is less easy for secular processes to form the more massive bulges of S0–Sb galaxies. The B/T ratio in these galaxies is large, and the galaxies tend to be very massive. Total bulge masses are at least $10^{10} - 10^{11}\ M_\odot$. The evidence from stellar populations (Section 8.1) is that the stars in these bulges formed quickly and long ago. We conclude that the stars in these bulges formed mostly during hierarchical clustering. That is, S0–Sb galaxies mainly contain classical bulges. Secular processes can contribute modestly to the growth of classical bulges, but evolution by half of a Hubble stage is expected to be unusual. Based on present star formation rates, Sab galaxies like NGC 4736 that have dominant pseudobulges should be rare.

In fact, they are not extremely rare, and even some S0s have pseudobulges. The above estimates are lower limits for at least two reasons. First, disk galaxies presumably contained more gas in the past. Second, some secular processes, such as buckling instabilities, do not depend on concurrent star formation. They elevate pre-existing disk stars into the pseudobulge.

6.2. Merger-Induced Versus Secular Star Formation in Bulges

Finally, we make a preliminary comparison of the relative importance of secular and merger-induced star formation in the present universe. As shown above, it is plausible that most of the stars in Sc–Sm (pseudo)bulges and a significant fraction of the stars in Sb–Sbc (pseudo)bulges formed as a result of secular evolution. Given the relative numbers of early- and late-type galaxies, classical bulges and pseudobulges are not very different in number. However, the masses of (mostly) classical bulges in early-type galaxies are at least one to two orders of magnitude larger than the masses of pseudobulges in late-type spirals. Integrated over the history of the universe, star formation caused by secular processes has contributed at most a few percent of bulge stars. The vast majority of bulge stars are believed to have formed in collapse and merger events.

However, most of these events occurred in the distant past. Observations show that merger rates increase dramatically with increasing cosmic lookback time (Patton et al. 2002, Conselice et al. 2003). The fractional contribution of galaxy interactions and mergers to the total present-day SFR in the universe has been estimated by many workers, starting with Larson & Tinsley (1978). Kennicutt et al. (1987) estimated that 6% $\pm$ 3% of current star formation is induced by galaxy-galaxy interactions. This contains two, partly compensating uncertainties. It underestimates dust-extincted star formation in bulges, but it overestimates bulge star formation because it includes a contribution from distant tidal interactions as well as mergers. How does this value compare to the contribution from secular evolution? In Section 5.3, we note that $\sim$10% of intermediate-type spirals contain circumnuclear disks or rings and that their star formation accounts for 10–80% of the current SFR in those galaxies. These same intermediate-type spirals dominate the current total cosmic SFR (Brinchmann et al. 2003). Combining these numbers suggests that a few percent of present-day star formation is attributable to secular processes. Thus, galaxy mergers and secular evolution produce comparable star formation in the present universe. Both contributions are small compared with the dominant source of star formation at $z = 0$, namely the quiescent star formation in the disks of spiral and irregular galaxies. Nevertheless, as argued in the Introduction, we live approximately at the epoch of transition when secular processes are overtaking mergers as the primary mechanism that forms stars in the central parts of galaxies. We emphasize again that all the estimates in Sections 6.1 and 6.2 are very uncertain.

7. COMPLICATIONS

This section covers issues that complicate the identification of pseudobulges. They do not threaten the conclusion that pseudobulges form by secular evolution of disks; on the contrary, they make it likely that such evolution has operated even in situations where this is not obvious. They highlight areas that need further work.

7.1. Pseudobulges Do Not Have To Be Flat

Several dynamical heating processes are expected to puff pseudobulges up in the axial direction. We are fortunate that some pseudobulges are disky enough so that we can detect the smoking gun that points to a secular origin. It is plausible that others are so similar to classical bulges that they cannot easily be recognized.

One heating mechanism that we have already discussed is bar buckling (Section 4.5). If the density profile along the ridge line of the bar is not too steep, then buckled bars produce box-shaped structures that can easily be recognized when they are seen edge-on.

Resonant vertical heating by the bar may also be important (Pfenniger 1984, 1985; Pfenniger & Norman 1990; Friedli 1999). It is not limited to the relatively

few stars that are in resonance at any one time, because the radii of all resonances change as the central concentration increases.

Another heating mechanism involves in-the-plane instabilities that result if the nuclear disk gets too dense for its velocity dispersion. Secular gas inflow is slow compared with the disk's rotation velocity and even the disk's radial velocity dispersion σ_r. If, as a result, star formation builds up the disk surface density μ without much changing σ_r, then the disk gets less stable. Toomre (1964) showed that violent instability sets in when $Q \equiv \sigma_r/\sigma_{\rm crit} \rightarrow 1$, where $\sigma_{\rm crit} = 3.36G\,\mu/\kappa$. Gas inflow increases both the density and the epicyclic frequency, but density wins and $\sigma_{\rm crit}$ increases as the evolution proceeds. As Q drops toward 1, instabilities should form and heat the growing pseudobulge in the disk plane. Toomre (1966) showed further that buckling instabilities heat the disk vertically if σ_r gets bigger than about 3.3 times the vertical velocity dispersion even if there is no bar. So heating in the plane results in heating perpendicular to the plane. Because the density increases rapidly toward the center, it is unlikely that the result will look box-shaped. Rather, the thickness of the pseudobulge is likely to be larger at smaller radii, much like in a classical bulge.

Finally, at radii that are smaller than the disk thickness, it is no longer relevant that the incoming gas comes from a disk. There is no reason why the innermost parts of a pseudobulge should be flattened at all.

7.2. Pseudobulges Do Not Have To Be Young

Most of this review emphasizes evolution in progress, because this is the easiest way to see that evolution is happening at all. However, we do not mean to create the mistaken impression that pseudobulges must be young or that they must be made of young stars.

Secular evolution is by definition slower than nonequilibrium processes such as mergers, but it can have timescales that are much shorter than a Hubble time. Rates are uncertain, but evolution is thought to be possible on timescales as short as ∼5 galactic rotations. Bars started to be reasonably abundant at least 5 Gyr ago (Abraham et al. 1999, van den Bergh 2002, van den Bergh et al. 2002). Therefore it is possible that secular evolution built some pseudobulges quickly $\gtrsim$5 Gyr ago and then stopped.

Also, heating by bars can elevate disk stars to scale heights characteristic of pseudobulges. These stars can be as old as the oldest disks.

So we expect that pseudobulges have a range of stellar population ages from nearly zero to at least 5 Gyr (e.g., Bouwens, Cayón & Silk 1999). Much older stellar populations are not out of the question; how much older is plausible is not known.

7.3. Demise of Bars II: Is Pseudobulge Formation Self-Limiting?

If building a central mass concentration of 5–10% of the disk mass destroys a bar, does secular evolution then stop? Do we already know the maximum bulge-to-disk ratio B/D that secular evolution can produce?

The answer is probably "no": (*a*) Many SB0 and SBa galaxies have bulge-to-disk ratios of $\sim$1. So bars can coexist with surprisingly large central mass concentrations. (*b*) Once bars grow nonlinear, simple heuristic arguments about how to make a successful bar lose force. In particular, it may no longer be necessary that the radius of ILR be small. (*c*) The simulations that demonstrate bar suicide do not take into account enough physics. Many do not include gas. Almost none allow the bar to interact with all of the components that we see in galaxies. The competition between angular momentum sinks that help to strengthen bars and the damaging effects of pseudobulge building may be weighted more in favor of the angular momentum sinks than current simulations suggest. (*d*) Gravitational tickling of an unbarred galaxy with an encounter (but not a merger) may re-excite a bar (Noguchi 1988; Gerin, Combes & Athanassoula 1990; Barnes & Hernquist 1991).

8. CAVEATS

8.1. Stellar Populations in Classical Bulges and Pseudobulges

Published studies of stellar populations and metallicities promote quite a different view of bulges than the one discussed in this paper. They emphasize that the stellar populations are generally old, metal-rich, and similar to those of elliptical galaxies. On the basis of such evidence, many papers suggest that observations of stellar populations are inconsistent with secular evolution and instead point to early and rapid formation. Do these results reveal a problem with the present picture?

The themes of this section are as follows: Most stellar population studies concentrate on early-type galaxies; their results are consistent with our conclusion that these generally contain classical bulges. In contrast, many Sbc and later-type bulges, plus a few early-type objects with independent evidence for pseudobulges, do contain young stars. However, some galaxies with clearcut evidence for pseudobulges certainly have old stellar populations. At present, we see no compelling collision between stellar population and secular evolution studies. But the situation is not clearcut, and a collision is possible. More than any other subject discussed in this review, the stellar populations of late-type (pseudo)bulges need further work to make sure that there is no fundamental problem or else to uncover it. We concentrate on a few seminal papers that illustrate these points.

Peletier et al. (1999) studied the $B - I$ versus $I - H$ color-color diagram of bulges. They have shown convincingly that dust absorption dominates the central colors in many galaxies, and that colors at the effective radius r_e of the bulge are much less affected by dust. Their conclusions are as follows:

For 13 bulges of S0–Sab galaxies, colors at r_e mostly show little scatter and are consistent with the colors of Coma cluster ellipticals. The authors conclude that the age spread of these bulges is small, at most 2 Gyr, and that the stars formed $\gtrsim$12 Gyr ago. Two early-type galaxies have blue colors indicative of younger ages. NGC 5854 is classified Sa, but Sandage & Bedke (1994) note: "The inner spiral

pattern [of two] is in the bulge (it forms the bulge) and has the form and the sense of the opening of a stubby S." This spiral is more consistent with a pseudobulge than with a classical bulge. Spiral structure requires a dynamically cold system, and indeed, the weighted mean of the best velocity dispersion measurements is 102 ± 4 km s^{-1} (Simien & Prugniel 1997; Vega Beltrán et al. 2001; Falcón-Barroso, Peletier & Balcells 2002). The second "young" bulge is in the S0 galaxy NGC 7457; Kormendy (1993) showed that this has an unusually small velocity dispersion indicative of a pseudobulge. Thus, of 13 early-type bulges discussed in Peletier et al. (1999), the only two that have young stellar populations also are pseudobulges.

Of four Sb bulges, one (NGC 5443) is young; it is also barred. The other three are made of old stars. It is important to note that these include the boxy pseudobulge NGC 5746 (Figure 15).

Peletier et al. (1999) noted that their three Sbc bulges are "considerably bluer, have lower surface brightness, show patchy dust and star formation together, and are rather different from the rest of the galaxies." So the sample is small, but the results in Peletier et al. (1999) are consistent with the present picture that secular evolution dominates late-type bulges but that early-type bulges, on the whole, are like ellipticals. One important new result is that at least one pseudobulge is made of old stars. Generally similar results were found by Bica & Alloin (1987).

Another result that is consistent with and even suggestive of secular evolution is a correlation between bulge color and the color of the adjacent part of the disk (Peletier & Balcells 1996, Gadotti & dos Anjos 2001). Bulges and disks both show large ranges in colors, but "bulges are more like their disk than they are like each other" (Wyse et al. 1997). Also, some bulge colors found in the above studies are indicative of young ages, especially for Sc–Sm galaxies (de Jong 1996c). Bulge and disk scale lengths and surface brightnesses also correlate (see the above papers; Courteau, de Jong, & Broeils 1996, Courteau 1996b). Courteau and collaborators have interpreted these correlations as products of "secular dynamical evolution. . .via angular momentum transfer and viscous [gas] transport."

Finally, Trager (2004) reviewed recent work which shows that bulges of S0/a–Sbc spirals span a large range of ages and [α-element/Fe] abundance enhancements. The latter are a particularly important indicator of star-formation history because α-elements are ejected by massive stars when they explode as supernovae of type II; their abundances are diluted with Fe when type I supernovae become important $\sim$1 Gyr after a starburst. After that, [α-element/Fe] can never again be much greater than the solar value. So overabundances of the α-elements indicate that almost all of the star formation occurred quickly (e.g., Terndrup 1993; Bender & Paquet 1995; Thomas, Greggio & Bender 1999; Thomas, Maraston & Bender 2002; Worthey, Faber & Gonzalez 1992). Trager reviewed evidence that bulges with high luminosities or velocity dispersions show α-element enhancements, but those with low luminosities or velocity dispersions do not. For example, many S0 bulges, which tend to be high in luminosity, tend to have α-element enhancements indicative of rapid formation (e.g., Bender & Paquet 1995; Fisher, Franx, &

Illingworth 1996). These results do not ring alarm bells, but they would be a more decisive test of secular evolution if they included more late-type galaxies.

It is well known that a few S0 bulges have post-starburst spectra, but these are more likely to be the result of galaxy accretions than processes that form either classical or pseudo bulges.

In summary, stellar population data appear reasonably consistent with the conclusion of previous sections that S0–Sb galaxies tend to have classical bulges, and that Sbc–Sm galaxies usually have pseudobulges. However, (*a*) the galaxy samples studied are too heavily weighed toward early-type galaxies to be a decisive test, and (*b*) there certainly exist galaxies that are difficult to understand. For example, while the boxy bulge of the S0 galaxy NGC 7332 is likely to be younger than its disk (Bender & Paquet 1995), the even more boxy bulge of NGC 5746 appears to be old (Peletier et al. 1999).

Finally, the best-studied boxy bulge is the one in our Galaxy. The low-absorption field that has received the most attention is Baade's window. At a Galactic latitude of -4°, it is well up into the boxy part of the bulge revealed by COBE (see figure 1 in Wyse, Gilmore, & Franx 1997). Still, it is almost along the minor axis, so there is a small chance that the stars that define the boxiness are not completely the same as the ones in Baade's window. In any case, the observations imply that bulge stars far from the Galactic plane are old (Terndrup 1993, Ortolani et al. 1995, Feltzing & Gilmore 2000, Kuijken & Rich 2002, Zoccali et al. 2003, all of which also review earlier work; for further review, see Sandage 1986; Wyse, Gilmore, & Franx 1997; Renzini 1999; Rich 1999). The absolute age is uncertain but is approximately 11–13 Gyr. Moreover, moderate α-element overabundances with respect to iron (McWilliam & Rich 1994, Barbuy et al. 1999) again imply rapid star formation over a period of $\lesssim$1 Gyr. Finally, the observed correlation that more metal-poor bulge/halo stars have more eccentric, plunging orbits continues to point to an early collapse with accompanying self-enrichment (Eggen, Lynden-Bell & Sandage 1962; Sandage 1986, 1990). The Galactic bulge is clearly older than a secular evolution picture can easily accommodate. If we try to solve this problem by postulating that the boxy structure was made by heating a pre-existing disk of old stars, then the fact that the bulge and the metal-poor halo are similar in age becomes a coincidence. Also, the Galactic center is currently forming stars at a rate that, if sustained for an appreciable fraction of a Hubble time, adds up to much of the stellar density observed there (Rich 1999). We argue in this paper for the importance of secular evolution, but we would be the last to suggest that the above results are easily understood. Clearly, solving them deserves high priority. On the other hand, the Galactic bulge is clearly boxy. At present, the only model that we have for its origin is via secular processes.

8.2. Can Minor Accretion Events Mimic Pseudobulge Growth?

This is certainly possible. Kannappan, Jansen & Barton (2004) found a correlation between blue-centered, star-forming bulges and evidence of tidal encounters with

neighboring galaxies. Well-known examples are M 82 and NGC 3077, which are connected to M 81 by H I tidal bridges (Yun, Ho & Lo 1994). Counterrotating gas and even stellar components in some galaxies also imply accretion. An example is NGC 4826 (Braun et al. 1994, Rubin 1994, Walterbos et al. 1994, Rix et al. 1995, Garcia-Burillo et al. 2003). However, NGC 4826's pseudobulge signature—a very low stellar velocity dispersion (Kormendy 1993)—is a property of corotating stars and therefore predates the accretion of counterrotating material and has not yet been affected by it. An example of a galaxy with pseudobulge characteristics that may instead be caused by a gas accretion is NGC 7457 (Kormendy & Illingworth 1983, Kormendy 1993, Peletier et al. 1999).

There are three reasons why we suggest that secular evolution accounts for more pseudobulges than do accretion events: (*a*) Many of the most recognizable pseudobulges occur in strongly barred and oval galaxies, especially in ones in which radial dust lanes imply that gas infall is ongoing now. (*b*) If galaxies approach each other closely enough to transfer gas, then their dark matter halos are likely already to overlap and they are likely to merge after a few more orbits. A configuration like the M 81-M 82-NGC 3077 encounter can last for a billion years but not for a significant fraction of a Hubble time and not at all without being recognizable. Most pseudobulge galaxies show no signs of tidal interactions in progress. (*c*) Inhaling a tiny, gas-rich dwarf does no damage to an existing disk, but a major merger heats a thin disk too much to be consistent with flat, edge-on galaxies.

Nevertheless, the relative importance of internal and externally driven secular evolution is not known and needs further study. It is likely that accretions create more than an occasional quasipseudobulge.

8.3. Disky Distortions in Elliptical Galaxies

Some ellipticals contain central disky distortions (see Bender et al. 1989, Kormendy & Djorgovski 1989, Bender 1990b, Kormendy & Bender 1996 for reviews). In the more extreme cases, the line-of-sight velocity distributions show asymmetries or even a two-component structure indicative of a cold, rotating nuclear disk embedded in a more slowly rotating elliptical host (e.g., Franx & Illingworth 1988; Bender 1990a; Bender, Saglia & Gerhard 1994; Scorza & Bender 1995). Because these disks are not self-gravitating, the processes discussed in this paper cannot operate. Therefore there must be some embedded nuclear disks in the earliest-type galaxies that are not related to the themes of this paper.

How are they produced? Minor accretion events in which an elliptical swallows a gas-rich dwarf almost certainly produce some of them, along with the central dust disks commonly observed in ellipticals (see Kormendy & Djorgovski 1989 for a review and Jaffe et al. 1994, van Dokkum & Franx 1995, and Martini et al. 2003 for *HST* images). There is evidence that dust disks gradually turn into small stellar disks (Kormendy et al. 1994, 2004). Alternatively, gas shed by dying stars in the elliptical may, in some cases, cool and fall to the center. These processes are

quite different from secular evolution driven by nonaxisymmetries in dominant, self-gravitating disks.

We do not know whether the tiny nuclear disks seen, for example, in NGC 3115 (e.g., Lauer et al. 1995, Scorza & Bender 1995, Kormendy et al. 1996b) and NGC 4594 (e.g., Burkhead 1991, Kormendy 1988, Seifert & Scorza 1996, Kormendy et al. 1996a) are more nearly related to pseudobulges or to the disky distortions discussed above. The dividing line between the above processes and those that make pseudobulges deserves further investigation. This uncertainty affects only a minority of disky components embedded in the largest, earliest-type classical bulges. It is not a problem for the identification of most pseudobulges in Sb and later-type galaxies.

9. CONCLUSION

9.1. A Preliminary Prescription for Recognizing Pseudobulges

Any prescription must cope with the expected continuum from pure classical bulges built by mergers and rapid collapse through objects with some E-like and some disk-like characteristics to pseudobulges built completely by secular processes. There are still many uncertainties. Keeping them in mind, a preliminary list of pseudobulge characteristics suggested by the previous sections are

1. The candidate pseudobulge is seen to be a disk in images, e.g., its apparent flattening is similar to that of the outer disk.
2. It is or it contains a nuclear bar (in relatively face-on galaxies).
3. It is box shaped (in edge-on galaxies).
4. It has a Sérsic index $n \simeq 1$ to 2.
5. It is more rotation-dominated than are the classical bulges in the $V_{\rm max}/\sigma - \epsilon$ diagram; e.g., $(V_{\rm max}/\sigma)^* > 1$.
6. It is a low-σ outlier in the Faber-Jackson (1976) correlation between (pseudo) bulge luminosity and velocity dispersion.
7. It is dominated by Population I material (young stars, gas, and dust), but there is no sign of a merger in progress.

If any of these characteristics are very well developed, it seems safe to identify the central component as a pseudobulge. The more that any of these characteristics apply, the safer the classification becomes. If several characteristics apply but all are relatively subtle, then the central component may be a pseudobulge or it may be a transition object.

Small bulge-to-total luminosity ratios B/T do not guarantee that the galaxy in question contains a pseudobulge, but if $B/T \gtrsim 1/3$ to $1/2$, it seems safe to conclude that the galaxy contains a classical bulge.

Based on these criteria, galaxies with classical bulges include M 31, M 81, NGC 2841, NGC 3115, and NGC 4594. Galaxies with prototypical pseudobulges include NGC 1291 (Figures 2, 14), NGC 1512 (Figures 3, 8), NGC 1353 (Figure 10), NGC 1365 (Figure 7), NGC 3945 (Figures 5, 14, 17), NGC 4371 (Figure 17), NGC 4736 (Figures 2, 8, 17, 20), and NGC 5377 (Figure 11). The classification of the bulge of our Galaxy is ambiguous; the observation that it is box shaped strongly favors a pseudobulge, but the stellar population age and α-element overabundance are most easily understood if the bulge is classical (Section 8.1).

9.2. Perspective

Secular evolution provides a new collection of physical processes that we need to take into account when we try to understand galaxies. Doing so has already led to significant progress. Thirty years ago, Hubble classification was in active and successful use. However, we also knew about a long list of commonly observed, regular features in disk galaxies, including lenses, boxy bulges, nuclear bars, and nuclear star clusters, that were not understood and not included in the classification schemes. In addition, we knew about uniquely peculiar galaxies (e.g., Arp 1966) that were completely outside the classification process. Now, almost all of the common features and peculiar galaxies have candidate explanations within one of two paradigms of galaxy evolution that originated in the late 1970s. The peculiar objects have turned out mostly to be interacting and merging galaxies. And many of the previously unexplained but common features of disk galaxies now are fundamental to our growing realization that galaxies continue to evolve secularly after the spectacular fireworks of galaxy mergers, dissipative collapse, and their attendant nuclear activity have died down.

ACKNOWLEDGMENTS

We are indebted to Ron Buta and Jerry Sellwood; to scientific editors Geoffrey Burbidge and Allan Sandage; and to the Nuker team, especially Sandy Faber and Scott Tremaine, for penetrating comments on the draft that resulted in important improvements in the final paper. We thank Ralf Bender, Martin Bureau, Andi Burkert, Leo Blitz, Ken Freeman, Sheila Kannappan, Mike Rich, and Guy Worthey for helpful discussions or for permission to quote results before publication. We are exceedingly grateful to Ron Buta and Marcello Carollo for making available many of the digital images used in the construction of figures. Additional figures were kindly made available by Lia Athanassoula, Martin Bureau, Ortwin Gerhard, and Linda Sparke. The color image of NGC 1326 in Figure 8 was constructed for this review by Zolt Levay of STScI from *UBV RI* and $H\alpha$, *HST* PC images provided by Ron Buta. We are most grateful to Mary Kormendy for extensive editorial help. Also, we thank Mark Cornell for technical support and for permission to quote results before publication. This review has made extensive use of the NASA/IPAC Extragalactic Database (NED), which is operated by JPL and Caltech under contract with NASA. We acknowledge the support of NSF grant AST-0307386 and NASA grant NAG5-8426.

LITERATURE CITED

Abraham RG, Merrifield MR, Ellis RS, Tanvir NR, Brinchmann J. 1999. *MNRAS* 308: 569

Aguerri JAL, Debattista VP, Corsini EM. 2003. *MNRAS* 338:465

Alonso-Herrero A, Knapan JH. 2001. *Astron. J.* 122:1350

Andersen DR, Bershady MA, Sparke LS, Gallagher JS, Wilcots EM. 2001. *Ap. J.* 551:L131

Andredakis YC. 1998. *MNRAS* 295:725

Andredakis YC, Peletier RF, Balcells M. 1995. *MNRAS* 275:874

Andredakis YC, Sanders RH. 1994. *MNRAS* 267:283

Aronica G, Athanassoula E, Bureau M, Bosma A, Dettmar R-J, et al. 2003. *Astrophys. Space Sci.* 284:753

Arp H. 1966. *Atlas of Peculiar Galaxies*. Pasadena: California Inst. of Technology

Arsenault R, Boulesteix J, Georgelin Y, Roy J-R. 1988. *Astron. Astrophys.* 200:29

Athanassoula E. 1992a. *MNRAS* 259:328

Athanassoula E. 1992b. *MNRAS* 259:345

Athanassoula E. 2002. *Astrophys. Space Sci.* 281:39

Athanassoula E. 2003. *MNRAS* 341:1179

Athanassoula E, Bosma A, Crézé M, Schwarz MP. 1982. *Astron. Astrophys.* 107:101

Athanassoula E, Misiriotis A. 2002. *MNRAS* 330:35

Bacon R, Bureau M, Cappellari M, Copin Y, Davies R, et al. 2002. In *Galaxies: The Third Dimension*, ed. M Rosado, L Binette, L Arias, p. 179. San Francisco: Astron. Soc. Pac. (astro-ph/0204129)

Balcells M. 2001. In *The Central Kiloparsec of Starbursts and AGN: The La Palma Connection*, ed. JH Knapen, JE Beckman, I Schlosman, TJ Mahoney, p. 140. San Francisco: Astron. Soc. Pac.

Balcells M. 2003. In *JENAM 2002 Galaxy Dynamics Workshop*. ESA. (astro-ph/0301647)

Balcells M, Graham AW, Domínguez-Palmero L, Peletier RF. 2003. *Ap. J.* 582:L79

Barbuy B, Renzini A, Ortolani S, Bica E, Guarnieri MD. 1999. *Astron. Astrophys.* 341:539

Barnes JE, Hernquist LE. 1991. *Ap. J.* 370:L65

Bender R. 1990a. *Astron. Astrophys.* 229:441

Bender R. 1990b. In *Dynamics and Interactions of Galaxies*, ed. R Wielen, p. 232. Berlin: Springer

Bender R, Burstein D, Faber SM. 1992. *Ap. J.* 399:462

Bender R, Burstein D, Faber SM. 1993. *Ap. J.* 411:153

Bender R, Paquet A. 1995. In *IAU Symposium 164, Stellar Populations*, ed. PC van der Kruit, G Gilmore, p. 259. Dordrecht: Kluwer

Bender R, Saglia RP, Gerhard OE. 1994. *MNRAS* 269:785

Bender R, Surma P, Döbereiner S, Möllenhoff C, Madejsky R. 1989. *Astron. Astrophys.* 217:35

Benedict GF, Higdon JL, Jefferys WH, Duncombe R, Hemenway PD, et al. 1993. *Astron. J.* 105:1369

Benedict GF, Howell DA, Jørgensen I, Kenney JDP, Smith BJ. 2002. *Astron. J.* 123:1411

Benedict GF, Smith BJ, Kenney JDP. 1996. *Astron. J.* 111:1861

Berentzen I, Heller CH, Shlosman I, Fricke KJ. 1998. *MNRAS* 300:49

Bertin G. 1983. *Astron. Astrophys.* 127:145

Bertola F, Capaccioli M. 1975. *Ap. J.* 200:439

Bertola F, Capaccioli M. 1977. *Ap. J.* 211:697

Bettoni D, Galletta G. 1994. *Astron. Astrophys.* 281:1

Bica E, Alloin D. 1987. *Astron. Astrophys. Suppl.* 70:281

Bica E, Alloin D, Schmidt AA. 1990. *Astron. Astrophys.* 228:23

Binggeli B, Barazza F, Jerjen H. 2000. *Astron. Astrophys.* 359:447

Binggeli B, Jerjen H. 1998. *Astron. Astrophys.* 333:17
Binggeli B, Sandage A, Tammann GA. 1985. *Astron. J.* 90:1681
Binggeli B, Sandage A, Tarenghi M. 1984. *Astron. J.* 89:64
Binney J. 1976. *MNRAS* 177:19
Binney J. 1978a. *MNRAS* 183:501
Binney J. 1978b. *Comments Ap.* 8:27
Binney J. 1980. *MNRAS* 190:873
Binney J. 1982. In *Morphology and Dynamics of Galaxies, Twelfth Advanced Course of the Swiss Society of Astronomy and Astrophysics*, ed. L Martinet, M Mayor, p. 1. Geneva Observatory: Sauverny
Binney J, Gerhard O. 1993. In *Back to the Galaxy*, ed. SS Holt, F Verter, p. 87. New York: AIP
Binney J, Gerhard OE, Stark AA, Bally J, Uchida KI. 1991. *MNRAS* 252:210
Binney J, Tremaine S. 1987. *Galactic Dynamics*. Princeton: Princeton Univ. Press
Binney JJ, Davies RL, Illingworth GD. 1990. *Ap. J.* 361:78
Blitz L, Spergel DN. 1991. *Ap. J.* 379:631
Block DL, Bertin G, Stockton A, Grosbøl P, Moorwood AFM, Peletier RF. 1994. *Astron. Astrophys.* 288:365
Block DL, Buta R, Puerari I, Knapen JH, Elmegreen BG, et al. 2002. In *The Dynamics, Structure and History of Galaxies*, ed. GS Da Costa, H Jerjen, p. 97. San Francisco: Astron. Soc. Pac.
Block DL, Puerari I, Knapen JH, Elmegreen BG, Buta R, et al. 2001. *Astron. Astrophys.* 375:761
Block DL, Wainscoat RJ. 1991. *Nature* 353:48
Böker T, Förster-Schreiber NM, Genzel R. 1997. *Astron. J.* 114:1883
Böker T, Laine S, van der Marel RP, Sarzi M, Rix H-W, et al. 2002. *Astron. J.* 123:1389
Böker T, Lisenfeld U, Schinnerer E. 2003a. *Astron. Astrophys.* 406:87
Böker T, Sarzi M, McLaughlin DE, van der Marel RP, Rix H-W, et al. 2003b. *Astron. J.* 127:105
Böker T, Stanek R, van der Marel RP. 2003c. *Astron. J.* 125:1073
Böker T, van der Marel RP, Mazzuca J, Rix H-W, Rudnick G, et al. 2001. *Astron. J.* 121:1473
Böker T, van der Marel RP, Vacca WD. 1999. *Astron. J.* 118:831
Boroson T. 1981. *Ap. J. Suppl.* 46:177
Boselli A, Lequeux J, Gavazzi G. 2002. *Astron. Astrophys.* 384:33
Bosma A. 1981a. *Astron. J.* 86:1791
Bosma A. 1981b. *Astron. J.* 86:1825
Bosma A, Ekers RD, Lequeux J. 1977a. *Astron. Astrophys.* 57:97
Bosma A, van der Hulst JM, Sullivan WT. 1977b. *Astron. Astrophys.* 57:373
Bouwens R, Cayón L, Silk J. 1999. *Ap. J.* 516:77
Braine J, Combes F, Casoli F, Dupraz C, Gérin M, et al. 1993. *Astron. Astrophys. Suppl.* 97:887
Braun R, Walterbos RAM, Kennicutt RC, Tacconi LJ. 1994. *Ap. J.* 420:558
Bresolin F, Kennicutt RC. 1997. *Ap. J.* 113:975
Brinchmann J, Charlot S, White SDM, Tremonti C, Kauffmann G, et al. 2003. *MNRAS.* In press (astro-ph/0311060)
Burbidge EM, Burbidge GR. 1959. *Ap. J.* 130:20
Burbidge EM, Burbidge GR. 1960. *Ap. J.* 132:30
Burbidge EM, Burbidge GR. 1962. *Ap. J.* 135:366
Bureau M, Freeman KC. 1999. *Astron. J.* 118:126
Burkhead MS. 1991. *Astron. J.* 102:893
Burstein D, Bender R, Faber SM, Nolthenius R. 1997. *Astron. J.* 114:1365
Buta R. 1986a. *Ap. J. Suppl.* 61:609
Buta R. 1986b. *Ap. J. Suppl.* 61:631
Buta R. 1988. *Ap. J. Suppl.* 66:233
Buta R. 1990. *Ap. J.* 351:62
Buta R. 1995. *Ap. J. Suppl.* 96:39
Buta R. 1999. *Astrophys. Space Sci.* 269-270: 79
Buta R. 2000. In *Toward a New Millennium in Galaxy Morphology*, ed. DL Block, I Puerari, A Stockton, D Ferreira, p. 79. Dordrecht: Kluwer
Buta R, Block DL. 2001. *Ap. J.* 550:243

Buta R, Combes F. 1996. *Fund. Cosmic Phys.* 17:95

Buta R, Corwin HG, Odewahn SC. 2004. In *The de Vaucouleurs Atlas of Galaxies*. Cambridge: Cambridge Univ. Press. In preparation

Buta R, Crocker DA. 1991. *Astron. J.* 102:1715

Buta R, Crocker DA. 1993. *Astron. J.* 105:1344

Buta R, Purcell GB. 1998. *Astron. J.* 115:484

Buta R, Treuthardt PM, Byrd GG, Crocker DA. 2000. *Astron. J.* 120:1289

Byrd G, Rautiainen P, Salo H, Buta R, Crocker DA. 1994. *Astron. J.* 108:476

Caon N, Capaccioli M, D'Onofrio M. 1993. *MNRAS* 265:1013

Carlberg RG. 1987. In *Nearly Normal Galaxies: From the Planck Time to the Present*, ed. SM Faber, p. 131. Berlin: Springer-Verlag

Carollo CM. 1999. *Ap. J.* 523:566

Carollo CM. 2004. In *Carnegie Observatories Astrophysics Series, Vol. 1: Coevolution of Black Holes and Galaxies*, ed. LC Ho, p. 232. Cambridge: Cambridge Univ. Press

Carollo CM, Ferguson HC, Wyse RFG, eds. 1999. *The Formation of Galactic Bulges*. Cambridge: Cambridge Univ. Press

Carollo CM, Stiavelli M. 1998. *Astron. J.* 115:2306

Carollo CM, Stiavelli M, de Zeeuw PT, Mack J. 1997. *Astron. J.* 114:2366

Carollo CM, Stiavelli M, de Zeeuw PT, Seigar M, Dejonghe H. 2001. *Ap. J.* 546:216

Carollo CM, Stiavelli M, Mack J. 1998. *Astron. J.* 116:68

Carollo CM, Stiavelli M, Seigar M, de Zeeuw PT, Dejonghe H. 2002. *Astron. J.* 123: 159

Cole S, Lacey C. 1996. *MNRAS* 281:716

Colina L, García Vargas ML, Mas-Hesse JM, Alberdi A, Krabbe A. 1997. *Ap. J.* 484:L41

Colina L, Wada K. 2000. *Ap. J.* 529:845

Combes F. 1991. In *IAU Symp. 146, Dynamics of Galaxies and Their Molecular Cloud Distributions*, ed. F Combes, F Casoli, p. 255. Dordrecht: Kluwer

Combes F. 1994. In *Mass-Transfer Induced Activity in Galaxies*, ed. I Shlosman, p. 170. Cambridge: Cambridge Univ. Press

Combes F. 1998. In *IAU Symp. 184, The Central Regions of the Galaxy and Galaxies*, ed. Y Sofue, p. 257. Dordrecht: Kluwer

Combes F. 2000. In *Dynamics of Galaxies: From the Early Universe to the Present*, ed. F Combes, GA Mamon, V Charmandaris, p. 15. San Francisco: ASP

Combes F. 2001. In *Galaxy Disks and Disk Galaxies*, ed. JG Funes, EM Corsini, p. 213. San Francisco: ASP

Combes F, Debbasch F, Friedli D, Pfenniger D. 1990. *Astron. Astrophys.* 233:82

Combes F, Gerin M, Nakai N, Kawabe R, Shaw MA. 1992. *Astron. Astrophys.* 259:L27

Combes F, Sanders RH. 1981. *Astron. Astrophys.* 96:164

Conselice CJ, Bershady MA, Dickinson M, Papovich C. 2003. *Astron. J.* 126:1183

Contopoulos G. 1980. *Astron. Astrophys.* 81:198

Contopoulos G, Mertzanides C. 1977. *Astron. Astrophys.* 61:477

Copin Y, Cretton N, Emsellem E. 2004. *Astron. Astrophys.* 415:889

Corsini EM, Debattista VP, Aguerri JAL. 2003. *Ap. J.* 599:L29

Courteau S. 1996a. *Ap. J. Suppl.* 103:363

Courteau S. 1996b. In *New Extragalactic Perspectives in the New South Africa*, ed. DL Block, JM Greenberg, p. 255. Dordrecht: Kluwer

Courteau S, de Jong RS, Broeils AH. 1996. *Ap. J.* 457:L73

Crosthwaite LP, Turner JL, Buchholz L, Ho PTP, Martin RN. 2002. *Astron. J.* 123:1892

Curran SJ, Polatidis AG, Aalto S, Booth RS. 2001a. *Astron. Astrophys.* 368:824

Curran SJ, Polatidis AG, Aalto S, Booth RS. 2001b. *Astron. Astrophys.* 373:459

Davidge TJ, Courteau S. 2002. *Astron. J.* 123:1438

Davies RL, Efstathiou G, Fall SM, Illingworth G, Schechter PL. 1983. *Ap. J.* 266:41

Debattista VP, Corsini EM, Aguerri JAL. 2002. *MNRAS* 332:65

Debattista VP, Williams TB. 2001. In *Galaxy Disks and Disk Galaxies*, ed. JG Funes, EM Corsini, p. 553. San Francisco: ASP

de Carvalho RR, da Costa LN. 1987. *Astron. Astrophys.* 171:66
de Jong RS. 1996a. *Astron. Astrophys. Suppl.* 118:557
de Jong RS. 1996b. *Astron. Astrophys.* 313:45
de Jong RS. 1996c. *Astron. Astrophys.* 313:377
de Jong RS, van der Kruit PC. 1994. *Astron. Astrophys. Suppl.* 106:451
de Souza RE, dos Anjos S. 1987. *Astron. Astrophys. Suppl.* 70:465
de Vaucouleurs G. 1948. *Ann. Astrophys.* 11:247
de Vaucouleurs G. 1959. *Handb. Phys.* 53:275
de Vaucouleurs G. 1963. *Ap. J. Suppl.* 8:31
de Vaucouleurs G. 1974. In *IAU Symp. 58, The Formation and Dynamics of Galaxies*, ed. JR Shakeshaft, p. 335. Dordrecht: Reidel
de Vaucouleurs G. 1975. *Ap. J. Suppl.* 29:193
de Vaucouleurs G, de Vaucouleurs A, Corwin HG, Buta RJ, Paturel G, Fouqué P. 1991. *Third Reference Catalogue of Bright Galaxies*. Berlin: Springer-Verlag
Devereux N. 1987. *Ap. J.* 323:91
Devereux NA, Kenney JDP, Young JS. 1992. *Astron. J.* 103:784
de Zeeuw PT, Bureau M, Emsellem E, Bacon R, Carollo CM, et al. 2002. *MNRAS* 329: 513
Díaz RJ, Dottori H, Vera-Villamizar N, Carranza G. 2002. In *Disks of Galaxies: Kinematics, Dynamics and Perturbations*, ed. E Athanassoula, A Bosma, R Mujica, p. 278. San Francisco: ASP
Díaz RJ, Pagel BEJ, Edmunds MG, Phillips MM. 1982. *MNRAS* 201:P49
Djorgovski S, Davis M. 1987. *Ap. J.* 313:59
Djorgovski S, de Carvalho R, Han M-S. 1988. In *The Extragalactic Distance Scale*, ed. S van den Bergh, CJ Pritchet, p. 329. San Francisco: ASP
D'Onofrio M, Capaccioli M, Caon N. 1994. *MNRAS* 271:523
D'Onofrio M, Capaccioli M, Merluzzi P, Zaggia S, Boulesteix J. 1999. *Astron. Astrophys. Suppl.* 134:437
Dressler A, Lynden-Bell D, Burstein D, Davies RL, Faber SM, et al. 1987. *Ap. J.* 313:42
Duus A, Freeman KC. 1975. In *La Dynamique des Galaxies Spirales*, ed. L Weliachew, p. 419. Paris: CNRS
Dwek E, Arendt RG, Hauser MG, Kelsall T, Lisse CM, et al. 1995. *Ap. J.* 445:716
Eggen OJ, Lynden-Bell D, Sandage AR. 1962. *Ap. J.* 136:748
Elmegreen BG. 1996. In *Barred Galaxies*, ed. R Buta, DA Crocker, BG Elmegreen, p. 197. San Francisco: ASP
Elmegreen BG, Elmegreen DM. 1985. *Ap. J.* 288:438
Elmegreen BG, Elmegreen DM, Brinks E, Yuan C, Kaufman M, et al. 1998. *Ap. J.* 503:L119
Elmegreen BG, Wilcots E, Pisano DJ. 1998. *Ap. J.* 494:L37
Elmegreen DM, Chromey FR, McGrath EJ, Ostenson JM. 2002. *Astron. J.* 123:1381
Elmegreen DM, Chromey FR, Santos M, Marshall D. 1997. *Astron. J.* 114:1850
Emsellem E, Greusard D, Combes F, Friedli D, Leon S, et al. 2001. *Astron. Astrophys.* 368:52
Englmaier P, Gerhard O. 1997. *MNRAS* 287:57
Erwin P. 2004. *Astron. Astrophys.* 415:941
Erwin P, Sparke LS. 1999. *Ap. J.* 521:L37
Erwin P, Sparke LS. 2002. *Astron. J.* 124:65
Erwin P, Sparke LS. 2003. *Ap. J. Suppl.* 146:299
Erwin P, Vega Beltrán JC, Graham AW, Beckman JE. 2003. *Ap. J.* 597:929
Eskridge PB, Frogel JA, Pogge RW, Quillen AC, Berlind AA. 2002. *Ap. J. Suppl.* 143:73
Eskridge PB, Frogel JA, Pogge RW, Quillen AC, Davies RL, et al. 2000. *Astron. J.* 119:536
Eskridge PB, Frogel JA, Taylor VA, Windhorst RA, Odewahn SC, et al. 2003. *Ap. J.* 586:923
Evans DS. 1951. *MNRAS* 111:526
Faber SM, Dressler A, Davies RL, Burstein D, Lynden-Bell D, et al. 1987. In *Nearly Normal Galaxies: From the Planck Time to the Present*, ed. SM Faber, p. 175. Berlin: Springer-Verlag
Faber SM, Jackson RE. 1976. *Ap. J.* 204:668
Falcón-Barroso J, Bacon R, Bureau M, Cappellari M, Davies RL, et al. 2004. *Astron. Nachr.* 325:92
Falcón-Barroso J, Peletier RF, Balcells M. 2002. *MNRAS* 335:741
Fall SM. 1981. *Ap. J.* 257:230

Fathi K, Peletier RF. 2003. *Astron. Astrophys.* 407:61
Feltzing S, Gilmore G. 2000. *Astron. Astrophys.* 355:949
Fisher D, Franx M, Illingworth G. 1996. *Ap. J.* 459:110
Fisher D, Illingworth G, Franx M. 1994. *Astron. J.* 107:160
Franx M, de Zeeuw T. 1992. *Ap. J.* 392:L47
Franx M, Illingworth GD. 1988. *Ap. J.* 327:L55
Freeman KC. 1970a. *Ap. J.* 160:811
Freeman KC. 1970b. In *IAU Symp. 38, The Spiral Structure of Our Galaxy*, ed. W Becker, G Contopoulos, p. 351. Dordrecht: Reidel
Freeman KC. 1975. In *IAU Symp. 69, Dynamics of Stellar Systems*, ed. A Hayli, p. 367. Dordrecht: Reidel
Freeman KC. 2000. In *Toward a New Millennium in Galaxy Morphology*, ed. DL Block, I Puerari, A Stockton, D Ferreira, p. 119. Dordrecht: Kluwer
Frei Z, Guhathakurta P, Gunn JE, Tyson JA. 1996. *Astron. J.* 111:174
Frenk CS, White SDM, Davis M, Efstathiou G. 1988. *Ap. J.* 327:507
Friedli D. 1996. In *Barred Galaxies*, ed. R Buta, DA Crocker, BG Elmegreen, p. 378. San Francisco: ASP
Friedli D. 1999. In *The Evolution of Galaxies on Cosmological Timescales*, ed. JE Beckman, TJ Mahoney, p. 88. San Francisco: ASP
Friedli D, Benz W. 1993. *Astron. Astrophys.* 268:65
Friedli D, Benz W. 1995. *Astron. Astrophys.* 301:649
Friedli D, Martinet L. 1993. *Astron. Astrophys.* 277:27
Friedli D, Pfenniger D. 1991. In *IAU Symp. 146, Dynamics of Galaxies and Their Molecular Cloud Distributions*, ed. F Combes, F Casoli, p. 362. Dordrecht: Kluwer
Friedli D, Wozniak H, Rieke M, Martinet L, Bratschi P. 1996. *Astron. Astrophys. Suppl.* 118:461
Gadotti DA, dos Anjos S. 2001. *Astron. J.* 122:1298
Gallagher JS, Goad JW, Mould J. 1982. *Ap. J.* 263:101
Gao Y, Solomon PM. 2004. *Ap. J. Suppl.* 152:63
García-Barreto JA, Dettmar R-J, Combes F, Gerin M, Koribalski B. 1991. *Rev. Mex. Astron. Astrofs.* 22:197
García-Burillo S, Combes F, Hunt LK, Boone F, Baker AJ, et al. 2003. *Astron. Astrophys.* 407:485
García-Burillo S, Sempere MJ, Combes F, Neri R. 1998. *Astron. Astrophys.* 333:864
Geha M, Guhathakurta P, van der Marel RP. 2002. *Astron. J.* 124:3073
Gerin M, Combes F, Athanassoula E. 1990. *Astron. Astrophys.* 230:37
Gerin M, Nakai N, Combes F. 1988. *Astron. Astrophys.* 203:44
Gerssen J, Kuijken K, Merrifield MR. 1999. *MNRAS* 306:926
Gerssen J, Kuijken K, Merrifield MR. 2003. *MNRAS* 345:261
Gnedin OY, Goodman J, Frei Z. 1995. *Astron. J.* 110:1105
Gordon KD, Hanson MM, Clayton GC, Rieke GH, Misselt KA. 1999. *Ap. J.* 519:165
Graham A. 2001. *Ap. J.* 121:820
Graham A, Lauer TR, Colless M, Postman M. 1996. *Ap. J.* 465:534
Greusard D, Friedli D, Wozniak H, Martinet L, Martin P. 2000. *Astron. Astrophys. Suppl.* 145:425
Griv E, Chiueh T. 1998. *Ap. J.* 503:186
Hackwell JA, Schweizer F. 1983. *Ap. J.* 265:643
Hasan H, Norman C. 1990. *Ap. J.* 361:69
Hasan H, Pfenniger D, Norman C. 1993. *Ap. J.* 409:91
Helfer TT, Thornley MD, Regan MW, Wong T, Sheth K, et al. 2003. *Ap. J. Suppl.* 145: 259
Heller CH, Shlosman I. 1996. *Ap. J.* 471:143
Ho LC, Filippenko AV, Sargent WLW. 1997. *Ap. J.* 487:568
Hughes MA, Alonso-Herrero A, Axon D, Scarlata C, Atkinson J, et al. 2003. *Astron. J.* 126:742
Hummel E, van der Hulst JM, Keel WC. 1987. *Astron. Astrophys.* 172:32
Illingworth G. 1977. *Ap. J.* 218:L43
Illingworth G, Schechter PL. 1982. *Ap. J.* 256:481

Inoue AK, Hirashita H, Kamaya H. 2000. *Astron. J.* 120:2415
Jaffe W, Ford HC, O'Connell RW, van den Bosch FC, Ferrarese L. 1994. *Astron. J.* 108:1567
Jarrett TH, Chester T, Cutri R, Schneider SE, Huchra JP. 2003. *Astron. J.* 125:525
Jarvis B. 1987. *Astron. J.* 94:30
Jarvis B. 1990. In *Dynamics and Interactions of Galaxies*, ed. R Wielen, p. 416. New York: Springer
Jarvis BJ. 1986. *Astron. J.* 91:65
Jarvis BJ, Dubath P, Martinet L, Bacon R. 1988. *Astron. Astrophys. Suppl.* 74:513
Jarvis BJ, Freeman KC. 1985. *Ap. J.* 295:324
Jogee S. 1998. In *Molecular gas and star formation in the inner kpc of starbursts and non-starbursts*. PhD thesis, Yale Univ.
Jogee S, Scoville NZ, Kenney JDP. 2004. *Ap. J.* In press (astro-ph/0402341)
Jogee S, Shlosman I, Laine S, Englmaier P, Knapen J, et al. 2002. *Ap. J.* 575:156
Jones DH, Mould JR, Watson AM, Grillmair C, Gallager JS, et al. 1996. *Ap. J.* 466:742
Jungwiert B, Combes F, Axon DJ. 1997. *Astron. Astrophys. Suppl.* 125:479
Kalnajs A. 1973. *Proc. Astron. Soc. Aust.* 2:174
Kalnajs A. 1996. In *Proc. Nobel Symp. 98, Barred Galaxies and Circumnuclear Activity*, ed. Aa Sandqvist, PO Lindblad, p. 165. Berlin: Springer-Verlag
Kannappan SJ, Jansen RA, Barton EJ. 2004. *Astron. J.* 127:1371
Kenney JDP, Wilson CD, Scoville NZ, Devereux NA, Young JS. 1992. *Ap. J. Lett.* 395:L79
Kennicutt RC. 1983. *Ap. J.* 272:54
Kennicutt RC. 1994. In *Mass-Transfer Induced Activity in Galaxies*, ed. I Shlosman, p. 131. Cambridge: Cambridge Univ. Press
Kennicutt RC. 1998a. *Annu. Rev. Astron. Astrophys.* 36:189
Kennicutt RC. 1998b. *Ap. J.* 498:541
Kennicutt RC, Chu Y-H. 1988. *Astron. J.* 95:720
Kennicutt RC, Edgar BK, Hodge PW. 1989. *Ap. J.* 337:761
Kennicutt RC, Keel WC, Blaha CA. 1989. *Astron. J.* 97:1022
Kennicutt RC, Keel WC, van der Hulst JM, Hummel E, Roettiger KA. 1987. *Astron. J.* 93:1011
Kennicutt RC, Schweizer F, Barnes JE. 1998. *Galaxies: Interactions and Induced Star Formation*. Berlin: Springer-Verlag
Kent SM. 1985. *Ap. J. Suppl.* 59:115
Kent SM. 1987a. *Astron. J.* 93:816
Kent SM. 1987b. *Astron. J.* 93:1062
Kent SM. 1988. *Astron. J.* 96:514
Kent SM, Dame TM, Fazio G. 1991. *Ap. J.* 378:131
Knapen JH, Beckman JE, Heller CH, Shlosman I, de Jong RS. 1995a. *Ap. J.* 454:623
Knapen JH, Beckman JE, Shlosman I, Peletier RF, Heller CH, de Jong RS. 1995b. *Ap. J.* 443:L73
Knapen JH, Pérez-Ramírez D, Laine S. 2002. *MNRAS* 337:808
Knapen JH, Shlosman I, Peletier RF. 2000. *Ap. J.* 529:93
Kormendy J. 1979a. In *Photometry, Kinematics and Dynamics of Galaxies*, ed. DS Evans, p. 341. Austin: Dept. Astron., Univ. Texas, Austin
Kormendy J. 1979b. *Ap. J.* 227:714
Kormendy J. 1981. In *The Structure and Evolution of Normal Galaxies*, ed. SM Fall, D Lynden-Bell, p. 85. Cambridge: Cambridge Univ. Press
Kormendy J. 1982a. In *Morphology and Dynamics of Galaxies, Twelfth Advanced Course of the Swiss Society of Astronomy and Astrophysics*, ed. L Martinet, M Mayor, p. 113. Sauverny: Geneva Obs.
Kormendy J. 1982b. *Ap. J.* 257:75
Kormendy J. 1984. *Ap. J.* 286:116
Kormendy J. 1988. *Ap. J.* 335:40
Kormendy J. 1993. In *IAU Symp. 153, Galactic Bulges*, ed. H Habing, H Dejonghe, p. 209. Dordrecht: Kluwer
Kormendy J, Bender R. 1996. *Ap. J.* 464:L119
Kormendy J, Bender R, Ajhar EA, Dressler A, Faber SM, et al. 1996a. *Ap. J.* 473:L91
Kormendy J, Bender R, Richstone D, Ajhar EA, Dressler A, et al. 1996b. *Ap. J.* 459:L57
Kormendy J, Cornell ME. 2004. In *Penetrating Bars Through Masks of Cosmic Dust: The*

Hubble Tuning Fork Strikes a New Note, ed. DL Block, KC Freeman, I Puerari, G Groess. Dordrecht: Kluwer. In press

Kormendy J, Dressler A, Byun Y-I, Faber SM, Grillmair C, et al. 1994. In *ESO/OHP Workshop on Dwarf Galaxies*, ed. G Meylan, P Prugniel, p. 147. Garching: ESO

Kormendy J, Djorgovski S. 1989. *Annu. Rev. Astron. Astrophys.* 27:235

Kormendy J, Gebhardt K, Macchetto FD, Sparks WBS. 2004. *Astron. J.* Submitted

Kormendy J, Illingworth G. 1982. *Ap. J.* 256:460

Kormendy J, Illingworth G. 1983. *Ap. J.* 265:632

Kormendy J, McClure RD. 1993. *Astron. J.* 105:1793

Kormendy J, Norman CA. 1979. *Ap. J.* 233:539

Kuijken K, Merrifield MR. 1995. *Ap. J.* 443:L13

Kuijken K, Rich RM. 2002. *Astron. J.* 124:2054

Laine S, Shlosman I, Knapen JH, Peletier RF. 2002. *Ap. J.* 567:97

Larson RB, Tinsley BM. 1978. *Ap. J.* 219:46

Lauberts A, Valentijn EA. 1989. *The Surface Photometry Catalogue of the ESO-Uppsala Galaxies*. Garching: ESO

Lauer TR. 1985. *Ap. J. Suppl.* 57:473

Lauer TR. 1987. In *Nearly Normal Galaxies: From the Planck Time to the Present*, ed. SM Faber, p. 207. New York: Springer

Lauer TR, Ajhar EA, Byun Y-I, Dressler A, Faber SM, et al. 1995. *Astron. J.* 110:2622

Lauer TR, Faber SM, Ajhar EA, Grillmair CJ, Scowen PA. 1998. *Astron. J.* 116:2263

Lauer TR, Faber SM, Currie DG, Ewald SP, Groth EJ, et al. 1992. *Ap. J.* 104:522

Lauer TR, Faber SM, Groth EJ, Shaya EJ, Campbell B, et al. 1993. *Astron. J.* 106:1436

Laurikainen E, Salo H. 2002. *MNRAS* 337:1118

Leitherer C, Schaerer D, Goldader JD, González Delgado RM, Robert C, et al. 1999. *Ap. J. Suppl.* 123:3

Lindblad B. 1958. *Stockholms Obs. Ann.* 20:No. 6

Lindblad B. 1959. *Handb. Phys.* 53:21

Lindblad PAB, Lindblad PO, Athanassoula E. 1996. *Astron. Astrophys.* 313:65

Lindblad PO. 1999. *Astron. Astrophys. Rev.* 9:221

Long KS, Charles PA, Dubus G. 2002. *Ap. J.* 569:204

Lütticke R, Dettmar R-J, Pohlen M. 2000a. *Astron. Astrophys. Suppl.* 145:405

Lütticke R, Dettmar R-J, Pohlen M. 2000b. *Astron. Astrophys.* 362:435

Lynden-Bell D. 1979. *MNRAS* 187:101

Lynden-Bell D. 1996. In *Proc. Nobel Symp. 98, Barred Galaxies and Circumnuclear Activity*, ed. Aa Sandqvist, PO Lindblad, p. 8. New York: Springer

Lynden-Bell D, Kalnajs AJ. 1972. *MNRAS* 157:1

Lynden-Bell D, Wood R. 1968. *MNRAS* 138:495

MacArthur LA, Courteau S, Holtzman JA. 2003. *Ap. J.* 582:689

Maciejewski W, Sparke LS. 2000. *MNRAS* 313:745

Maoz D, Barth AJ, Ho LC, Sternberg A, Filippenko AV. 2001. *Astron. J.* 121:3048

Maoz D, Barth AJ, Sternberg A, Filippenko AV, Ho LC, et al. 1996. *Astron. J.* 111:2248

Márquez I, Durret F, González Delgado RM, Marrero I, Masegosa J, et al. 1999. *Astron. Astrophys. Suppl.* 140:1

Martinet L. 1995. *Fund. Cosmic Phys.* 15:341

Martini P, Pogge RW. 1999. *Astron. J.* 118:2646

Martini P, Regan MW, Mulchaey JS, Pogge RW. 2003. *Ap. J. Suppl.* 146:353

Matthews LD, Gallagher JS. 2002. *Ap. J. Suppl.* 141:429

Matthews LD, Gallagher JS, Krist JE, Watson AM, Burrows CJ, et al. 1999a. *Astron. J.* 118:208

Matthews LD, Gallagher JS, van Driel W. 1999b. *Astron. J.* 118:2751

McWilliam A, Rich RM. 1994. *Ap. J. Suppl.* 91:749

Merrifield MR. 1996. In *IAU Colloq. 157, Barred Galaxies*, ed. R Buta, DA Crocker, BG Elmegreen, p. 179. San Francisco: ASP

Merrifield MR, Kuijken K. 1995. *MNRAS* 274:933

Merrifield MR, Kuijken K. 1999. *Astron. Astrophys.* 345:L47

Merritt D, Sellwood JA. 1994. *Ap. J.* 425:551
Mihalas D, Routly PM. 1968. *Galactic Astronomy*. San Francisco: Freeman
Miller RH, Smith BF. 1979. *Ap. J.* 227:785
Minkowski R. 1962. In *IAU Symp. 15, Problems of Extra-Galactic Research*, ed. GC McVittie, p. 112. New York: Macmillan
Minniti D, Olszewski EW, Rieke M. 1993. *Ap. J.* 410:L79
Möllenhoff C, Heidt J. 2001. *Astron. Astrophys.* 368:16
Möllenhoff C, Matthias M, Gerhard OE. 1995. *Astron. Astrophys.* 301:359
Moore B. 1994. *Nature* 370:629
Morgan WW. 1951. *Publ. Obs. Univ. Mich.* 10:33
Morgan WW. 1958. *Publ. Astron. Soc. Pac.* 70:364
Mulchaey JS, Regan MW. 1997. *Ap. J.* 482:L135
Mulchaey JS, Regan MW, Kundu A. 1997. *Ap. J. Suppl.* 110:299
Navarro JF, Eke VR, Frenk CS. 1996. *MNRAS* 283:L72
Navarro JF, Frenk CS, White SDM. 1996. *Ap. J.* 462:563
Navarro JF, Frenk CS, White SDM. 1997. *Ap. J.* 490:493
Nilson P. 1973. *Uppsala General Catalogue of Galaxies*. Uppsala: Uppsala Astron. Obs.
Noguchi N. 1988. *Astron. Astrophys.* 203:259
Norman CA. 1984. In *Formation and Evolution of Galaxies and Large Structures in the Universe*, ed. J Audouze, JTT Van, p. 327. Dordrecht: Reidel
Norman CA, Sellwood JA, Hasan H. 1996. *Ap. J.* 462:114
O'Connell RW. 1983. *Ap. J.* 267:80
Ortolani S, Renzini A, Gilmozzi R, Marconi G, Barbuy B, et al. 1995. *Nature* 377:701
Paglione TAD, Wall WF, Young JS, Heyer MH, Richard M, et al. 2001. *Ap. J. Suppl.* 135:183
Patsis PA, Athanassoula E, Grosbøl P, Skokos Ch. 2002. *MNRAS* 335:1049
Patton DR, Pritchet CJ, Carlberg RG, Marzke RO, Yee HKC, et al. 2002. *Ap. J.* 565:208
Peletier RF, Balcells M. 1996. *Astron. J.* 111:2238
Peletier RF, Balcells M, Davies RL, Andredakis Y, Vazdekis A, et al. 1999. *MNRAS* 310:703
Pence WD, Blackman CP. 1984. *MNRAS* 207:9
Pérez-Ramírez D, Knapen JH, Peletier RF, Laine S, Doyon R, Nadeau D. 2000. *MNRAS* 317:234
Pfenniger D. 1984. *Astron. Astrophys.* 134:373
Pfenniger D. 1985. *Astron. Astrophys.* 150:112
Pfenniger D. 1996a. *In Barred Galaxies*, ed. JA Sellwood, p. 273. San Francisco: ASP
Pfenniger D. 1996b. In *Proc. Nobel Symp. 98, Barred Galaxies and Circumnuclear Activity*, ed. Aa Sandqvist, PO Lindblad, p. 91. New York: Springer
Pfenniger D. 2000. In *Toward a New Millennium in Galaxy Morphology*, ed. DL Block, I Puerari, A Stockton, D Ferreira, p. 149. Dordrecht: Kluwer
Pfenniger D, Friedli D. 1991. *Astron. Astrophys.* 252:75
Pfenniger D, Norman C. 1990. *Ap. J.* 363:391
Phillips AC. 1993. *Star formation in barred spiral galaxies*, PhD thesis, Univ. Wash.
Phillips AC, Illingworth GD, MacKenty JW, Franx M. 1996. *Astron. J.* 111:1566
Piner BG, Stone JM, Teuben PJ. 1995. *Ap. J.* 449:508
Pogge RW. 1989. *Ap. J. Suppl.* 71:433
Pompea SM, Rieke GH. 1990. *Ap. J.* 356:416
Prendergast KH. 1964. *Astron. J.* 69:147
Prendergast KH. 1983. In *IAU Symp. 100, Internal Kinematics and Dynamics of Galaxies*, ed. E Athanassoula, p. 215. Dordrecht: Reidel
Quillen AC, Kuchinski LE, Frogel JA, DePoy DL. 1997. *Ap. J.* 481:179
Raha N, Sellwood JA, James RA, Kahn FD. 1991. *Nature* 352:411
Regan MW. 2000. *Ap. J.* 541:142
Regan MW, Sheth K, Vogel SN. 1999. *Ap. J.* 526:97
Regan MW, Teuben P. 2003. *Ap. J.* 582:723
Regan MW, Vogel SN, Teuben PJ. 1997. *Ap. J.* 482:L143
Regan MW, Thornley MD, Helfer TT, Sheth K, Wong T, et al. 2001. *Ap. J.* 561:218
Renzini A. 1999. In *The Formation of Galactic Bulges*, ed. CM Carollo, HC Ferguson, RFG

Wyse, p. 9. Cambridge: Cambridge Univ. Press
Rest A, van den Bosch FC, Jaffe W, Tran H, Tsvetanov T, et al. 2001. *Astron. J.* 121:2431
Rich RM. 1999. In *The Formation of Galactic Bulges*, ed. CM Carollo, HC Ferguson, RFG Wyse, p. 54. Cambridge: Cambridge Univ. Press
Rix H-W, Kennicutt RC, Braun R, Walterbos RAM. 1995. *Ap. J.* 438:155
Rix H-W, Zaritsky D. 1995. *Ap. J.* 447:82
Roberts WW, Huntley JM, van Albada GD. 1979. *Ap. J.* 233:67
Roberts WW, Roberts MS, Shu FH. 1975. *Ap. J.* 196:381
Rubin VC. 1994. *Astron. J.* 107:173
Rubin VC, Ford WK, Peterson CJ. 1975. *Ap. J.* 199:39
Ryder SD, Knapen JH, Takamiya M. 2001. *MNRAS* 323:663
Saglia RP, Bender R, Dressler A. 1993. *Astron. Astrophys.* 279:75
Sakamoto K, Okamura SK, Ishizuki S, Scoville NZ. 1999. *Ap. J.* 525:691
Sakamoto K, Okamura S, Minezaki T, Kobayashi Y, Wada K. 1995. *Astron. J.* 110:2075
Salo H, Rautiainen P, Buta R, Purcell GB, Cobb ML, et al. 1999. *Astron. J.* 117:792
Sandage A. 1961. *The Hubble Atlas of Galaxies*. Washington, DC: Carnegie Inst. Wash.
Sandage A. 1975. In *Stars and Stellar Systems*, Vol. 9: *Galaxies and the Universe*, ed. A Sandage, M Sandage, J Kristian, p. 1. Chicago: Univ. Chicago Press
Sandage A. 1986. *Annu. Rev. Astron. Astrophys.* 24:421
Sandage A. 1990. *JRASC* 84:70
Sandage A, Bedke J. 1994. *The Carnegie Atlas of Galaxies*. Washington, DC: Carnegie Inst. Wash.
Sandage A, Brucato R. 1979. *Astron. J.* 84:472
Sanders DB, Mirabel IF. 1996. *Annu. Rev. Astron. Astrophys.* 34:749
Sanders RH, Prendergast KH. 1974. *Ap. J.* 188:489
Sanders RH, Tubbs AD. 1980. *Ap. J.* 235: 803
Schinnerer E, Böker T, Meier DS. 2003. *Ap. J.* 591:L115
Schinnerer E, Maciejewski W, Scoville N, Moustakas LA. 2002. *Ap. J.* 575:826
Schmidt AA, Bica E, Alloin D. 1990. *MNRAS* 243:620
Schmidt M. 1959. *Ap. J.* 129:243
Schwarz MP. 1981. *Ap. J.* 247:77
Schwarz MP. 1984. *MNRAS* 209:93
Schweizer F. 1980. *Ap. J.* 237:303
Schweizer F. 1990. In *Dynamics and Interactions of Galaxies*, ed. R Wielen, p. 60. New York: Springer
Scorza C, Bender R. 1995. *Astron. Astrophys.* 293:20
Scoville NZ, Matthews K, Carico DP, Sanders DB. 1988. *Ap. J.* 327:L61
Seifert W, Scorza C. 1996. *Astron. Astrophys.* 310:75
Seigar M, Carollo CM, Stiavelli M, de Zeeuw PT, Dejonghe H. 2002. *Astron. J.* 123:184
Seigar MS, James PA. 1998. *MNRAS* 299:672
Sellwood JA. 1981. *Astron. Astrophys.* 99: 362
Sellwood JA. 1985. *MNRAS* 217:127
Sellwood JA. 1993a. In *IAU Symp. 153, Galactic Bulges*, ed. H Habing, H Dejonghe, p. 391. Dordrecht: Kluwer
Sellwood JA. 1993b. In *Back to the Galaxy*, ed. SS Holt, F Verter, p. 133. New York: AIP
Sellwood JA, Debattista VP. 1996. In *Proc. Nobel Symp. 98, Barred Galaxies and Circumnuclear Activity*, ed. Aa Sandqvist, PO Lindblad, p. 43. New York: Springer
Sellwood JA, Moore EM. 1999. *Ap. J.* 510: 125
Sellwood JA, Sparke LS. 1988. *MNRAS* 231: 25P
Sellwood JA, Wilkinson A. 1993. *Rep. Prog. Phys.* 56:173
Sérsic JL. 1968. *Atlas de Galaxias Australes*. Córdoba: Obs. Astron. Univ. Nac. Córdoba
Sérsic JL. 1973. *Publ. Astron. Soc. Pac.* 85:103
Sérsic JL, Pastoriza M. 1965. *Publ. Astron. Soc. Pac.* 77:287
Sérsic JL, Pastoriza M. 1967. *Publ. Astron. Soc. Pac.* 79:152
Shaw M. 1993. *Astron. Astrophys.* 280:33

Shaw M, Axon D, Probst R, Gatley I. 1995. *MNRAS* 274:369
Shaw M, Wilkinson A, Carter D. 1993a. *Astron. Astrophys.* 268:511
Shaw MA. 1987. *MNRAS* 229:691
Shaw MA, Combes F, Axon DJ, Wright GS. 1993b. *Astron. Astrophys.* 273:31
Shen J, Sellwood JA. 2004. In *Carnegie Observatories Astrophysics Ser.*, Vol. 1: *Coevolution of Black Holes and Galaxies*, ed. LC Ho. Cambridge: Cambridge Univ. Press. In press (astro-ph/0303130)
Sheth K, Vogel SN, Regan MW, Teuben PJ, Harris AI, Thornley MD. 2002. *Astron. J.* 124:2581
Shields JC, Filippenko AV. 1992. In *Relationships Between Active Galactic Nuclei and Starburst Galaxies*, ed. AV Filippenko, p. 267. San Francisco: ASP
Shlosman I, Frank J, Begelman MC. 1989. *Nature* 338:45
Simien F, de Vaucouleurs G. 1986. *Ap. J.* 302:564
Simien F, Prugniel Ph. 1997. *Astron. Astrophys. Suppl.* 126:15
Simkin SM, Su HJ, Schwarz MP. 1980. *Ap. J.* 237:404
Sørensen S-A, Matsuda T, Fujimoto M. 1976. *Astrophys. Space Sci.* 43:491
Sparke LS, Gallagher JS. 2000. *Galaxies in the Universe: An Introduction*. Cambridge: Cambridge Univ. Press
Sparke LS, Sellwood JA. 1987. *MNRAS* 225:653
Spitzer L, Schwarzschild M. 1951. *Ap. J.* 114:385
Spitzer L, Schwarzschild M. 1953. *Ap. J.* 118:106
Talbot RJ, Jensen EB, Dufour RJ. 1979. *Ap. J.* 229:91
Terndrup DM. 1993. In *The Minnesota Lectures on Clusters of Galaxies and Large-Scale Structure*, ed. RM Humphreys, p. 9. San Francisco: ASP
Thomas D, Greggio L, Bender R. 1999. *MNRAS* 302:537
Thomas D, Maraston C, Bender R. 2002. *Astrophys. Space Sci.* 281:371
Thronson HA, Hereld M, Majewski S, Greenhouse M, Johnson P, et al. 1989. *Ap. J.* 343:158
Toomre A. 1964. *Ap. J.* 139:1217
Toomre A. 1966. In *Geophysical Fluid Dynamics, Notes on the 1966 Summer Study Program at the Woods Hole Oceanogr. Inst.*, No. 66–46, p. 111
Toomre A. 1977a. In *The Evolution of Galaxies and Stellar Populations*, ed. BM Tinsley, RB Larson, p. 401. New Haven: Yale Univ. Obs.
Toomre A. 1977b. *Annu. Rev. Astron. Astrophys.* 15:437
Toomre A, Toomre J. 1972. *Ap. J.* 178:623
Tóth G, Ostriker JP. 1992. *Ap. J.* 389:5
Trager SC. 2004. In *Carnegie Observatories Astrophysics Ser.*, Vol. 4: *Origin and Evolution of the Elements*, ed. A McWilliam, M Rauch, p. 391. Cambridge: Cambridge Univ. Press
Tremaine S. 1989. In *Dynamics of Astrophysical Disks*, ed. JA Sellwood, p. 231. Cambridge: Cambridge Univ. Press
Tremaine S, Ostriker JP. 1982. *Ap. J.* 256: 435
Tremaine SD, Ostriker JP, Spitzer L. 1975. *Ap. J.* 196:407
Trujillo I, Asensio Ramos A, Rubiño-Martín JA, Graham AW, Aguerri JAL, et al. 2002. *MNRAS* 333:510
Usui T, Saito M, Tomita A. 1998. *Astron. J.* 116: 2166
Usui T, Saito M, Tomita A. 2001. *Astron. J.* 121: 2483
van den Bergh S. 1960a. *Ap. J.* 131:215
van den Bergh S. 1960b. *Ap. J.* 131:558
van den Bergh S. 1976a. *Ap. J.* 203:764
van den Bergh S. 1976b. *Ap. J.* 206:883
van den Bergh S. 1986. *Astron. J.* 91:271
van den Bergh S. 1991. *PASP* 103:609
van den Bergh S. 1995. *Astron. J.* 110:613
van den Bergh S. 2002. *Publ. Astron. Soc. Pac.* 114:797
van den Bergh S, Abraham RG, Whyte LF, Merrifield MR, Eskridge PB, et al. 2002. *Astron. J.* 123:2913
van den Bosch FC, Jaffe W, van der Marel RP. 1998. *MNRAS* 293:343

van der Kruit PC. 1976. *Astron. Astrophys.* 52:85
van der Kruit PC, Jiménez-Vicente J, Kregel M, Freeman KC. 2001. *Astron. Astrophys.* 379:374
van der Kruit PC, Searle L. 1981a. *Astron. Astrophys.* 95:105
van der Kruit PC, Searle L. 1981b. *Astron. Astrophys.* 95:116
van der Kruit PC, Searle L. 1982. *Astron. Astrophys.* 110:61
van Dokkum PG, Franx M. 1995. *Astron. J.* 110:2027
van Driel W, Rots AH, van Woerden H. 1988. *Astron. Astrophys.* 204:39
Vega Beltrán JC, Pizella A, Corsini EM, Funes JG, Zeilinger WW, et al. 2001. *Astron. Astrophys.* 374:394
Verolme EK, Cappellari M, Copin Y, van der Marel RP, Bacon R, et al. 2002. *MNRAS* 335:517
Wakamatsu K-I, Hamabe M. 1984. *Ap. J. Suppl.* 56:283
Waller WH, Fanelli MN, Keel WC, Bohlin R, Collins NR, et al. 2001. *Astron. J.* 121:1395
Walterbos RAM, Braun R, Kennicutt RC. 1994. *Astron. J.* 107:184
Warren MS, Quinn PJ, Salmon PJ, Zurek WH. 1992. *Ap. J.* 399:405
Weiland JL, Arendt RG, Berriman GB, Dwek E, Freudenreich HT, et al. 1994. *Ap. J.* 425:L81
Weiner BJ, Sellwood JA, Williams TB. 2001a. *Ap. J.* 546:931
Weiner BJ, Williams TB, van Gorkom JH, Sellwood JA. 2001b. *Ap. J.* 546:916
Wilson CD. 1995. *Ap. J.* 448:L97
Windhorst RA, Taylor VA, Jansen RA, Odewahn SC, Chiarenza CAT, et al. 2002. *Astrophys. J. Suppl.* 143:113
Wong T, Blitz L. 2000. *Ap. J.* 540:771
Worthey G, Faber SM, Gonzalez JJ. 1992. *Ap. J.* 398:69
Wozniak H, Friedli D, Martinet L, Martin P, Bratschi P. 1995. *Astron. Astrophys. Suppl.* 111:115
Wyse RFG, Gilmore G, Franx M. 1997. *Annu. Rev. Astron. Astrophys.* 35:637
Young JS, Devereux NA. 1991. *Ap. J.* 373:414
Young JS, Scoville NZ. 1991. *Annu. Rev. Astron. Astrophys.* 29:581
Yun MS, Ho PTP, Lo KY. 1994. *Nature* 372:530
Zhang Q, Fall SM. 1999. *Ap. J.* 527:L81
Zhang X. 1996. *Ap. J.* 457:125
Zhang X. 1998. *Ap. J.* 499:93
Zhang X. 1999. *Ap. J.* 518:613
Zhang X. 2003. *J. Korean Astron. Soc.* 36:223 (astro-ph/0301655)
Zoccali M, Renzini A, Ortolani S, Greggio L, Saviane I, et al. 2003. *Astron. Astrophys.* 399:931
Zwicky F. 1957. *Morphological Astronomy*. Berlin: Springer

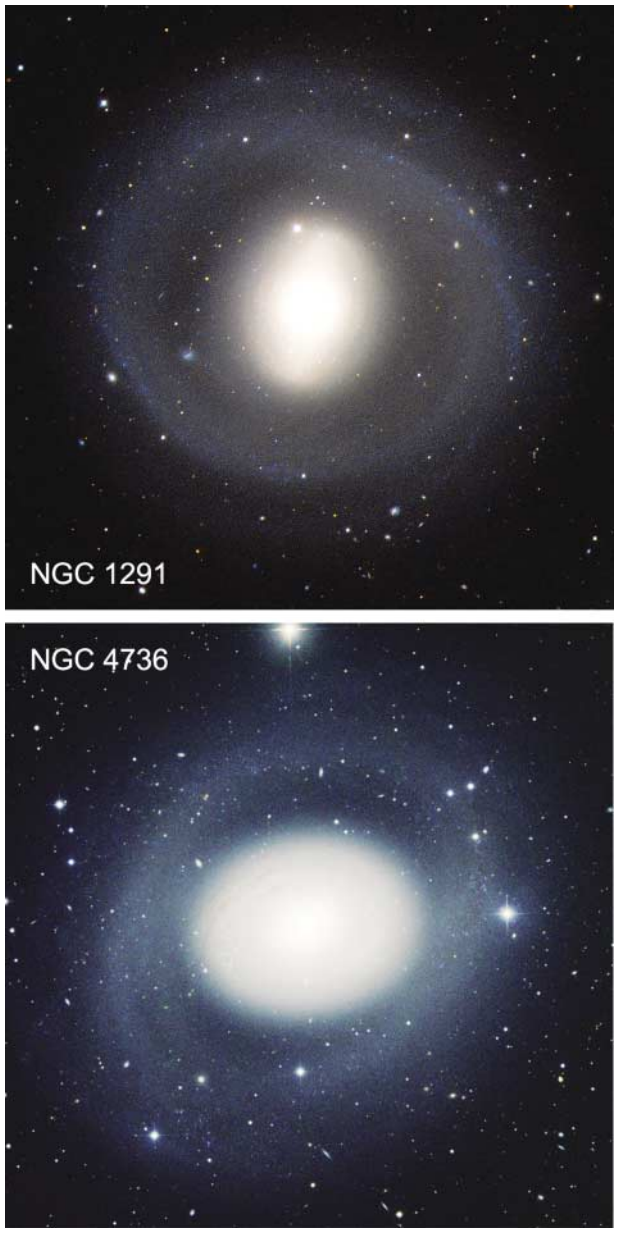

Figure 2 Prototypical outer rings in barred and unbarred galaxies. NGC 1291 is an (R)SB(lens)0/a galaxy—it has a bar embedded in a lens of the same major-axis diameter (see also Kormendy 1979b). NGC 4736 is classified (R)SA(r)ab. This figure shows how blue the outer rings are: They are dominated by young stars. Both rings also contain H I gas (van Driel et al. 1988, Bosma et al. 1977b). Sources: NGC 1291 (Buta, Corwin, & Odewahn 2003); NGC 4736 (NOAO).

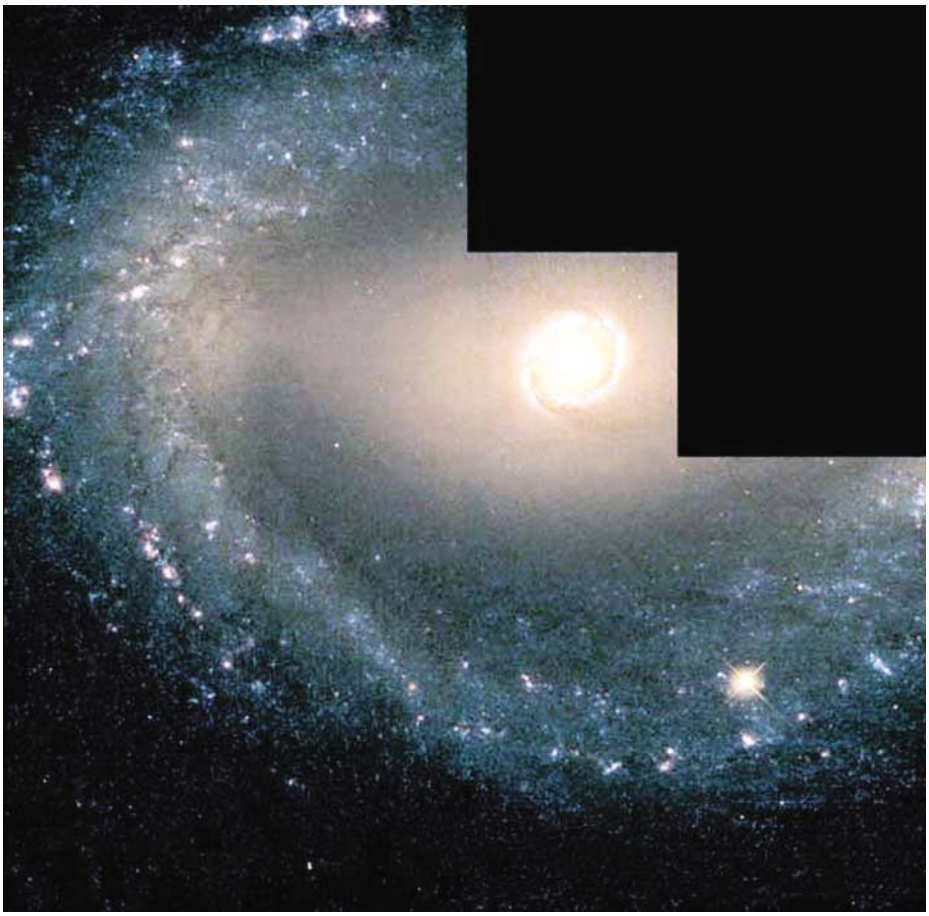

Figure 3 NGC 1512, an SB(r)ab galaxy imaged with HST by Maoz et al. (2001). This figure (courtesy NASA and ESA) illustrates the stellar population of inner rings. As is common in intermediate-Hubble-type galaxies, the bar in NGC 1512 is made of old, red stars and the disk is made of young, blue stars. This figure shows that the inner ring has the same stellar population as the disk, not the bar. Also seen at center is a nuclear star-formation ring that is shown at higher magnification in Figure 8 and the start of a well-developed, curved dust lane (cf. Figures 6–8) that extends out of the field of view to the right. The corresponding dust lane on the other side is visible near the central ring but not at larger radii. The outer parts of NGC 1512 are illustrated by Sandage & Bedke (1994), who note that NGC 1512 is morphologically normal except for some distortion of its outer spiral structure (not shown here) by a tidal encounter with neighboring NGC 1510.

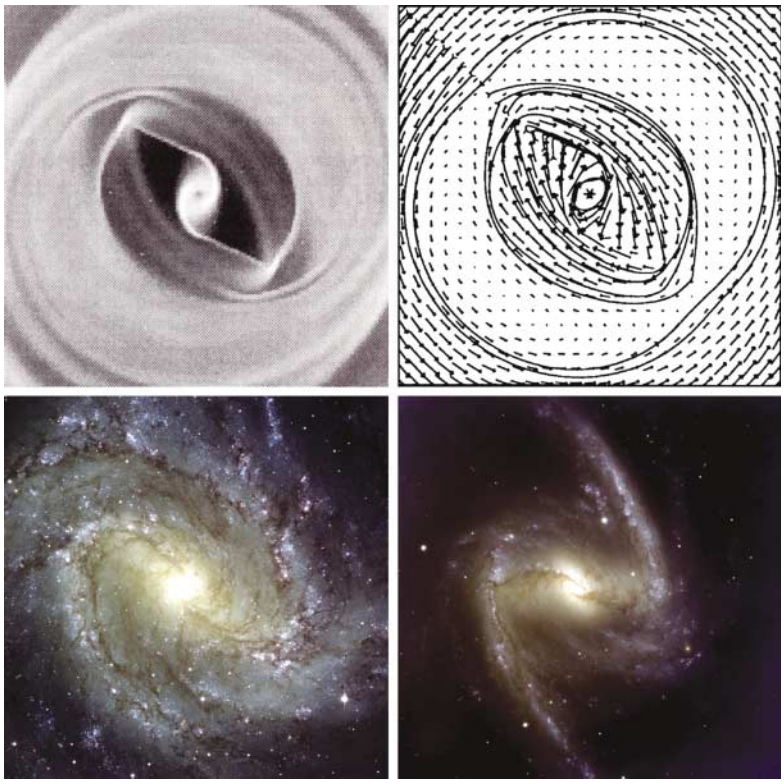

Figure 7 Comparison of the gas response to a bar (model 001 by Athanassoula 1992b) with NGC 5236 (*left*) and NGC 1365 (*right*). The galaxy images were taken with the VLT and are reproduced courtesy of ESO. In the models, the bar potential is oriented at 45° to the horizontal, parallel to the bar in NGC 5236. The bar axial ratio is 0.4, and its length is approximately half of the box diagonal. The top-right panel shows the velocity field; arrow lengths are proportional to flow velocities. Discontinuities in gas velocity indicate the presence of shocks; these are where the gas density is high in the density map at top left. High gas densities are identified with dust lanes in the galaxies. The model correctly reproduces the observations that (*a*) dust lanes are offset in the forward (rotation) direction from the ridge line of the bar; (*b*) they are offset by larger amounts nearer the center; and (*c*) very near the center, they curve and become nearly azimuthal. As emphasized by the velocity field, the shocks in the model and the dust lanes in the galaxy are signs that the gas loses energy. Therefore it must fall toward the center. In fact, both galaxies have high gas densities and active star formation in their bright centers (e.g., Crosthwaite et al. 2002; Curran et al. 2001a,b).

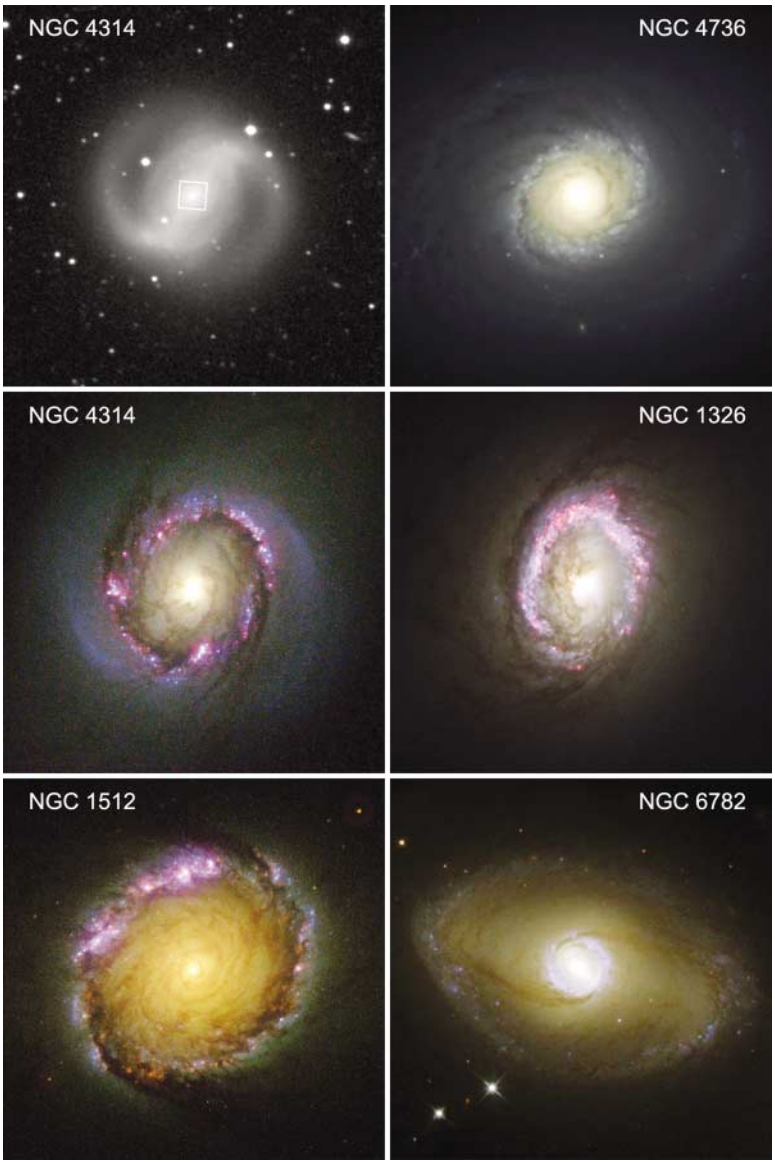

Figure 8 Nuclear star-formation rings in barred and oval galaxies. For NGC 4314, a wide-field view is at top left; for NGC 4736, the wide-field view is as in Figure 2. Sources: NGC 4314 (Benedict et al. 2002); NGC 4736 (NOAO); NGC 1326 [Buta et al. 2000 and Zolt Levay (STScI)]; NGC 1512 (Maoz et al. 2001); NGC 6782 (Windhorst et al. 2002 and the Hubble Heritage Program).

Annual Review of Astronomy and Astrophysics
Volume 42, 2004

CONTENTS